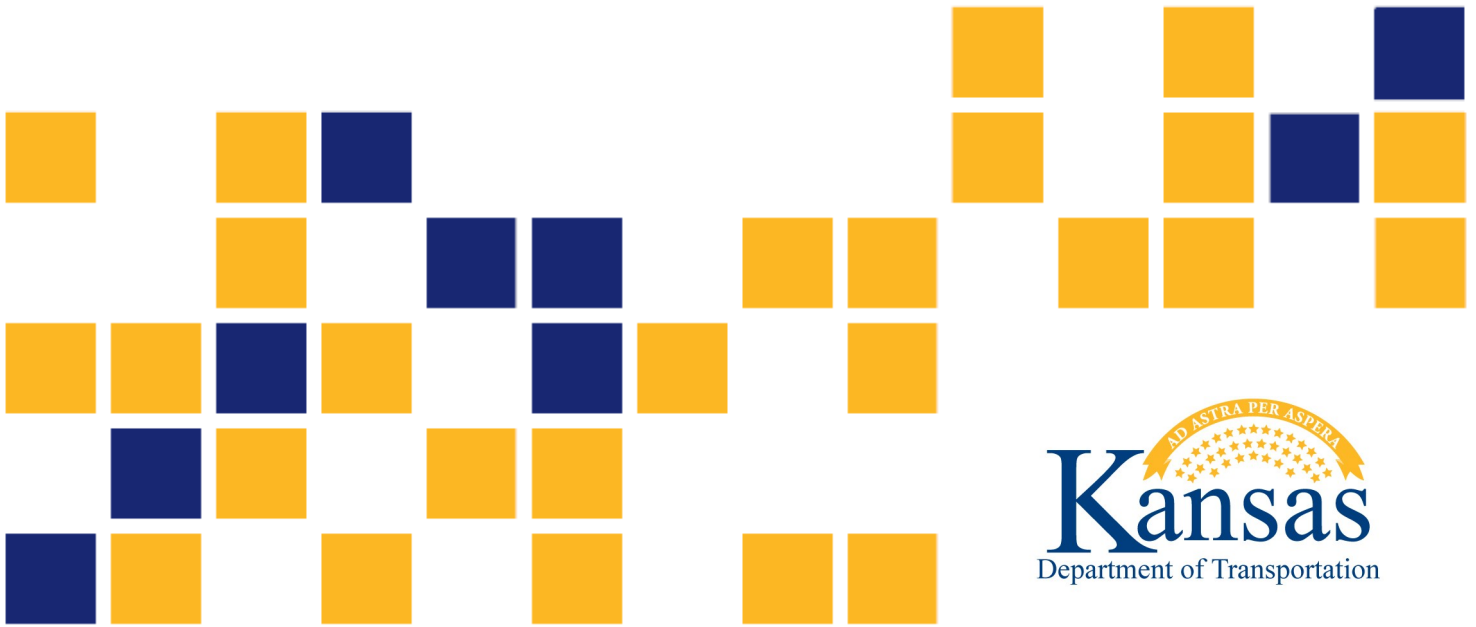# Evaluation of Low-Quality Recycled Concrete Pavement Aggregates for Subgrade Soil Stabilization

Massoumeh Tavakol
Stacey Kulesza, Ph.D., P.E.
Christopher Jones, Ph.D.
Xingdong Wu
Mustaque Hossain, Ph.D., P.E.

Kansas State University Transportation Center

Kansas
Department of Transportation

1	Report No. K-TRAN: KSU-16-2 P2	2	Government Accession No.	3	Recipient Catalog No.		
4	**Title and Subtitle** Evaluation of Low-Quality Recycled Concrete Pavement Aggregates for Subgrade Soil Stabilization			5	**Report Date** July 2024		
				6	**Performing Organization Code**		
7	**Author(s)** Massoumeh Tavakol; Stacey Kulesza, Ph.D., P.E.; Christopher Jones, Ph.D.; Xingdong Wu; Mustaque Hossain, Ph.D., P.E.			8	**Performing Organization Report No.**		
9	**Performing Organization Name and Address** Kansas State University Transportation Center Department of Civil Engineering 2118 Fiedler Hall 1701C Platt Street Manhattan, KS 66506-5000			10	**Work Unit No. (TRAIS)**		
				11	**Contract or Grant No.** C2081		
12	**Sponsoring Agency Name and Address** Kansas Department of Transportation Bureau of Research 2300 SW Van Buren Topeka, Kansas 66611-1195			13	**Type of Report and Period Covered** Final Report January 2016 – July 2019		
				14	**Sponsoring Agency Code** RE-0688-01		
15	**Supplementary Notes** See also K-TRAN: KSU-16-2 P1 for a companion report titled *Evaluation of Low-Quality Recycled Concrete Pavement Aggregates for Portland Cement-Treated Base*. For more information write to address in block 9.						

16 **Abstract**

Recycled concrete aggregate (RCA) is the byproduct of the demolition of concrete structures and pavements. The use of RCA to replace quarried aggregates in paving projects is one way to utilize these materials and alleviate concerns regarding this increasing waste stream. In this study, a low-plasticity clay in Kansas was stabilized using RCA and three stabilizing materials (lime, Class C fly ash, and a combination of portland cement and fly ash). Candidate mixtures with varying proportions of chemical stabilizers and D-cracked aggregates were evaluated using the standard Proctor, unconfined compressive strength, linear shrinkage, and California Bearing Ratio tests. Microstructure characteristics of selected mixtures were explored using scanning electron microscopy (SEM) and energy-dispersive X-ray tests. Laboratory test results indicated that RCA, in conjunction with all cementitious materials except lime, improved clay strength, stiffness, and shrinkage properties. SEM results also indicated that RCA causes a low void space and a dense arrangement of soil particles. RCA effectively improved evaluated mixture properties when an adequate soil-RCA bond was reached using chemical agents. The long-term performance of full-depth flexible pavements with stabilized mixtures as subgrade was assessed in the AASHTOWare Pavement ME Design (commonly known as MEPDG) software, and the life-cycle cost of flexible pavements with stabilized mixtures was estimated for a 40-year design period. Economic analysis results indicated that RCA is cost-effective only if it is used with a combination of fly ash and portland cement in a mass ratio of 1:1.

17	**Key Words** Recycled materials, Mix design, Soil stabilization, Materials tests, Economic analysis		18	**Distribution Statement** No restrictions. This document is available to the public through the National Technical Information Service www.ntis.gov.		
19	**Security Classification (of this report)** Unclassified	20	**Security Classification (of this page)** Unclassified	21	**No. of pages** 155	22	**Price**

This page intentionally left blank.

Evaluation of Low-Quality Recycled Concrete Pavement Aggregates for Subgrade Soil Stabilization

Final Report

Prepared by

Massoumeh Tavakol
Stacey Kulesza, Ph.D., P.E.
Christopher Jones, Ph.D.
Xingdong Wu
Mustaque Hossain, Ph.D., P.E.

Kansas State University Transportation Center

A Report on Research Sponsored by

THE KANSAS DEPARTMENT OF TRANSPORTATION
TOPEKA, KANSAS

and

KANSAS STATE UNIVERSITY TRANSPORTATION CENTER
MANHATTAN, KANSAS

July 2024

PREFACE

The Kansas Department of Transportation's (KDOT) Kansas Transportation Research and New-Developments (K-TRAN) Research Program funded this research project. It is an ongoing, cooperative, and comprehensive research program addressing transportation needs of the state of Kansas utilizing academic and research resources from KDOT, Kansas State University and the University of Kansas. Transportation professionals in KDOT and the universities jointly develop the projects included in the research program.

NOTICE

The authors and the state of Kansas do not endorse products or manufacturers. Trade and manufacturers names appear herein solely because they are considered essential to the object of this report.

This information is available in alternative accessible formats. To obtain an alternative format, contact the Office of Public Affairs, Kansas Department of Transportation, 700 SW Harrison, 2nd Floor – West Wing, Topeka, Kansas 66603-3745 or phone (785) 296-3585 (Voice) (TDD).

DISCLAIMER

The contents of this report reflect the views of the authors who are responsible for the facts and accuracy of the data presented herein. The contents do not necessarily reflect the views or the policies of the state of Kansas. This report does not constitute a standard, specification, or regulation.

Abstract

Recycled concrete aggregate (RCA) is the byproduct of the demolition of concrete structures and pavements. The use of RCA to replace quarried aggregates in paving projects is one way to utilize these materials and alleviate concerns regarding this increasing waste stream. In this study, a low-plasticity clay in Kansas was stabilized using RCA and three stabilizing materials (lime, Class C fly ash, and a combination of portland cement and fly ash). Candidate mixtures with varying proportions of chemical stabilizers and D-cracked aggregates were evaluated using the standard Proctor, unconfined compressive strength, linear shrinkage, and California Bearing Ratio tests. Microstructure characteristics of selected mixtures were explored using scanning electron microscopy (SEM) and energy-dispersive X-ray tests. Laboratory test results indicated that RCA, in conjunction with all cementitious materials except lime, improved clay strength, stiffness, and shrinkage properties. SEM results also indicated that RCA causes a low void space and a dense arrangement of soil particles. RCA effectively improved evaluated mixture properties when an adequate soil-RCA bond was reached using chemical agents. The long-term performance of full-depth flexible pavements with stabilized mixtures as subgrade was assessed in the AASHTOWare Pavement ME Design (commonly known as MEPDG) software, and the life-cycle cost of flexible pavements with stabilized mixtures was estimated for a 40-year design period. Economic analysis results indicated that RCA is cost-effective only if it is used with a combination of fly ash and portland cement in a mass ratio of 1:1.

Acknowledgments

Table of Contents

List of Tables

List of Figures

Chapter 1: Introduction

1.1 Background

Natural aggregate resources, although vast, are finite. The cost of using natural aggregates in construction projects is rising due to the scarcity of economic sources, especially near urban areas, and increasing haul distances. In addition, the depletion of natural resources has undesirable environmental impacts; thus, environmental regulations further limit the opening of new quarries or the expansion of existing aggregate quarries (Verian et al., 2013). Unfortunately, construction waste produced in the United States and around the world continues to increase each year (Gonzalez & Moo-Young, 2004). The massive production of construction waste raises economic and environmental concerns, particularly related to landfilling (Oikonomou, 2005). However, the use of recycled concrete aggregate (RCA) as a substitute for virgin aggregates helps conserve natural aggregates and reduces the amount of waste entering landfills while conserving significant amounts of energy used to process and transport virgin aggregates and remove construction waste (Verian et al., 2013).

1.2 Problem Statement

Although many state Departments of Transportation (DOTs) have used recycled concrete as aggregates in pavement construction, the acceptance of RCA usage in pavement applications has varied (Verian et al., 2013; Cabalar et al., 2017). The properties of RCA differ from those of natural aggregates primarily due to the recycled mortar in RCA, which consequently alters pavement layer performance. As such, many highway agencies are reluctant to use RCA in the surface layer, choosing instead to primarily utilize these materials in unbound bases. Although experience using RCA for subgrade soil stabilization is limited, especially RCA from low-quality sources such as D-cracked pavements, RCA usage offers the potential for pavement performance improvement, elimination of ever-increasing waste stream, and reduction of costs associated with subgrade soil stabilization. D-cracking is a form of concrete pavement deterioration that appears on the pavement surface as a series of closely spaced cracks generally parallel to transverse and longitudinal joints. Coarse aggregates are susceptible to D-cracking. Freeze-thaw (F-T) cycles and

moisture are the primary contributors to D-cracking. To date, no known work has evaluated the effectiveness of a combination of RCA and chemical stabilizers for subgrade soil stabilization.

1.3 Objective

The primary objective of this study was to investigate the suitability of D-cracked RCA for subgrade stabilization for hot-mix asphalt (HMA) pavements. This research also evaluated the strength, stiffness, and shrinkage potential of clay subgrade beneath HMA pavements stabilized using D-cracked RCA and various stabilizers. The selected stabilizers were lime, Class C fly ash, and a combination of portland cement and Class C fly ash. Potential soil improvement was assessed via compaction, unconfined compressive strength (UCS), California Bearing Ratio (CBR), and linear shrinkage tests. In addition, this study used scanning electron microscopy (SEM) and energy dispersive X-ray (EDX) analysis to investigate the RCA-clay interaction to identify the effects of RCA on the microstructure of stabilized mixtures. Finally, this research sought to predict the long-term performance of stabilized mixtures using the AASHTOWare Pavement ME Design software and assess the potential cost savings of using RCA via life-cycle cost analysis (LCCA).

Chapter 2: Literature Review

2.1 Introduction

Each year, two billion tons of aggregate are produced in the United States, with an expected annual increasing trend (Gonzalez & Moo-Young, 2004). Annual construction waste produced from building demolition is currently estimated to be 123 million tons (Gonzalez & Moo-Young, 2004). According to the U.S. Environmental Protection Agency (EPA), the generation of debris from construction, demolition, and renovation of residential and nonresidential buildings in the United States was almost 170 million tons in 2003 (EPA, 2014), and the total amount of waste generated in the European Union was more than 2.5 billion tons in 2012, of which 34% was due to construction and demolition (Silva et al., 2016). The massive consumption of raw natural resources and substantial production of construction waste raise economic and environmental concerns (Oikonomou, 2005). Landfilling is the most common method of waste management for construction materials, but this method has negative environmental impacts and high costs. Consequently, state agencies have begun to consider recycling as a viable option for construction projects (Gonzalez & Moo-Young, 2004).

2.2 Recycled Concrete Aggregates

RCA is the product of demolishing concrete structures and pavements (McNeil & Kang, 2013). Initial demolition waste recycling dates back to post-World War II in Germany, followed by worldwide research that revealed promising performances of recycled aggregates (Rao et al., 2007). Figure 2.1 shows a percentage estimation of various construction materials in demolition waste (Oikonomou, 2005).
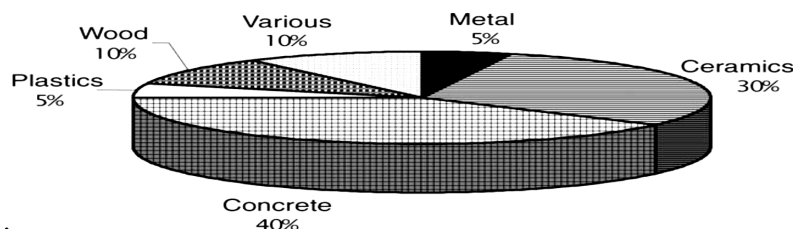
Figure 2.1: Approximate Basic Composition of Demolition Wastes
Source: Oikonomou (2005)

Three main types of materials are produced from recycling construction and demolition waste (Silva et al., 2016): RCAs that contain a minimum of 90%, by mass, of portland cement-based wastes and natural aggregates; recycled masonry aggregates (RMAs) that contain a minimum of 90%, by mass, of aerated and lightweight concrete blocks, ceramic bricks, blast-furnace slag bricks and blocks, ceramic roofing tiles and shingles, and sand-lime bricks; and mixed recycled aggregates (MRAs) that contain less than 90%, by mass, of RCA and RMA.

The use of RCA in construction is prevalent in the worldwide building industry. In Great Britain, 10% of aggregates are RCA, while Holland used 78,000 tons of RCA in 1994, and Germany has attempted to recycle 40% of building waste since 1991 (Oikonomou, 2005). Recycled concrete has also been used as an aggregate source, specifically a paving material, in the United States since the 1940s (Verian et al., 2013). In fact, U.S. Route 66 in Illinois was one of the first applications of RCA in concrete pavement mixtures (Epps et al., 1980). Approximately 100 RCA-incorporated concrete paving projects were identified in the 1990s, some of which included D-cracked and alkali-silica reaction-damaged recycled materials (Snyder et al., 1994).

Although RCA aggregates mostly performed well in previous projects, negative experiences have also been recorded. For example, RCA-jointed reinforced concrete pavements constructed with mesh-reinforced panels longer than 20 ft have been shown to quickly develop mid-panel transverse cracks that deteriorate rapidly due to inadequate aggregate interlock across the cracks because of RCA (Snyder, 2016). Undoweled RCA concrete pavements also have occasionally developed faulting more quickly than pavements with natural aggregates (Snyder, 2016). In addition, concrete properties and subsequent performance may be adversely affected by RCA (Verian et al., 2013). Because recycled aggregates consist of original aggregates and mortar, mortar quality and quantity influence the physical properties of recycled aggregates. The porosity of mortar depends on the water-to-cement ratio of the parent concrete. The crushing procedure and recycled aggregate size also influence the amount of mortar produced. Absorption capacity of recycled aggregates is one of the most critical RCA properties that influences properties of fresh and hardened concrete made from RCA. A limit of 30% coarse recycled aggregate has been suggested for structural concrete (Etxeberria et al., 2007).

2.3 Physical Properties of RCA

A considerable amount of research has evaluated physical properties of RCA, and almost all studies have suggested common RCA characteristics, as summarized in Table 2.1 and Table 2.2. RCA particles are comprised of reclaimed aggregates, reclaimed mortar, or both. Thus, properties of the parent concrete and the amount of reclaimed mortar affect RCA characteristics. Recycled mortar creates an increasingly porous system in the RCA, and the presence of mortar attached to RCA produces large areas of aggregate-cement paste interfaces known as the interfacial transition zone (ITZ). ITZ is the weakest area in concrete where potential failure may occur (Dastgerdi et al., 2019; Verian et al., 2013). As mentioned, the mortar in RCA is the primary factor that negatively impacts RCA performance. A high amount of mortar in RCA is usually associated with increased absorption capacity, decreased specific gravity, considerable plastic shrinkage, reduced particle strength, low abrasion resistance, and consequently high cracking rate in pavements with recycled aggregate. The RCA aggregates are relatively angular and rough-textured particles when obtained from concrete slab crushing processes (Verian et al., 2013).

Table 2.1: Typical Properties of Natural Aggregates and RCA
Source: Snyder (2016)

Property	Natural Aggregate	RCA
Absorption capacity (%)	0.8–3.7	3.7–8.7
Specific gravity	2.4–2.9	2.1–2.4
L.A. abrasion test mass loss (%)	15–30	20–45
Sodium sulfate soundness test mass loss (%)	7–21	18–59
Magnesium sulfate soundness test mass loss (%)	4–7	1–9
Chloride content (lb/yd^3)	0–2	1–12

Table 2.2: Typical Properties of Concrete with RCA Compared to Natural Aggregate Concrete

Source: Snyder (2016)

Property	Coarse RCA Only	Coarse and Fine RCA
Compressive strength	0%–24% lower	15%–40% lower
Tensile strength	0%–10% lower	10%–20% lower
Variability of strength	Slightly greater	Slightly greater
Modulus of elasticity	10%–33% lower	25%–40% lower
Coefficient of thermal expansion/contraction	0%–30% higher	0%–30% higher
Permeability	0%–500% higher	0%–500% higher
Specific gravity	0%–10% lower	5%–15 % lower

2.4 RCA Production

RCA is produced by crushing and sorting existing concrete into desired aggregate sizes. The recycling process typically entails primary and secondary crushing stages. In the primary crushing stage, jaw crushers provide optimal size distribution and reduce the material size to 3–4 inches. A secondary crushing obtains desired maximum coarse aggregate size and produces round, less angular particles (Silva et al., 2016). The three main types of crushers used in concrete recycling are jaw, cone, and impact. Each crushing process removes different amounts of mortar from the original aggregate particles. The type of crushing device used and the number of processing stages influence the size and shape of the resulting aggregates. The amount of mortar removal and final grain size distribution is also a function of the natural aggregate properties within the crushed RCA (Verian et al., 2013).

2.5 Common Applications of RCA

RCA can be a substitute for almost any conventional virgin aggregate. Because of the presence of reclaimed mortar, RCA is also useful in additional applications such as unstabilized (granular) base and subbase layers as well as cement-treated base layers. RCA has also been incorporated as the primary or only aggregate source in new concrete pavements. Other RCA applications in pavement construction include shoulders, median barriers, sidewalks, and curbs and gutters. RCA applications in building and bridge foundations and even structural concrete

have also been reported (Cavalline, 2022). In addition, RCA has been used successfully in new asphalt pavement and asphalt-stabilized base applications. Other applications of RCA include granular fill and erosion control (i.e., riprap). RCA usage has been suggested for soil stabilization, pipe bedding, landscape materials, railroad ballast, agricultural soil treatments (similar to soil modification using lime), treatment of acidic lake waters, trickling filters and effluent treatment, components of sulfur dioxide (SO_2) scrubbers, masonry block production, and artificial reefs to establish oyster beds (American Concrete Pavement Association, 2009).

2.6 Incorporation of RCA into Pavements

Although recycled concrete can be used for all pavement layers, the use of RCA in base and subbase layers is the most common usage (American Concrete Pavement Association, 2009). Of the 41 states that allowed RCA in highway applications in 2004, only Idaho, Maryland, and Oregon did not use RCA as base aggregate. Additionally, 15 states used RCA in a surfacing layer. Colorado, Idaho, Illinois, Michigan, Minnesota, North Dakota, South Carolina, Texas, Virginia, West Virginia, and Wyoming allowed RCA in portland cement concrete, while only Florida, Illinois, Louisiana, Michigan, Minnesota, Mississippi, Virginia, and Utah allowed RCA in hot-mix asphalt (HMA). The remaining states used RCA as "miscellaneous aggregate" (Federal Highway Administration [FHWA], 2004).
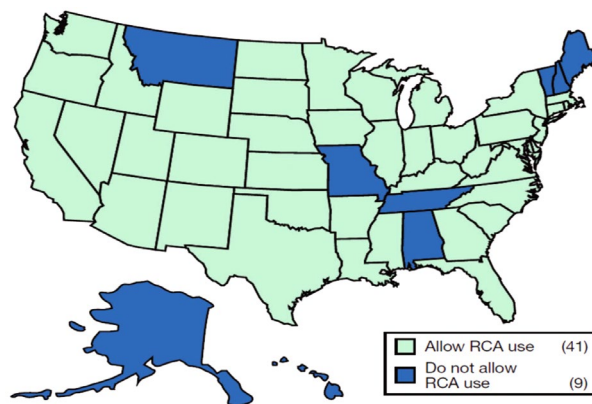
Figure 2.2: States' Usage of RCA in Pavement and Other Applications
Source: FHWA (2004)

7

2.7 Previously Damaged RCA in Paving Applications

RCA from D-cracked or pavements damaged from alkali-silica reaction (ASR) has been used in new paving projects. Two major projects, US-59 near Worthington, Minnesota, and I-80 in Wyoming, included severely D-cracked and ASR-damaged concrete pavements, respectively. The first project, built in 1980, was a jointed plain concrete pavement. Although transverse cracking and severe faulting developed, D-cracking did not occur. In the second project, done in 1985, successful measures such as the use of low-alkali Type II cement, the incorporation of high-quality virgin aggregates, and the use of Class F fly ash were taken to prevent the recurrence of ASR damage. In the project in Wyoming, ASR was not observed until 2015, approximately 30 years after reconstruction (Snyder, 2016).

In another RCA-focused study, Verian et al. (2013) claimed that concrete made with RCA from D-cracked pavement has F-T resistance performance identical to conventional concrete when aggregate size is limited to ¾". They also found that recycled concrete from ASR-damaged concrete shows minimal recurrence of ASR if precautions are taken, such as using low-alkali cement, because reclaimed mortar in RCA is inherently nonreactive. Therefore, concrete with processed RCA from ASR-damaged concrete should have less ASR potential than concrete containing virgin reactive siliceous aggregates.

2.8 Considerations in RCA Usage

The use of RCA in PCC pavement can lead to decreased strength, high permeability, and increased shrinkage potential. However, the use of pozzolanic materials such as fly ash reduces the high permeability caused by reclaimed mortar, resulting in more durable concrete. Reducing the mortar content by decreasing the size of RCA to less than its original aggregate size during production is another way to mitigate the effects of RCA. Studies have shown that an adjustment to mix design proportions also can compensate for changes in properties when using RCA in concrete. In addition, research has shown no significant impact on compressive strength and F-T resistance of concrete if up to 30% of coarse aggregate is replaced with RCA (Verian et al., 2013). The use of fine RCA in concrete mixtures has generally been associated with mixture workability

problems, reduction in strength and elastic modulus, and significant increases in volumetric instability due to the old mortar in RCA (Verian et al., 2013).

2.9 State DOT Requirements for RCA Usage

Specifications regarding the use of recycled materials vary widely from state to state. The five states with the greatest amount of recycled material usage are Texas, Virginia, Michigan, Minnesota, and California. These states strongly encourage the use of RCA in unbound pavement base/subbase courses (Westover et al., 2007). A national survey of RCA usage as granular material in pavement base and subbase layers was conducted by Rutgers University in 2008. Twenty-five states and one Canadian province responded to the survey that was distributed through the American Association of State Highway and Transportation Officials (AASHTO), as shown in Figure 2.3 (Bennert & Maher, 2008).

Figure 2.3: Participating States (shaded) in the AASHTO RCA Survey
Source: Bennert and Maher (2008)

Survey questions included RCA usage as a pavement material, specifications or practices for levels of permeability, material blending practices, use of filter fabric (if any), problems regarding RCA usage or permeability, and related ASR issues. A portion of the survey results are shown in Table 2.3 and Table 2.4. Eighteen of the 26 responses (69%) indicated use of RCA for pavement base courses, 12 (46%) for pavement subbase and base courses, eight (31%) for various material purposes, and five states do not use RCA at all. In addition, 15 agencies use RCA alone as a pavement layer material and six use a blend of RCA with other materials. Of the 18 respondents that use RCA alone, nine agencies use gradation to specify material properties; the rest of the agencies use criteria such as sand equivalent, F-T stability, composition, and durability with gradation to specify material properties. Finally, 13 respondents blend RCA with other materials. Two of these agencies specify a percentage of RCA to virgin material by weight, six use gradation, and the remaining five use criteria such as sand equivalent, F-T stability, composition, Atterberg limits, AASHTO A-1a, and durability in combination with gradation to specify material properties.

Survey responses showed a wide range of sources of RCA material for use in pavement base and subbase layers; however, most responses indicated that the sources were recycled concrete pavement and structures. Results also revealed that 20 of the agencies do not monitor RCA pavement performance. The six states that monitored RCA performance are Louisiana, Illinois, Nebraska, Ohio, Virginia, and Washington. Illinois and Virginia indicated no difference in performance when compared to virgin aggregates, while the remaining four states commonly identified pavement permeability as the main issue. Specifically, Louisiana and Nebraska address permeability by controlling the material specification (i.e., gradation). No state sets a permeability requirement for the base or subbase material or monitors the permeability of RCA when used in base or subbase layers. Finally, 10 of the responding states do not permit RCA with ASR; the states that accept RCA with ASR use it in their base or subbase materials but do not pretreat ASR-damaged RCA prior to pavement usage (Bennert & Maher, 2008).

Table 2.3: RCA Usage in Base or Subbase Layers by AASHTO Members

Source: Bennert and Maher (2008)

State	Base or Subbase?	Performance of pavements with RCA	ASR-damaged RCA Permitted?
Arizona	-		Yes
California	Both		Yes
Colorado	Both		Yes
D.C.	Base	Works good in areas with no groundwater problems	No
Florida	Base		
Georgia	Base		No
Hawaii	None		No
Illinois	Both	No difference seen.	Yes
Kentucky	Both		No
Louisiana	Both	Material specification compliance and good construction methods are dictating performance rather than choice of aggregate.	Yes
Maine	None		
Maryland	Base		Yes
Minnesota	Base		Yes
Nebraska	Not common	Great stability but poor permeability. Used coarser gradation of RCA, overall good performance, but more expensive. Thus not used as often.	Yes
Nevada	None		
Ohio	None	Looked at the material performance using F-T testing and found high breakdown of the materials as compared to virgin materials. Found high amounts of tufa and clogging of the drainage.	No
Oregon	Subbase		No
Tennessee	Both		No
Utah	Both		Yes
Virginia	Both	When used no difference is seen.	Yes
Washington	Both		No
West Virginia	None		-
Wyoming	Both		Yes
Ontario	Both		No

Table 2.4: Specifications for RCA Usage in Base or Subbase Layers by AASHTO Members

Source: Bennert and Maher (2008)

State	How used?	Material properties specification (used alone)	Material properties specification (used blended)
Arizona	Blended		Percent of RCA to virgin materials by weight, 50% max.
California	Blended		Gradation, up to 100% RCA allowed.
Colorado	Alone	Gradation	
D.C.	Alone	Gradation	
Florida	Alone	Gradation, Sulfate Soundness, LA Abrasion	Atterberg limits, stabilized subgrade of min. Bearing Ratio of 40.
Georgia	Alone	Gradation and Sand Equivalent	
Illinois	Alone	Gradation	Gradation and composition.
Kentucky	Alone	Gradation	Gradation.
Louisiana	Blended		Specified gradation in all uses, some uses allow blending, some don't. LA abrasion, Sulfate Soundness testing.
Maryland	Alone	Gradation, LA, Modified Proctor, pH	
Minnesota	Blended		Gradation.
Nebraska	Alone	Gradation	
Oregon	Alone	F-T stability, Gradation	Gradation.
Tennessee	Alone	Gradation	
Utah	Alone/Blended		All virgin aggregate requirements, A-1a, NP, wear, soundness.
Virginia	Alone/Blended	Allows crushed concrete alone or blended	20% min.
Washington	Alone/Blended	Should meet all the specs for the specific use	Should meet all the specs for the specific use.
Wyoming	Blended		Percent of RCA to virgin material by weight, 50% avg.
Ontario	Alone	Gradation	

2.10 Soil Stabilization

Soil stabilization refers to techniques to treat and improve the engineering properties of unsatisfactory natural soil for a specific use (Yoder & Witczak, 1975). For pavement purposes, soil stabilization is used in poor subgrade conditions, for dust or moisture control, and to salvage old roads (Yoder & Witczak, 1975). Soil stabilization methods are categorized as mechanical, physical, chemical, biological, and electrical treatments (Latifi et al., 2016). Selection of the desired method for highway subgrade soil stabilization depends on soil properties, economic benefits, and conditions of the project, and benefits resulting from soil stabilization provide economic justification for the process (Banda, 2003; Yoder & Witczak, 1975).

Mechanical stabilization, which is the process of physically changing soil properties to enhance soil-particle interlock and to produce desirable engineering characteristics, is accomplished through compaction or blending and is typically implemented to improve strength or plasticity (Banda, 2003; Jones et al., 2010). Sufficient strength can often be achieved through additional compaction. For example, an exceptionally heavy roller can be used to help pavements meet subgrade design requirements on certain subgrade materials. Compaction enhances aggregate interlock, thereby reducing air-void content, pore connectivity, and subsequent moisture susceptibility. Blending is defined as the mixing of materials with different properties, typically particle size distribution or plasticity, to form a material with improved characteristics. Blending often involves adding coarse aggregates to fine in-situ material (Jones et al., 2010).

Polymer-manufactured products such as geotextile fabrics, geogrids, and geocells are often used to improve subgrade soil properties when stabilizing with geosynthetics (Banda, 2003). Geosynthetics, which are placed between the pavement structure and the subgrade (typically untreated), offer temporary or long-term improvement because they enhance the structural integrity of pavements (Jones et al., 2010). Geosynthetics specifically allow drainage within the pavement structure without loss of finer subgrade particles. The Kansas Department of Transportation (KDOT) sometimes uses a geosynthetic under a granular base to prevent lateral movement of fine aggregates and allow water to drain.

Chemical stabilization requires the addition of selected stabilizers to the soil, resulting in a chemical reaction and consequently improving or modifying the soil's physical properties (Banda,

2003). Chemicals that can be used for soil stabilization include cementing agents, modifiers, waterproofing agents, water retaining agents, water retarding agents, and miscellaneous chemicals. Cementing agents used for soil stabilization principally include portland cement, lime kiln dust in combination with portland cement, cement kiln dust, lime, fly ash, and bitumen (Yoder & Witczak, 1975).

Stabilizers can be categorized into three groups based on the mechanism of stabilization. Stabilizers such as hydrated lime, portland cement, and fly ash are one group, while byproduct stabilizers such as cement kiln dust, lime kiln dust, and other forms of byproduct lime comprise another group. These two stabilizer groups are considered traditional admixtures, which means they rely primarily on calcium exchange and pozzolanic reaction to stabilize soil. The third group of stabilizers are nontraditional stabilizers, including sulfonated oils, potassium compounds, ammonium chloride, enzymes, and polymers. These materials rely on a mechanism that differs from traditional stabilization. However, due to uncertainties associated with the use of nontraditional stabilizers and performance limitations on comparative test programs, traditional stabilizers such as lime and portland cement are the most commonly used admixtures (Petry & Little, 2002).

2.11 Cement for Soil Stabilization

Portland cement has been successfully used for base course and subbase course stabilization. Although granular soil, silty soil, and lean clays are able to be stabilized using portland cement, cement is not suitable for the stabilization of organic materials or soils subject to seasonal frost heave (Maher et al., 2005; Yoder & Witczak, 1975). Properties of soils stabilized with portland cement demonstrate increased strength, decreased compressibility, reduced swell potential, and increased durability due to cement stabilization. A hard-bound, impermeable layer is formed as the result of soil-cement stabilization (Maher et al., 2005). Although portland cement is most commonly used for base courses due to the effective strength gain of soil-cement mixtures, such stabilization is rarely used for surfacing due to the brittle nature of cement-stabilized materials, which increases surface-layer susceptibility to cracking under traffic loads (Yoder & Witczak, 1975; Maher et al., 2005).

2.11.1 Mechanism of Soil-Cement Stabilization

Portland cement is comprised of tricalcium silicate ($3CaO.SiO_2$), dicalcium silicate ($2CaO.SiO_2$), tricalcium aluminate ($3CaO.Al_2O_3$), and tetra calcium aluminoferrite ($4CaO.Al_2O_3.Fe_2O_3$). Cementitious products are produced as these components come into contact and react with water. The following reactions occur between water and portland cement components (Banda, 2003):

$$2(3CaO.SiO_2) + 6H_2O \rightarrow 3CaO.2SiO_2.3H_2O + 3Ca\,(OH)_2$$

$$2(2CaO.SiO_2) + 4H_2O \rightarrow 3CaO.2SiO_2.3H_2O + Ca\,(OH)_2$$

And consequently,

$$3CaO.Al_2O_3 + 12H_2O + Ca\,(OH)_2 \rightarrow 3CaO.Al_2O_3.Ca\,(OH)_2.12H_2O$$
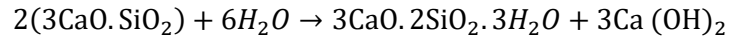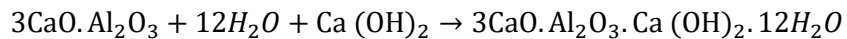
Calcium silicate hydrate (CSH), $3CaO.2SiO_2.3H_2O$, and calcium aluminate hydrate (CAH), $3CaO.Al_2O_3.Ca(OH)_2.12H_2O$, are the primary cementitious products. The hydration of cement products produces calcium ions, and the subsequent cation ion exchange with soil particles causes flocculation and agglomeration of the soil. Flocculated soil particles are stabilized with produced cementitious materials (CSH and CAH). Calcium hydroxide formed from cement hydration is more reactive than ordinary lime, and when dissociated from cement hydration, the calcium hydroxide provides free calcium that reacts with pozzolans, or finely divided siliceous or siliceous/aluminous materials that form cementitious products when mixed with water and lime. The reaction of pozzolans in clay with calcium forms more CSH and CAH, a reaction known as a pozzolanic reaction. Details of pozzolanic reaction are as follows (Banda, 2003):

$$Ca^{++} + OH^- + silica\ from\ clay\ (SiO_2) \rightarrow CSH$$

$$Ca^{++} + OH^- + Alumina\ from\ clay\ (Al_2O_3) \rightarrow CAH$$
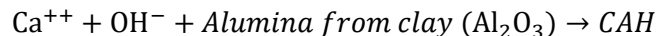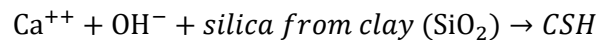
The additional CSH and CAH are secondary cementitious materials produced from the pozzolanic reaction with clay. Further strength is achieved from these secondary products because they glue the flocculated clay particles to their point of contact. Pozzolanic reaction can continue for months or even years after mixing as long as the calcium, soluble silica, and alumina are present. Stabilized clay gains more long-term strength with increased curing time and additional pozzolanic reactions. However, cementitious strength (short-term) of primary CSH and CAH is much stronger than the secondary products (Banda, 2003).

2.11.2 Soil-Cement Mixture Design

Mix design procedure depends on the desired engineering properties after stabilization (Banda, 2003). The Portland Cement Association (PCA) has developed requirements for AASHTO soils A-1 to A-7 to determine the durability of soil-cement mixtures based on maximum weight losses under wet-dry (ASTM D559) and F-T (ASTM D560) tests. However, due to decreased required time and increased availability of equipment and trained technicians, many state DOTs currently define minimum unconfined compressive strength (UCS) (ASTM D1633) as the requirement for soil-cement stabilization instead of durability testing. However, durability is not guaranteed even if a specified strength is achieved (Petry & Little, 2002).

The design process to attain certain strength requirements based on the reviewed literature first requires the classification and gradation of untreated soil according to current ASTM standards. Second, the estimated cement design content must be selected using available guidelines. The PCA requirement for cement selection based on soil classification is the most common source found in the literature, as shown in Table 2.5. Third, the design process requires the execution of moisture density tests (standard or modified Proctor) and control mixture strength via UCS tests (Kestler, 2009; Banda, 2003). This procedure could be followed for any type of chemical stabilizer, with the primary difference in procedure being the estimated initial binder percentage.

Table 2.5: Cement Requirement for Stabilization Based on AASHTO Soil Groups
Source: Little and Nair (2009); PCA (1992)

AASHTO Soil Group	Usual Range in Cement Requirement		Estimated Cement Content
	% by Volume	% by Weight	% by Weight
A-1-a	5–7	3–5	5
A-1-b	7–9	5–8	6
A-2	7–10	5–9	7
A-3	8–12	7–11	9
A-4	8–12	7–12	10
A-5	8–12	8–13	10
A-6	10–14	9–15	12
A-7	10–14	10–16	13

2.12 Fly Ash for Soil Stabilization

The combustion of coal in electric power plants produces finely graded particles known as fly ash. These particles generally are spheres ranging in size from 0.01 μm to 100 μm (Ozdemir, 2016). Fly ash is a pozzolan that primarily consists of silicon, aluminum, iron, and calcium oxides and is classified as either Class F or Class C. According to ASTM C618, *Standard Specification for Coal Fly Ash and Raw or Calcined Natural Pozzolan for Use in Concrete*, when the sum of $SiO_2+Al_2O_3+Fe_2O_3$ is a minimum 50%, fly ash is classified as Class C; when the sum of $SiO_2+Al_2O_3+Fe_2O_3$ is greater than 70%, it is classified as Class F fly ash (Banda, 2003). Class F fly ash has pozzolanic properties, whereas Class C fly ash has pozzolanic and cementitious properties. Class C fly ash, the most popular type of fly ash for soil stabilization in the Midwest, is also known as a high calcium fly ash because it typically contains more than 10% CaO and has a self-cementing property (in the presence of water) due to its high lime (CaO) content (Banda, 2003). The reaction of CaO with the pozzolans (SiO_2, Al_2O_3, Fe_2O_3) in the presence of water forms cementitious materials that bind inert material together (Ozdemir, 2016). The mechanism of forming cementitious materials is as follows (Tastan et al., 2011; Banda, 2003):

$$CaO + H_2O \rightarrow Ca\,(OH)_2$$
$$Ca\,(OH)_2 \rightarrow Ca^{++} + 2OH^-$$
$$Ca^{++} + OH^- + silica\ from\ clay\ (SiO_2) \rightarrow CSH$$
$$Ca^{++} + OH^- + Alumina\ from\ clay\ (Al_2O_3) \rightarrow CAH$$
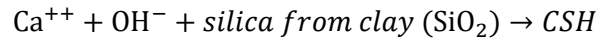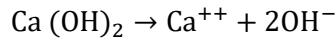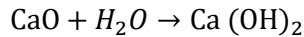
Fly ash can be used in highway construction to enhance strength properties and control shrink-swell properties of expansive soils (Zha et al., 2008). It also acts as a drying agent to reduce soil moisture to permit compaction. The primary reasons for using fly ash in soil stabilization are to improve the compressive and shear strength of soils and stabilize silt-sized particles that are likely to become unstable in the presence of moisture. Although the self-cementitious properties of Class C fly ash allow it to be used as a stand-alone material, a cementitious agent (i.e., lime, lime kiln dust, cement kiln dust, or cement) is needed when using Class F fly ash in soil stabilization. The plasticity of soils treated with Class C fly ash is influenced by the type of clay minerals present in the soil and the soil-adsorbed water. Fly ash may cause excessive swelling if

more than 10% sulfates exist in the soil. In addition, organic soils are difficult to stabilize using fly ash (American Coal Ash Association, 2003).

2.13 Lime

Burned limestone ($CaCO_3$), calcium oxide (CaO), or calcium hydroxide ($Ca(OH)_2$) products are often used to stabilize soil, although quick lime (CaO) is a more effective stabilizer than hydrated lime. Soils with plasticity indexes ranging from 10 to 50 usually react and can be stabilized with lime, but a pozzolan is required for soils with a plasticity index less than 10. Fly ash has been commonly used with lime to stabilize those soils. Heavy clays also may be effectively stabilized with lime. Among various clay minerals (i.e., montmorillonite, kaolinite, illite, chlorite), montmorillonite is most reactive with lime (Bell, 1993).

Lime stabilizes soils in two ways. The first process utilizes cation exchange in which divalent calcium ions (Ca^{++}), provided by the addition of lime to clay soil, replace weaker monovalent ions such as sodium (Na^+) or potassium (K^+) on the surface of clay particles. The pH of the soil also increases with the addition of lime, causing accelerated cation exchange, resulting in the flocculation and agglomeration of clay soil. The second process is the pozzolanic reaction of Ca^{++} with clay pozzolans, as described in Section 2.11.1.

2.14 UCS Requirement for Chemical Soil Stabilization

The PCA and the United States Army Corps of Engineers (USACE) methods are the most common methods for stabilized layer design. These methods consider the UCS of the stabilized mixtures to be their primary design criteria; however, no minimum UCS value has been universally agreed upon by highway agencies (Guthrie et al., 2002). Table 2.6 summarizes a literature review of used/proposed UCS for stabilized layer design.

18

Table 2.6: Minimum UCS of Stabilized Soil with Various Stabilizers

Reference	Cement (psi)	Lime (psi)	Fly ash or combination with cement (psi)
Bell (1993)	406, 7 days	-	-
Gomez and Anderson (2012)	250, 7 days	-	-
Kestler (2009)	250, 7 days	250, 28 days	250, 28 days
Danyluk (1986)	250, 7 days	-	-
USACE (1994) Rigid Pavements	200, 7 days	200, 28 days	200, 28 days
USACE (1994) Flexible Pavements	250, 7 days	250, 28days	250, 28 days
Little and Nair (2009)	200–400, 7 days (clay soil)	Base-Subbase layer (Min=50, Max=200)	-
Petry and Little (2002)	203–760, no age specified	230–290, after 24 h capillary soak	-
Maher et al. (2005)	125–500, no age specified	100–400, no age specified	100–510, no age specified
KDOT (2007)	-	Min 5% of the soil weight	Only Class C allowed (fly ash with UCS > 500 psi.)

2.15 RCA Usage for Subgrade Soil Stabilization

Chemical or mechanical techniques, or a combination of both, are often used to stabilize subgrade soil. For example, pavements in Australia are typically stabilized with coarse aggregate, stabilizer (e.g., cement), and pozzolans (e.g., clay) (Chakrabarti & Kodikara, 2003). Although natural aggregates have been extensively used for mechanical stabilization of subgrade soil, to date there is little known work on the application of RCA for subgrade soil stabilization.

Arulrajah et al. (2012) characterized five recycled construction and demolition materials in terms of their basic properties, shear strength parameters, resilient modulus (M_r), and permanent deformation. RCA was found to have geotechnical properties equivalent or superior to typical quarry subbase materials. Poon and Chan (2006) showed that use of RCA increases the optimum moisture content (OMC) and decreases the maximum dry density (MDD) of subgrade materials. California Bearing Ratio (CBR) values (unsoaked and soaked) of subbase materials prepared with 100% RCA were lower than CBR values of natural subbase materials. Cabalar et al. (2017)

evaluated mixtures of 0%, 10%, 20%, 30%, 40%, 50%, and 100% clay and RCA and concluded that the addition of clay into all gravel-sized RCA materials increases the OMC of RCA. The MDD value of the clay-RCA mixtures prepared at OMC increased up to a certain content of clay and then decreased. Cabalar et al. (2017) concluded that adding any percentage of clay to the RCA increased energy absorption, potentially enhancing pavement response to severe dynamic loads.

2.16 D-Cracking

D-cracking is a form of concrete pavement deterioration that originates in the coarse aggregate particles. A series of slightly inclined cracks start at the bottom of the slab and propagate upward. D-cracking appears on the pavement surface as a series of closely spaced cracks that sever the coarse aggregate generally parallel to transverse and longitudinal joints and pavement free edges, as shown in Figure 2.4.

Figure 2.4: Development of D-Cracking Along Joints
Source: Schwartz (1987)

2.16.1 Mechanism of D-Cracking

The development of hydraulic pressures in aggregate pores and concrete causes internal damage and D-cracking. Cracks originate in coarse aggregates due to excessive pressure generated by water infiltrated from joints and existing moisture beneath the pavement. If pressure in saturated coarse aggregates surpasses the internal strength of aggregate, then cracks initiate. Existing cracks become wider with continued freezing and thawing, consequently causing excessive pressure.

These cracks can eventually progress to the surface. Figure 2.5 shows crack formation in coarse aggregates.
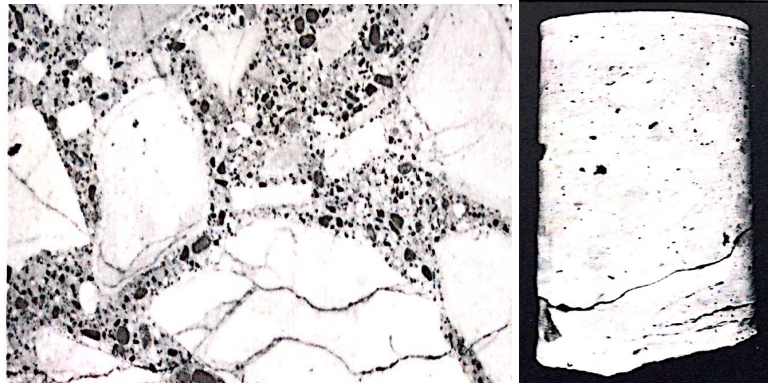
Figure 2.5: D-Cracking in Coarse Aggregates with Crack Initiation from Bottom
Source: Schwartz (1987)

The basic mechanism by which excessive pressure develops in coarse aggregates is not well understood. However, all proposed theories recognize moisture, F-T cycles, and excessive pressure building within some coarse aggregates, especially sedimentary aggregates, as primary contributors to D-cracking (Schwartz, 1987).

2.16.2 Factors Influencing D-Cracking Development

Considerable research has identified factors that influence the development of D-cracking in pavements. Noted factors include environmental conditions, aggregates (coarse or fine), cement, pavement design, traffic, and drainage. Environmental conditions such as repeated F-T cycles and degree of saturation affect D-crack development. The degree of saturation is critical since bridge decks do not develop D-cracking because slabs are not regularly exposed to free water and are permitted to dry periodically. Coarse aggregates with D-cracking potential are the primary reason for D-cracking. Factors such as pore structure composition, sorption (absorption-adsorption), particle size, and bulk specific gravity have been shown to influence D-cracking potential in coarse aggregate. Particle size has also emerged as a definite cause of D-cracking in all research, although the type of fine aggregate and amount of cement do not have any significant effect on D-cracking (Schwartz, 1987). Research has proven that pavement design alone is unable to prevent D-cracking,

although an adequate underdrain system could effectively reduce the rate of D-cracking development. Traffic characteristics do not contribute to the initiation of D-cracking, but high traffic volumes and heavy loads accelerate deterioration (Schwartz, 1987).

2.16.3 Laboratory Methods to Determine D-Cracking Susceptibility

As mentioned, the development of D-cracking in concrete pavements primarily depends on the coarse aggregate in a concrete mixture. Therefore, the first step in identifying the D-cracking potential of susceptible aggregates is to identify susceptible coarse aggregates using two groups of test methods. The first group of tests correlates aggregate properties with field performance, while the second group simulates the concrete pavement service environment and predicts concrete performance by conducting tests on aggregates or concrete specimens. Tests on concrete specimens are assumed to have better correlation with field performance because coarse aggregates behave differently when enclosed in mortar than in "bare" condition when subjected to freezing and thawing. Aggregate property tests include sorption tests, the Iowa pore index test, and the mercury porosimeter test. Environmental simulation tests include rapid F-T tests, the powers critical dilation test, and a single-cycle slow freeze test (Schwartz, 1987).

2.16.4 Countermeasures to Prevent or Minimize D-Cracking

Current consensus is the only way to completely prevent D-cracking is to eliminate D-cracking-susceptible coarse aggregates in concrete mixtures. Other methods can slow the rate of deterioration, but they do not eliminate D-cracking. However, reducing the maximum size of coarse aggregates can significantly increase D-cracking resistance. If nondurable aggregates must be used, size reduction is the most effective approach for strengthening their application. Other methods include blending susceptible aggregates with durable aggregates and beneficiating potentially harmful aggregates via separation of aggregates based on specific gravity. Material and construction specifications set limits on the maximum size of certain aggregates and the amount of such aggregates, or they eliminate them entirely. Certain aggregate characteristics can also be restricted, such as specific gravity, but a combined field and laboratory test program is required. Performance history of aggregate sources should be monitored, and susceptible sources must be identified and rejected if necessary. For mixture design, blending durable aggregates with mineral

aggregates, ensuring adequate air entrainment (to increase frost resistance of the concrete), and increasing the proportion of fine aggregates can minimize D-cracking. In Kansas, D-cracking is controlled primarily by limiting the use of limestone coarse aggregates, which are believed to be the primary cause of D-cracking (Schwartz, 1987).

2.17 Shrinkage Cracking

Shrinkage cracking is a major issue associated with chemically stabilized materials in pavement construction. Shrinkage cracks usually initiate as single isolated cracks that propagate to form multiple cracks, especially under traffic loads. Pavement performance is negatively affected by shrinkage cracks due to a reduction in the overall stiffness of the pavement structure. If shrinkage cracking occurs on the surface layer, water infiltration into underlying layers and erosion of stabilized materials through the formed pathways become concerns. The adverse effects of shrinkage cracks can be mitigated by regular crack sealing, but this mitigation results in increased maintenance costs and lower ride quality (Kodikara & Chakrabarti, 2001). The problem of reflected shrinkage cracking from a treated subgrade or subbase through an overlying untreated base layer into surface layers is a significant concern in stabilized base materials. To minimize negative effects and ensure a uniform stable platform for pavement structure, the possibility of shrinkage cracking must be considered from the early stage of mix design (Kodikara & Chakrabarti, 2001; Jones et al., 2010). Severe shrinkage cracking may be prevented by pre-cracking cementitious stabilized materials after final compaction, compacting the layer at the lowest possible moisture content with the required density and strength (not applicable for all mixtures), and curing the layer correctly (Jones et al., 2010).

Drying shrinkage is defined as observed strain developed with the loss of moisture (Guthrie et al., 2002). Although various processes contribute to drying shrinkage, moisture loss during dehydration is the most prevalent process. In this process, suction develops in the pore water as a result of moisture loss, bringing the solid particles together and causing shrinkage cracking. Development of this suction (i.e., matric suction) depends on pore size distribution of the solid particles. Another form of suction, osmotic suction, develops due to the chemical gradient between

pore water and adsorbed water in particles. The contribution of osmotic suction to shrinkage is less significant than the matric suction (Guthrie et al., 2002).

2.18 Mechanism of Shrinkage in Stabilized Clay-Aggregate Mixtures

Clay-aggregate-cement mixture shrinkage is influenced by the shrinkage of each component and combination of components. Hydrated lime is produced due to the instant hydration reactions of cement with water in the soil, followed by secondary reactions of hydrated lime and clay that produce secondary products via cation exchange and flocculation-agglomeration. These reactions improve moisture stability and soil strength, and the increased interparticle bond of soil reduces moisture susceptibility (Kodikara & Chakrabarti, 2001). Shrinkage of a soil-cement mixture initially decreases due to clay stabilization. After reaching a minimum, however, shrinkage increases when additional cement is added to the mixture (George, 1968). The increased shrinkage may be due to increased hydration of cement gel particles, which causes more shrinkage. However, shrinkage of clay-aggregate-cement mixtures has been shown to be less than shrinkage of clay-cement mixtures (Kodikara & Chakrabarti, 2001; George, 1968).

Similarly, tensile stresses can develop due to drying shrinkage of stabilized mixtures that are restrained from free movement, as is the case for most field conditions. When tensile strength of the material is less than the developed tensile stresses, material fracture or macrocracking occurs. Macrocracks may significantly reduce the stiffness of the stabilized pavement layers.

Although the most common methods for the design of stabilized layers, the PCA and USACE methods, are based on strength and durability requirements, most state DOTs focus only on compressive strength (Guthrie et al., 2002). Highway agencies share little consensus regarding the selection of a minimum strength requirement. While low cement contents have been shown to improve the long-term performance of stabilized layers, some highway agencies have adopted high strength requirements, resulting in unsatisfactory pavement performance. For example, the Texas DOT has shrinkage cracking on thousands of highway miles with cement-stabilized base layers designed to reach 700 psi (Guthrie et al., 2002). Based on PCA (1956), a 7-day UCS of 300–400 psi provides higher bearing capacity, durability, and shrinkage properties. For general subgrade improvement, a soaked UCS between 30 and 60 psi is considered sufficient. Any attempt to

achieve higher strength than target project strength requirements could be a waste of stabilizer and potentially lead to shrinkage-related problems. In fact, stabilizer contents above 4% of the dry soil weight may be uneconomical and, depending on soil properties, lead to complications related to shrinkage (Jones et al., 2010).

Little (1998) suggested that the shrinkage properties of lime-stabilized materials are directly related to the ultimate strength and ultimate modulus of the mixtures. To successfully distribute traffic loads without damaging the pavement structure, the stabilized layer should be stiff but not too rigid to cause excessive shrinkage cracking. Therefore, a range of acceptable values should be determined for resilient modulus (M_r) or UCS for pavement design. By establishing target limits on UCS and M_r, the level of shrinkage cracking and fracture damage in stabilized bases could be controlled. A range of values of back-calculated (from field falling weight deflectometer (FWD) testing) M_r values, typically 30,500–508,000 psi, were found to be structurally effective for load distribution but not so stiff as to induce excessive shrinkage cracking distress (Little, 1998). Pavement modulus could be approximated by the UCS-M_r relationship, as shown in Figure 2.6.
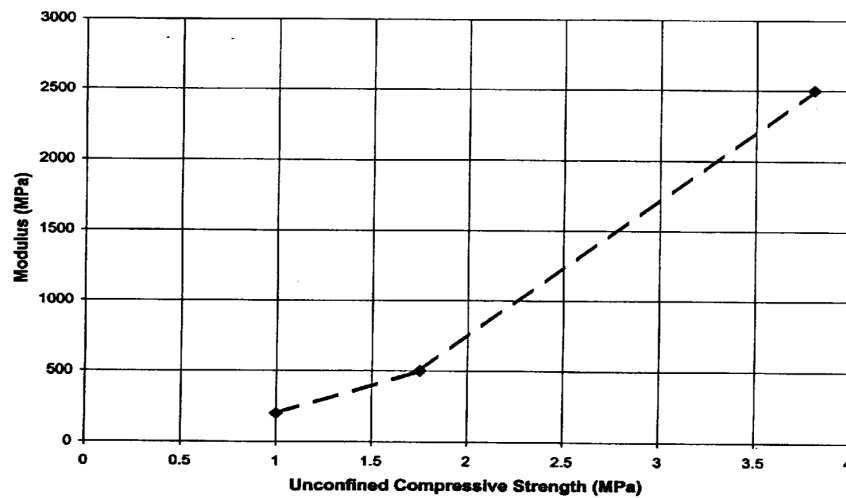
Figure 2.6: Design Relationship between UCS and M_r for Lime-Stabilized Subgrade Pavement Layers
Source: Little (1998)

2.19 Evaluation of Shrinkage Cracking

The shrinkage cracking of soil-cement mixtures is a function of binder content, strength, and drying shrinkage. Various laboratory test methods are available for evaluating potential shrinkage cracking.

2.19.1 Evaluation of Binder Content, Strength, and Shrinkage

George (1968) studied 12 soils containing various amounts of kaolinite and montmorillonite clay. Beam samples sized 3 inches × 3 inches × 11.25 inches were prepared based on the ASTM standard for making and curing soil-cement compression and flexure tests. Cement requirements for mixtures were evaluated via F-T test (ASTM D560), and linear shrinkage of mixtures with 3%–10% cement was measured at certain intervals. Total shrinkage was found to be a function of the type and amount of clay, compaction effort, mixing temperature, and molding moisture. Moisture had the most impact on shrinkage. Kaolinite soil-cement mixtures showed a faster shrinkage rate than montmorillonite soil-cement mixtures. In addition, the conclusion was made that shrinkage of clay soil is primarily a function of the fine fraction in the soil, while hydrated cement paste is the main cause of shrinkage in sands and sandy soils. Compaction at high densities significantly reduced shrinkage, but shrinkage increased with increased mixing temperatures. Shrinkage of mixtures first decreased with increased cement content but then increased after reaching a minimum. Discovery of an optimum cement content that would result in a minimum amount of shrinkage was suggested. The optimum cement content for minimum shrinkage of all soils was lower than the cement content required to make durable soil-cement based on the F-T tests.

Bhandari (1973) evaluated the effect of factors such as curing period, degree of saturation, cement content, and dry density on shrinkage during moist curing of cement-stabilized soils. A cement-stabilized soil containing 40% kaolinite clay and 60% sand was selected and studied. Samples cured for 84 days showed two behavior zones with respect to the curing period. Behavior change was observed at the 7-day point. A relatively large proportion of shrinkage occurred at very early stages of curing, but no extensive cracking developed in that period. Cement content did not have any effect on moist-cured shrinkage for the selected cement-stabilized mixture.

Rawlings et al. (1988) assessed the influence of cement content and material characteristics on drying shrinkage. Results of laboratory tests, shown in Figure 2.7, were related to the performance of recently constructed cement-treated pavements in southeast Queensland. Two materials, a natural soil aggregate material (material A) and a crushed soil aggregate material (material B), were used in the study. Material A had a high plastic fines content, which represented a poor-quality paving material, while material B had a low fine (low plasticity) content, which represented a quality paving material. Results of the laboratory study and field observations identified clay particles (specifically mineralogy with high plasticity, such as smectite) as the primary contributors to the shrinkage mechanism of cement-treated materials. The study also showed that sufficient cement must be provided to achieve adequate pavement strength and erosion resistance. The researchers investigated cement contents of 2%, 3%, 4%, and 5%, noting that additional cement may further improve results. Increased cement content increased the strength, elastic modulus, and abrasion resistance of pavement mixtures. Shrinkage increased slightly for high cement contents.
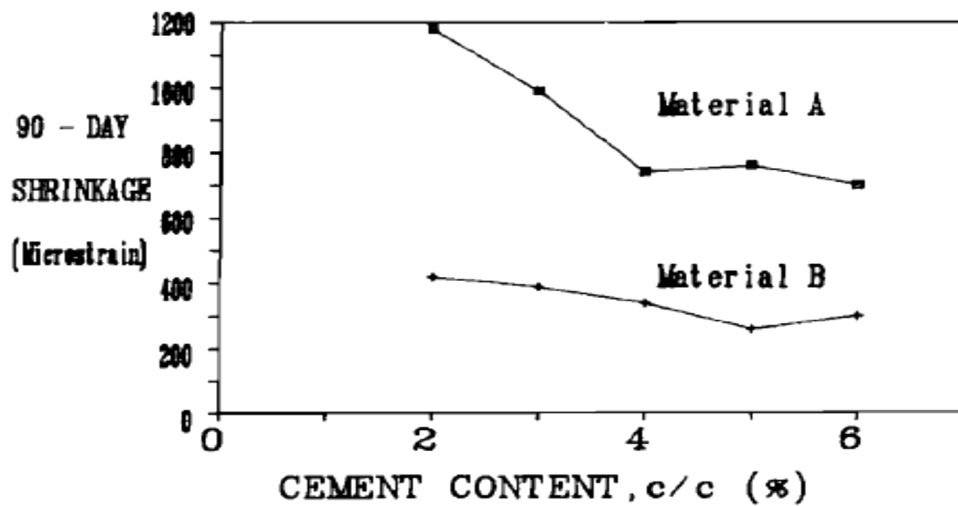
Figure 2.7: 90-Day Shrinkage versus Cement Content
Source: Rawlings et al. (1988)

Walker (1995) studied the effects of soil characteristics and cement content on the physical properties of stabilized soil blocks. A range of modified soils with a broad spectrum of plasticity characteristics were formed using mixtures of clay and river sand. Soil-cement blocks were

compacted, cured for 28 days, and then tested, as shown in Figure 2.8. Saturated and dry UCS were determined, and drying shrinkage of blocks was measured. A shrinkage limit of 0.1% was proposed for the soil-cement blocks. Based on the results, durability and strength improved by an increase in cement content, and the plasticity index had more impact on shrinkage than cement content. A cement content of 5%–10% was recommended for use in soil-cement blocks when the plasticity index was between 5 and 15. Walker (1995) added that cement stabilization with manual presses is not appropriate when the plasticity index is above 20–25 range.

Figure 2.8: Test Sample and Setup for Shrinkage Testing
Source: Walker (1995)

Guthrie et al. (2002) evaluated compressive strength, shrinkage, durability, and moisture susceptibility of cement-aggregate mixtures with three levels of Type I portland cement. Two types of aggregates, limestone and recycled concrete, were used, and samples were treated with 1.5%, 3.0%, and 4.5% cement. Tests included a compressive strength test (Tex-120-E), a developed linear shrinkage test, the South African wheel tracker erosion test (durability assessment), and a tube suction test (moisture susceptibility). Rectangular beam samples of 3 inches × 3 inches × 18 inches were tested for linear shrinkage. An Australian specification was used to judge sample performances. Based on the Australian standard, shrinkage strain should not exceed 0.000250 inches/in. after 21 days. Limestone samples that were tested for shrinkage at 50% relative humidity (RH) experienced shrinkage that exceeded the specified maximum limit in all cases. In addition, shrinkage strain increased with increased cement content. For recycled aggregates tested at 100%

RH, drying shrinkage decreased by increasing cement content from 1.5% to 3%. However, drying shrinkage increased after another 1.5% increase in cement content.

Based on the results of strength, durability, and moisture susceptibility, the use of 3% cement for stabilizing limestone and 1.5% cement for recycled concrete was suggested.

Chakrabarti and Kodikara (2003) investigated the properties of locally stabilized pavement materials. Laboratory testing evaluated UCS, shrinkage cracking, and capillary behavior of crushed basaltic rocks stabilized with cement and lime binders. The UCS of the mixtures, which was a function of binder quantity, increased significantly with increased binder content. Linear shrinkage was measured according to Australian standard AS 1289.3.4.1-1995. Shrinkage decreased for up to 4% cement content and then increased. As shown in Figure 2.9, the rate of drying shrinkage was high early in the study but steadied after 21 days.
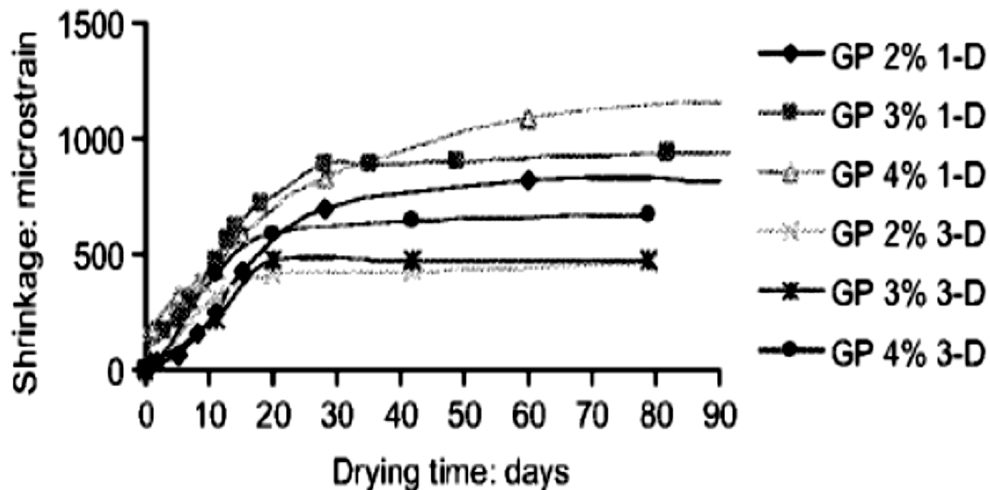
Figure 2.9: Drying Shrinkage over Time
Source: Chakrabarti & Kodikara (2003)

2.19.2 Shrinkage Testing of Stabilized Clay-Aggregate Mixtures

No standard procedure currently exists for shrinkage testing of soil-aggregate stabilized mixtures, so researchers have used standard methods to evaluate linear shrinkage of concrete or have followed modified methods based on regional needs or material. George (1968) conducted a study to determine factors that affect shrinkage and associated cracking mechanism. Twelve soils

29

represented a range in size and mineralogy, including kaolinite and montmorillonite clays. Soil-cement mixtures at various cement contents were prepared, and linear shrinkage of the molded soil cement beams was measured. The research procedure first approximated the cement content requirement via F-T tests in accordance with ASTM D560-57. Specimens above and below the minimum requirement were then investigated for shrinkage testing. A minimum of two beams, each measuring 3 inches × 3 inches × 11.25 inches, were prepared. Immediately after molding, specimens were stored at 100% RH at 72 ± 4 °F for 1–28 days. Upon completion of moist curing, the beams were air dried at 72 ± 4 °F and 55% RH, and a dial gauge comparator (precision up to 0.0001 inches) was used to measure linear shrinkage. Length change and weight, the principal measurements, were taken periodically during curing. Shrinkage was expressed in percentage based on the nominal length of samples (11.25 inches).

Guthrie et al. (2002) performed shrinkage testing of beam samples for two sources of cement-stabilized aggregates: virgin limestone aggregates and 100% RCA. Cement levels were 1.5%, 3%, and 4.5%, and no replicate samples were tested due to limited materials. Beams with dimensions of 3 inches × 3 inches × 18 inches were constructed in three lifts inside a metal form, with each lift compacted by 56 blows of a 10-lb hammer dropped from a height of 18 inches. Samples were removed from the form after curing in an environmental chamber maintained at 100% RH and 77 °F. Metal gauge studs were glued onto the ends of the samples with epoxy to facilitate shrinkage measurements over the following 21 days. Specimens of limestone aggregates were tested at 50% RH and 72 °F. Since limited RCA was available, the samples made for F-T testing were also used for shrinkage testing and kept at 100% RH for the duration of testing. The Australian specification that shrinkage strain should not exceed 0.000250 inches/in. after 21 days was followed. Only one RCA mixture with 3% cement passed the requirement.

Chakrabarti and Kodikara (2003) evaluated the performance of crushed basaltic rock stabilized with various types and quantities of cementitious materials. Drying shrinkage tests for basaltic crushed rock stabilized mixtures were performed according to Australian standard AS 1012.13-1992. The known quantity of stabilized mix was compacted in two layers into a rectangular steel mold measuring 3 inches × 3 inches × 11 inches. A standard Proctor hammer was used to compact the materials. Two gauge studs were placed at the center of the end sections during

compaction to facilitate shrinkage measurement. Duplicate specimens were cured for 24 hours at 90% RH or above and an air temperature of 21–24 °C. The specimens were subsequently dried at 50% RH and air temperature of 22 °C. A horizontal length comparator with a digital micrometer capable of measuring at least 0.001 mm was used to measure initial length of the specimen according to AS 1012.13-1992. Specimen lengths were recorded at gradually increasing intervals for up to 90 days while the specimens were kept in a controlled environment of 22 °C and 50% RH. Shrinkage in microstrain was calculated at the specific times.

ASTM C157 (2017), the test method commonly followed to measure the shrinkage of soil cement mixtures, determines length changes in hardened hydraulic cement mortar and concrete specimens made in the laboratory and exposed to controlled temperatures and moisture. However, this study modified the method to observe differences between concrete and soil-cement mixtures. ASTM C157 requires three specimens of identical dimensions, with specimen sizes depending on maximum aggregate size. The mix was then placed in the molds in approximately two layers, samples were demolded after 23 hours curing in the moist room, and the initial comparator reading was taken. The specimens remained in lime-saturated water until 28 days. The second comparator reading was taken after curing in lime-saturated water, and then the specimen was stored in water or 50% ± 4% RH. Other measurements were taken at certain intervals. Length change could be calculated at any age after the initial comparator reading. All reviewed shrinkage measurement procedures were essentially the same, with minor variations to satisfy the unique needs of each research study. Table 2.7 summarizes the reviewed methods.

Table 2.7: Summary of All Reviewed Shrinkage Testing Methods

Method	No. of samples	Size (in.)	Initial curing	Air curing	Final reading (days)
George (1968)	2	3 × 3 × 11.25	Moist room 100% RH/1–28 days	55% RH	-
Guthrie et al. (2002)	-	3 × 3 × 18	100% RH/24 hr.	50% RH	21
Chakrabarti and Kodikara (2003)	2	3 × 3 × 11	Moist room 90%+ RH/24 hr.	50% RH	90
ASTM C157 (2017)	3	Min: 3 × 3 × 11.25 Max: 5 × 5 × 16	Moist room 100% RH 24hr/immersion in lime-saturated water for 28 days	50% ± 4 RH	476/or 7 days intervals up to change length<0.001%

2.20 California Bearing Ratio Test

The CBR test, originally developed by the California Division of Highways, determines soil load deformation curves in the laboratory. Because CBR is affected by soil grain size distribution, moisture, and density, soil samples are compacted to specified densities, soaked in water for four days, and tested to determine the strength of soil relative to a standard crushed rock. A penetration test is conducted using standard CBR equipment. CBR is defined as:

$$CBR = \frac{unit\ load\ for\ 0.1\ piston\ penetration\ in\ test\ specimen\ (Ib/in^2)}{unit\ load\ for\ piston\ penetration\ in\ standard\ crushed\ rock (Ib/in^2)}$$

Equation 2.1

The unit load for standard crushed rock is usually 1,000 psi (Garber & Hoel, 2014). Samples are typically compacted at optimum moisture content using three compactive efforts, CBR is measured for material samples using each compactive effort, and the results are graphically depicted (Yoder & Witczak, 1975).

In pavement design, CBR is used to characterize pavement materials and subgrade strength, and an ASTM test is commonly used to characterize the CBR of soil-cement mixtures. The 1993 *AASHTO Guide for Design of Pavement Structures* (AASHTO, 1993) specifies that the main design input for pavement materials is resilient modulus (M_r). However, due to the complexity and expenses associated with moduli testing, CBR, commonly used as a design parameter, could be converted to an equivalent M_r with correlation factors. The AASHTO (1993) design procedure allows the correlated value (Garber & Hoel, 2014).

Many specifications require a minimum 15% CBR for the subgrade layer. CBR values higher than 80% are usually characterized as excellent compacted pavement subgrade (Hossain & Mol, 2011). Conversely, subgrade soils with CBR less than 6% and UCS values less than 7 psi are considered unstable and require stabilization, especially for pavement applications (Bandara et al., 2015; Ozdemir, 2016). Previous research that has studied the effect of soil stabilization on CBR has reported higher CBR values for stabilized mixtures (Bell, 1993; Hossain & Mol, 2011; Ozdemir, 2016).

2.21 Mechanistic-Empirical Pavement Design

State highway agencies have used the AASHTO guide as the primary pavement design procedure for decades (Islam et al., 2019). However, the AASHTO procedure that was developed based on road test data from 1958 to 1960 had many limitations. For example, the design procedure, which relied on empirical equations derived from the data, is now outdated for current traffic, materials, and construction techniques. Additionally, the AASHO road test was performed for a single geographic location, one type of subgrade, one type of HMA, one type of portland cement concrete mixture, and a limited number of axle load applications. Therefore, the *Mechanistic-Empirical Pavement Design Guide* (MEPDG), developed under the National Cooperative Highway Research Program (NCHRP) 1-37A project, was developed to satisfy the need for a design method that covers conditions beyond the limited AASHTO road test (AASHTO, 2015). The MEPDG considers input parameters that influence pavement performance, including traffic, climate, pavement structure, and material properties; pavement responses such as stresses, strains, and deflections are calculated mechanistically. Incremental damage over time is computed based on pavement responses and are empirically related to observed pavement distresses (AASHTO, 2015).

Many state highway agencies, including KDOT, are transitioning from the AASHTO (1993) design procedure to the recently developed MEPDG for new and reconstructed pavements. For example, the AASHTOWare Pavement ME Design (PMED) software incorporates MEPDG procedure into pavement design (Islam et al., 2018; Islam et al., 2019). This study utilized version 2.6.2.2 of PMED released in September 2022.

2.22 Life-Cycle Cost Analysis

LCCA is an economic analysis technique that considers the design and service life of pavements and evaluates the long-term economic efficiency of competing alternatives. The initial and discounted future agency, user, and other relevant costs over the life of alternatives are incorporated. For pavement design, the LCCA must be done during the project design stage (FHWA, 2002). LCCA is a subcategory of benefit-cost analysis (BCA), in which the agency has already decided to undertake a project. While BCA can be used to determine whether a project

should be initiated, LCCA determines the most cost-effective means to achieve a project's objectives. LCCA is applied only to compare project implementation alternatives yielding similar levels of service and benefits. BCA, however, considers the benefits and costs of alternatives, allowing comparison between alternatives that do not yield similar benefits or do not achieve the same objectives (FHWA, 2002).

The only costs included in LCCA are differential costs among alternatives. Common costs for all alternatives are generally not included in analysis and only noted in the text description of costs. The LCCA period is the time span over which alternatives are evaluated, and long-term cost differences must be sufficiently captured in the analysis period. The Federal Highway Administration (FHWA) recommends a minimum 35-year analysis period for all pavement projects. The net present worth (NPV) is the economic efficiency indicator used in LCCA. Future costs are estimated and rediscounted to the present value using a real discount rate that should reflect historical trends. Although the historical long-term trend for the discount rate nationally suggests a value of 4.0%, 3%–5% is also an acceptable range. KDOT refers to Appendix C: Discount Rates for Cost-Effectiveness, Lease-Purchase, and Related Analyses of the OMB Circular No. A-94 to set the discount rate for the LCCA. The discount rate, which is typically updated annually in December, varies significantly, however, and is not always in the range of 3%–5%. In 2018, the discount rate was 1.0%, compared to 0.5% in 2019.

The most significant costs of LCCA typically are the initial construction and user costs. Routine maintenance costs may have only a marginal effect on cost estimations, particularly when they are discounted over the 30- to 40-year analysis period. Salvage value, which is the remaining value of an alternative at the end of the analysis period, may be included in analysis as a negative cost when desired (Walls & Smith, 1998).

2.23 Microstructural Studies Using Scanning Electron Microscopy

Microstructural studies increase understanding of macroscopic behavior and physical properties of compacted and natural soils. Macroscopic soil properties such as distribution and connectivity of pores, particle size, shape and distribution, arrangement of grains, and grain-to-grain contacts can be explained via microstructural studies (Romero & Simms, 2008). A common

method for soil microstructural study is SEM, a microscopy technique that uses electron beams to produce magnified images with high resolution. In SEM, an image is generated by scanning the surface with a focused electron beam to determine if the electron signal is either direct scattering or emitted from the sample. The energy, intensity, and location of detected electrons are used to create an image. An EDX detector can also be paired with an SEM to determine the chemical composition of elements in the sample. The interactions of SEM and EDX can reveal information about the specimen's composition, topography, crystallography, and other properties (Sabahfar, 2016). Figure 2.10 shows a schematic of emitted signals.
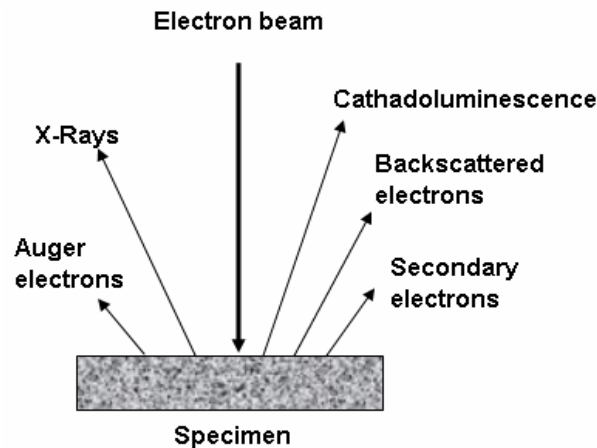
Figure 2.10: Emitted Signal due to Interaction of Electron Beam and Specimen
Source: Hafner (2007)

Al-Swaidani et al. (2016) evaluated the effect of natural pozzolan on geotechnical properties of lime-stabilized clayey soil. SEM and EDX were used to study the microstructure and chemical composition of the treated soils. Results showed significant changes in the microstructure of the treated soil. Based on EDX analysis, distinct peaks of Ca, Si, and Al elements indicated the presence of cementitious reaction products on the surface of treated clay. Improved properties of treated soil, such as increased flocculation (i.e., aggregation) of clayey particles and continuous pore structure, were attributed to the formation of cementitious compounds. The cementitious compounds were characterized by their high strength and low volume change, resulting in treated soil with improved plasticity, stiffness, compaction properties, and shrinkage.

Choobbasti and Kutanaei (2017) used SEM and EDX to study the microstructure of cement-stabilized sandy soil with nanosilica. The addition of nanoparticles created a cement-treated sand mixture with a compact microstructure. EDX detected increased intensity of the CSH peak and decreased intensity of the $Ca(OH)_2$ peak. SEM results showed unstable lumps at high concentrations of nanosilica due to insufficient resistance to unconfined compressive loads (Choobbasti & Kutanaei, 2017). Latifi et al. (2017) used a field emission scanning electron microscopic (FESEM) test to study the modification of soil structure treated with low-carbon nontraditional additives. Cementitious products formed into a white gel that filled the void space in the soil structure. Increased curing time resulted in additional pores filled with cementing products. Observed changes in the surface of soil particles resulted from the formation of cementitious products and changes in the soil fabric. The conclusion was made that the developed cementitious products in pores bonded the soil particles together. Denser fabric and cementation bonds were the main contributors to improved shear strength and compressibility parameters (Latifi et al., 2017).

Chapter 3: Methodology

3.1 Introduction

This study utilized laboratory testing and performance modeling to investigate the suitability of RCA for clay subgrade soil stabilization beneath HMA pavements. A total of 36 mixtures, including five control and 31 chemically stabilized mixtures were developed following the USACE method of stabilizing pavement subgrade. Physical properties of all materials, such as gradation, compaction curve, toughness, and soundness of aggregates, were assessed. The mixtures were then evaluated using UCS, linear shrinkage, and CBR tests. Experimental results were used in the AASHTOWare PMED software to predict the performance of pavements with designed mixtures. The cost savings of RCA versus the KDOT method for subgrade stabilization were evaluated using LCCA. This chapter discusses the materials, mixture design procedure, laboratory tests, MEPDG method, and LCCA.

3.2 Materials

Materials used in this study consisted of two sources of RCA, one source of clay, three chemical agents (i.e., lime, Class C fly ash, and portland cement), and water. RCA samples were collected from pavements with D-cracking: one from Topeka Blvd in Topeka, Kansas, and one from the Kansas City (KC) International airport runway. The slabs from these sources were crushed to a maximum aggregate size of 1 in. Coarse aggregates in the original Topeka mix design were quarried by Martin-Marietta from the east Topeka plant. The KC coarse aggregate was also produced by Martin-Marietta from the Sunflower quarry in De Soto, Kansas. Both coarse aggregates were limestone.

The clay, obtained from a local source in Kansas, was stabilized with RCA and chemical stabilizers. The soil was classified in the laboratory as lean clay (CL) according to the unified soil classification system (USCS) with a liquid limit of 38 and plasticity index of 15. Figure 3.1 shows the RCA and clay used to assess RCA effectiveness for clay subgrade stabilization.
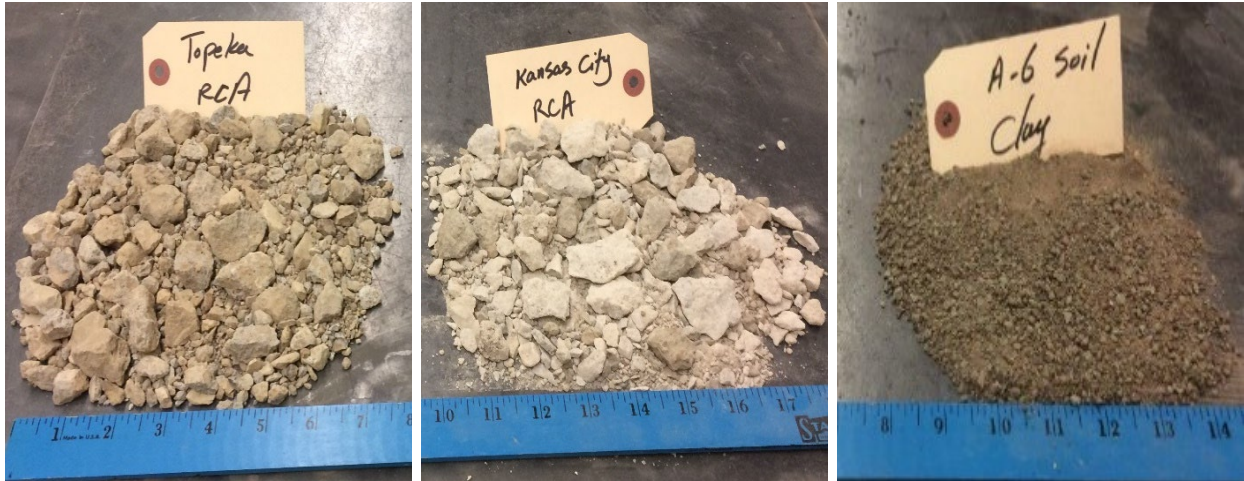
Figure 3.1: Topeka RCA, KC RCA, and Clay

Silty soil was also obtained to evaluate RCA effectiveness for mechanical stabilization in silty soils. The soil had a liquid limit of 32 and a plasticity index of 10 and was classified as a lean clay (CL) according to the Unified Soil Classification System (ASTM 2487). This soil was selected because it classified as AASHTO group A-4, or a silty soil. According to the design procedure followed in this study, if the UCS of stabilized mixtures increased compared to the control 100% silty soil, RCA would be considered an effective method for mechanical stabilization. Thus, the silty soil was mixed with RCA at various percentages and tested for UCS.

Type II portland cement, Class C fly ash, and lime were used as chemical agents (binders). Fly ash and lime were used alone in the mixtures, while portland cement was used with fly ash. The selected chemical agents are the most common agents used for pavement applications in Kansas. All chemical agents were obtained from local sources and passed KDOT requirements as specified in KDOT (2015) standard specifications. Specifically, fly ash complied with physical requirements of ASTM D5239 (2012) and chemical requirements of ASTM C618 (2017) per KDOT specifications. KDOT requires use of Class C fly ash with self-cementing properties and 7-day compressive strength higher than 500 psi for soil stabilization (KDOT, 2015). Table 3.1 compares the chemical properties of Class C fly ash used in this study and ASTM C618 requirements.

Table 3.1: Chemical and Physical Properties of Studied Class C Fly Ash

Property	ASTM C618	Class C fly ash used[*]
Cumulative SiO_2-Al_2O_3-Fe_2O_3, min. %	50.0	63
Sulfur trioxide (SO_3), max, %	5.0	1.4
Moisture content, max, %	3.0	0.07
Loss on ignition, max, %	6.0	0.27
Fineness, amount retained on #325 sieve, %	26.6	34 max.
Water requirement, % of cement control	95	105 max.
Soundness, autoclave expansion or contraction, %	0.06	0.8 max.

[*]Average of four chemical analysis reports, a complete report is provided in Appendix A, Figure A.1.

KDOT allows hydrated or quicklime for treating soil aggregates with a minimum of 90% lime index. This study used lime hydrated with a minimum 90% lime index as calcium hydroxide, produced by the Mississippi Lime company. Portland cement conformed to all requirements of AASHTO M 85 (2017), *Standard Specification for Portland Cement*, with a few modifications as stated in KDOT specifications on cementitious materials (KDOT, 2015). Figure 3.2 compares chemical and physical properties of Type II portland cement used in this study with AASHTO M 85 requirements, and Figure 3.2 shows the applied chemical agents. Mixing water was potable tap water that passed visual examination as specified by KDOT (2015).

Table 3.2: Chemical and Physical Properties of Studied Portland Cement

Property	AASHTO M 85	Type II (MH) Portland Cement *
SiO2 (%)	-	20.2
Al2O3 (%)	6.0 max.	4.7
Fe2O3 (%)	6.0 max.	3.1
Cao (%)	-	64.0
7-days Compressive strength (psi)	2,760 min.	5,060
Initial time of setting, Vicat (min)	45–375	97
Blaine Fineness	260-430	361
Specific gravity	-	3.18

[*]Complete mill report is provided in Appendix A, Figure A.2.

Figure 3.2: Applied Chemical Agents (Hydrated Lime, Portland Cement, Class C Fly Ash)

RCA was sieved over a 1-in. sieve to remove deleterious materials, dried to a constant mass at a temperature of 140 °F, and stored in the laboratory under ambient room temperature (65–75 °F) until it was incorporated into the mixtures. The clay was originally stored outside and contained vegetation and organic materials. Visible vegetation roots and deleterious materials were removed from the clay by hand, and then the clay was submerged under water in pans and repeatedly stirred to separate organic material from the clay. All floating organics were removed using sieves so that all floating vegetation was removed without altering soil particle distribution. The clay was dried in an oven to a constant mass at a temperature of 140 °F, the dry clay was thoroughly broken up to avoid reducing the natural size of individual particles, and all soil was then processed through a No. 4 sieve. The material gathered through the sieve was stored in the laboratory under ambient laboratory temperature (65–75 °F). The moisture contents of stored RCA and clay were recorded before incorporating the materials into the mixtures, and then they were dried in an oven to a constant mass if any moisture existed. The RCA and clay soil were brought to room temperature before they were incorporated into the mixtures.

3.3 Sieve Analysis of Coarse and Fine RCA Aggregates

The sieve analysis test was performed on RCA aggregates according to ASTM C136 (2014), *Standard Test Method for Sieve Analysis of Fine and Coarse Aggregates*. A sample with a minimum weight of 22 lb was prepared and dried to a constant mass at a temperature of 230 ±

10 °F. The dry mass of the sample was recorded as the original dry mass to the nearest 0.1%, and the sample was then washed over the No. 200 sieve until the wash water was clear. The washed sample was dried to a constant mass and recorded as the dry mass after wash. Washed aggregates were separated into two portions of passing and retained on the No. 4 sieve for further sieving. The total percentage of material retained on each sieve was calculated based on the total original dry mass of the sample. The percentage passing through the No. 200 sieve was calculated using the original dry mass and the dry mass after washing.

3.4 Particle Size Analysis, Atterberg Limits, and Specific Gravity

Particle sizes of the clay and the silty-clay soil were determined using ASTM D422 (2007), *Standard Test Method for Particle Analysis of Soils*. The distribution of particle sizes smaller than 0.0029 inches was determined via the hydrometer test, while the distribution of larger particles was determined via sieving. A 152H hydrometer was used in this study (Figure 3.3). The liquid limit, plastic limit, and the plasticity index of clay and silty soil were identified according to ASTM D4318 (2017), *Standard Test Method for Liquid Limit, Plastic Limit, and Plasticity Index of Soils.* The same procedure was followed to measure Atterberg limits of the mixtures of RCA, clay, and the stabilized mixtures developed in this study. To allow for curing, the chemically stabilized mixtures were kept at room temperature for 60 minutes after the addition of water while covered to prevent moisture loss. The curing time was in accordance with specifications explained in Section 3.8.

Figure 3.3: Hydrometer and Specific Gravity Test on Clay

3.5 Specific Gravity and Absorption

Specific gravities of clay and RCA were measured in the lab using various procedures for soil solids passing through a No. 4 sieve, as well as coarse and fine aggregates. The specific gravity of clay was determined according to the standard procedure ASTM D854 (2014), *Specific Gravity of Soil Solids by Water Pycnometer*, in which a water pycnometer determines the specific gravity of soil solids passing through a No. 4 sieve (Figure 3.3). The Kansas standard test method KT-6 (2004), *Specific Gravity and Absorption of Aggregates,* was used to determine the specific gravity and absorption of coarse and fine aggregates. Coarse aggregate was defined as the portion retained on the No. 4 sieve, and fine aggregate was all aggregates passing through the No. 4 sieve and remaining on the No. 200 sieve.

3.6 Soundness of Aggregates

The KTMR-21 (1999), *Soundness & Modified Soundness of Aggregates by Freezing and Thawing*, procedure was followed to determine RCA aggregate resistance to disintegration by F-T. The test method permits two classes of aggregates: official quality and Class I aggregate. Both classes, however, accounted for only the coarse portion of RCA aggregate. The primary difference between the two categories was test sample gradation and preparation. The test sample for official quality was the portion of aggregate covering 0.0937–0.75 inches. The official quality was selected for this study because it more accurately represented RCA aggregate gradation. The prepared test

sample was placed in an open-top container and subjected to 25 cycles of F-T. The cycles were a minimum of 2 hours of freezing at -20 °F–0°F, followed by 40 min. of thawing in a water tank. The test sample was washed over the No. 12 sieve after F-T cycles were complete. The aggregates were brought to saturated surface condition (SSD) and sieved as specified in KTMR-21. The mass retained on each sieve was recorded, and aggregate soundness was calculated.

3.7 Los Angeles Abrasion Test

Test procedure ASTM C131 (2006), *Resistance to Degradation of Small-Size Coarse Aggregate by Abrasion and Impact in the Los Angeles Machine*, was followed to measure the degradation of RCA coarse aggregate. The test sample was prepared by reducing the sample to the requirements of gradation B of the standard Los Angeles (LA) test method. Gradation B was selected because it was nearest to the size range of RCA aggregate.

3.8 Standard Proctor Test

The standard Proctor test was used to determine the relationship between molding water content, dry unit weight of soils, and RCA (compaction curve) compacted in standard molds as specified in ASTM D698 (2012), *Laboratory Compaction Characteristics of Soil Using Standard Effort*. This method covered only materials with 30% or less mass retained on the 0.75-in. sieve with no previous compaction in the laboratory. According to ASTM D698, three alternative methods (A, B, and C) are based on material gradation. Only methods A and C were applied to this research. Method A applied to materials with 25% or less mass retained on the No. 4 sieve, and method C was used if 30% or less mass was retained on the 0.75-in. sieve. The test fraction of material was the portion of total specimen used for the compaction test. For method A, the test fraction was passed through the No. 4 sieve, and in method C, the test fraction was passed through the 0.75-in. sieve. A correction was needed if the specimen contained more than 5%, by mass, oversized fraction that was not used in the compaction test. In this study, the percentage of the oversized fraction was less than 5%, and no correction was required. Samples were compacted using the standard effort (12,400 ft-lbf/ft^3), as specified in ASTM D698, which involved dropping a 5.5 lb hammer from a height of 12.0 inches. Standard effort can be calculated as follows:

$$\text{Energy} = \frac{(5.5 \text{ lb/blow})(\# \text{ of blows/layer})(3 \text{ layers})(1 \text{ ft})}{\text{Volume of the mold (ft}^3)}$$

Equation 3.1

A 4-in. and a 6-in. standard Proctor mold was used for methods A and C, respectively. Samples were compacted in three layers, with 25 blows of the standard hammer for method A and 56 blows for method C.

Material preparation included sieving clay over the No. 4 sieve (method A) and RCA over the 0.75-in. sieve (method C). ASTM D698 permitted two methods of moist and dry preparation. Dry preparation was for damp materials that were not friable, so the water content had to be reduced by air or oven drying. All soil and aggregates used in this study were oven dried to a constant mass with temperatures less than 140 °F. For mixtures with clay and RCA, each material was prepared separately and then mixed for further compaction testing. Five sub-specimens were prepared from the test fraction, and five different molding water contents, as corresponded to the estimated optimum water content, were added to each sub-specimen. ASTM D698 requires at least two sub-specimens on the wet side and two sub-specimens on the dry side of the OMC. Recommended variation in water content is 2%, but molding water content increments should not exceed approximately 4%.

All clay or blends of RCA-clay were mixed and kept in containers covered with plastic wraps for 24 ± 4 hr. Mixtures were cured for 60 min. The curing time was selected based on the literature (ASTM D3551, 2017; Banda, 2003; Parsons et al., 2001) and trial samples made in the lab. After curing, each specimen was compacted following the procedure outlined in ASTM D698.

The soil was compacted in three equal layers of approximately 2.5 inches in thickness. The sample top surface was trimmed, and any existing hole was filled with the unused or trimmed soil. The soil was pressed into the hole, and the surface was straightened using the sharp edge of a spatula. For samples with gravel-sized particles (samples containing RCA), the area around the particle was trimmed or the particle was removed from the surface to achieve an even surface. Once an even surface was prepared, the mass of the sample, the mold, and the baseplate were measured to the nearest gram. Molding water content was obtained using a representative sample from the bottom, middle, and top of the mold to incorporate all three layers. The mass of the

representative sample conformed to the requirements of ASTM D2216 (2010), *Standard Test Methods for Laboratory Determination of Water (Moisture) Content of Soil and Rock by Mass*. A compaction curve representing the best fit of molding water content versus dry unit weight was plotted, which required a minimum of four points, two on each side of the OMC. Based on the compaction curve, the OMC was determined to the nearest 0.1%, and MDD was determined to the nearest 0.1 lbs/ft³.

3.9 Stabilized Soil-Cement Mixture Design Procedure

This study followed the USACE (1994) method with minimal modifications to design stabilized soil-cement mixtures. Modifications were made to meet KDOT needs and anticipate unforeseen effects of RCA on the mixtures. The USACE method is based on strength and durability requirements. Although mixture durability should be assessed through applicable F-T testing procedures, similar to most state DOTs, KDOT focuses only on compressive strength (Guthrie et al., 2002). This focus on strength is due to minimal required testing time and increased availability of equipment and trained technicians. Therefore, the objective of mixture design in this study was to achieve a target strength, as evaluated by the UCS test described in Section 3.9.2.

The USACE requires a design UCS of 250 psi to stabilize subgrade soil for flexible pavements regardless of the stabilizer type. The required mixture age to achieve such strength depends on the type of stabilizer used (USACE, 1994). According to USACE requirements, the target UCS was determined to be 28 days for all chemical stabilizers. The UCS was also measured at 7 days for comparison. Mixture design required standard Proctor compaction and UCS tests. Mixtures of 100% clay, 50% clay-50% RCA, and 100% RCA with different stabilizers were developed, and mixtures containing only clay (i.e., 100% clay) were studied as control mixtures to obtain base binder requirements for clay stabilization. To assess the effectiveness of RCA in clay stabilization, RCA replaced 50% of clay by weight, resulting in a second blend of 50% clay and 50% RCA. Mixtures of 100% RCA were also studied to gather additional information about characteristics of RCA materials.

3.9.1 Estimation of Initial Binder Content

According to the USACE method, the first step in the design of mixtures with different types of chemical stabilizers is to estimate the initial percentage of binder, which refers to a percentage of chemical agent initially selected to achieve the design target strength. This section describes procedures to estimate this percentage. Additional percentages of binder were added according to the initial estimation.

3.9.1.1 Estimation of Initial Percentage of Lime

The first step in the design of lime mixtures was to estimate the initial percentage of lime according to ASTM D6276 (2006), *Using pH to Estimate the Soil-Lime Proportion Requirement for Soil Stabilization*. Therefore, various soil (passing the No. 40 sieve) slurries with water and differing percentages of lime were made, and the lowest percentage of lime in soil-lime mixtures with a pH of 12.4 was the approximate lime percentage for stabilizing that soil. The range of lime content in this study was 2%–12%. Figure 3.4 shows the prepared samples and pH meter used in this study. Once the initial lime percentage was fixed, as based on the total dry weight of soil, a standard Proctor test (per ASTM D698) was performed on the mixture with the estimated initial lime content. The UCS samples at measured compaction properties were then made according to ASTM D1632 (2017), *Standard Practice for Making and Curing Soil-Cement Compression and Flexure Test Specimens in the Laboratory*, and tested according to ASTM D1633 (2017), *Standard Test Methods for Compressive Strength of Molded Soil-Cement Cylinders*.

Figure 3.4: Estimation of Initial Lime Content
Source: ASTM D6276 (2006)

3.9.1.2 Estimation of Initial Fly Ash Content

The first design step for fly ash mixes was to estimate the initial percentage of fly ash. According to the USACE method, this percentage can be estimated using two methods. This study utilized the first method due to shorter required testing time, although for mixtures of clay and RCA, results were verified using the second method. A moisture content close to the OMC of soil-fly ash mixtures was estimated using the OMC of the soil or RCA blends as the estimated OMC for the fly ash-soil mixtures. Then a single-point compaction test was conducted on fly ash contents of 10%–20% while the water content remained constant. A plot of dry density versus fly ash content was drawn, and the fly ash content yielding MDD was determined from the plot and selected as the initial design binder content. The standard Proctor test was performed on the mixture with the estimated initial fly ash content. The OMC and MDD obtained for the initial mixtures were used to make other trial mixes with different percentages of binder. The UCS samples were made following ASTM D1632 and tested according to ASTM D1633.

3.9.1.3 Estimation of Initial Percentage of Fly Ash with Portland Cement

The estimated initial percentages of fly ash, as described in Section 3.9.1.2, were used as the total binder for a combination of fly ash and portland cement. A ratio of portland cement to fly ash yielding the highest strength was determined using trial UCS samples with cement to fly ash ratios of 1:1 and 1:2. The same steps were followed as for fly ash-only mixtures.

3.9.2 Unconfined Compressive Strength Test

The second step in the design of stabilized mixes was to test the selected trial mixtures for UCS. According to the USACE method, making and curing soil-cement samples for the UCS test should follow procedures outlined in ASTM D1632, and the test should be performed per ASTM D1633. This section describes the methods for making, curing, and testing UCS samples.

ASTM D1632 identifies a standard UCS specimen as being cylindrical with a diameter of 2.8 inches and a height of 5.6 inches. However, the procedure permits the molding of larger or smaller specimens if a height equal to twice the diameter of the sample is used. The USACE method dictates the use of samples with diameters of 4 inches and heights of 8 inches when more than 35% of material is retained on the No. 4 sieve. All mixtures incorporating clay required specimens measuring 3 inches × 6 inches, whereas 100% RCA mixtures required specimens measuring 4 inches × 8 inches based on ASTM requirements. To maintain a uniform specimen size, this study made trial specimens measuring 4 inches × 8 inches for all mixtures. However, specimens containing clay did not develop sufficient early strength and failed when removed from the mold. Because the small test specimens (3 inches × 6 inches) did not effectively represent 100% RCA formed primarily from coarse aggregates, the sample size in this study varied according to ASTM D1632 requirements. Measured strength decreased as the specimen size increased. However, the effect was negligible when comparing a 4-in. and a 3-in. specimen (Mindess et al., 2002).

ASTM D1632 requires three replicate UCS samples. The designed soil and water quantities were based on compaction results (ASTM D698) for the OMC and MDD of the mixture with the initial binder content. The cement amount was calculated according to results of the initial binder content estimation. Percentages above and below the initially estimated binder content were also tested (typically 2%–3%).

Mixing of soil-cement materials was allowed by hand or in a laboratory mixer. Only 100% RCA mixes were mixed using a mechanical mixer because the quantity of material was high and hand mixing was insufficient. Batches of soil-cement were made to leave approximately 10% excess after molding test specimens. The mixes were covered with plastic wraps to protect against loss of water. A mellowing time of 1 hour was selected according to trial mixes and the

recommendation of ASTM D3551 (2017), *Standard Practice for Laboratory Preparation of Soil-Lime Mixtures Using Mechanical Mixer*. ASTM D1632 does not specify a minimum mixing time, so this study adhered to minimum requirements of ASTM C192 (2016). Specimen molding began with coating the mold with commercial form oil. A predetermined mass of the uniformly mixed soil-cement was placed in the mold to make a sample at MDD and OMC of known dimensions. A minimum of six samples for testing at 7 and 28 days were made. A compression testing machine with a capacity of 5,000 lbf compacted samples by applying a static load with a strain rate of 0.5 inches/min until the specimen measured 6 inches or 8 inches in height. Because ASTM D1632 does not specify a loading rate for the mechanical compaction of samples, this study used trial and error to fabricate a properly compacted specimen with no visible holes in order to select the compaction rate. Figure 3.5 shows the machines used for mechanical mixing and sample compaction. Based on this procedure, samples should be cured in the mold for a minimum of 12 hour before extracting from the mold. Study specimens were not sturdy enough for early removal of the mold, so the trial specimens were cured for 24 ± 2 hour in a moist room with an RH of 50% while covered with plastic sheets. A hydraulic sample extruder was used to extrude samples from the molds, and then specimens were transferred to a moist room with +96% RH. Specimens were tested in moist conditions directly after removal from the moist room after reaching the specified age of curing (i.e., 7 or 28 days).

Figure 3.5: Mixing and Compaction of Soil-Cement Mixes

This study followed method B of ASTM D1633 (2017) to measure the UCS of compacted and cured soil-cement specimens using a test specimen with a height-to-diameter ratio equal to 2. The increased height-to-diameter ratio of method B, as compared to the 1.5 ratio of method A, resulted in a more accurate UCS measurement because it reduced complex stress conditions that may occur during the shearing of method A (ASTM D1633, 2017). A compression testing machine with a capacity of 11,000 lbf was used to test the samples by automatically controlling a loading rate of 0.05 inches/min. The sample was placed on the lower bearing block of the testing machine directly under the upper block, and the vertical axis of the specimen was aligned with the center of the seating blocks. A continuous static load was automatically applied to the specimen with no shock to maintain a constant strain rate of 0.05 inches/min. The maximum load carried by the specimen during the test before sample failure was recorded to calculate the UCS of the mixture. Sample failure was defined as the formation of a macrocracks in the sample or a sudden decline in the carried load, where a microcrack could be seen without magnification. Figure 3.6 shows the test set up and a failed sample. Compressive strength of the specimen was calculated to the nearest 10 psi by dividing the maximum load carried by the specimen by the cross-sectional area of the sample.
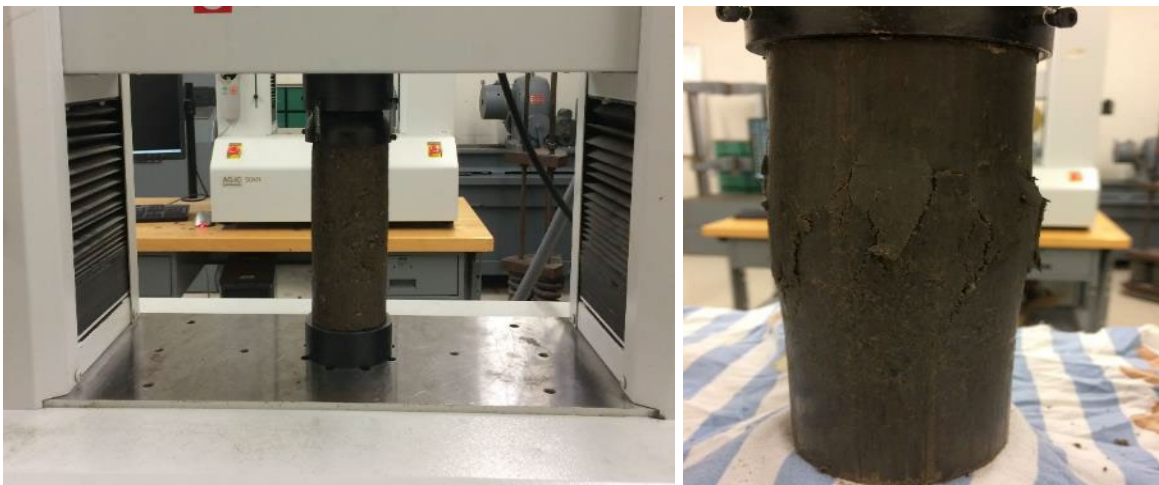
Figure 3.6: Unconfined Compression Test
Source: ASTM D1633 (2017)

3.10 Performance Testing of Selected Soil-Cement Mixtures

The performance of designed soil-cement mixtures was tested using linear shrinkage and CBR tests. This section describes experimental methods for testing soil-cement mixture performances with respect to shrinkage and mixture stiffness.

3.10.1 Shrinkage Test on Soil-Cement Mixtures

Shrinkage testing in this study was conducted according to ASTM C157, *Standard Test Method for Length Change of Hardened Hydraulic-Cement Mortar and Concrete* (ASTM C157, 2017), to determine length changes of mortar and concrete specimens made in the laboratory and exposed to controlled conditions of temperature and moisture. The test procedure measured length change to assess the potential for volumetric expansion or contraction due to causes other than applied force and temperature changes. This procedure was selected due to lack of a procedure for measuring shrinkage of soil-cement mixtures with aggregates larger than the No. 40 sieve. However, modifications were made to allow for compaction and length measurement of soil-cement samples.

All shrinkage samples were rectangular beams measuring 3 inches × 3 inches × 11.25 inches, as specified in ASTM C157 for mixtures with aggregates smaller than 1 in. Each mixture was mixed according to the previously outlined procedure for making and curing soil-cement mixtures in Section 3.9.2. Shrinkage molds were one-compartment steel molds conforming to the requirements of ASTM C490 (2017), *Use of Apparatus for the Determination of Length Change of Hardened Cement Paste, Mortar, and Concrete*. Each gauge stud was held in place by the end plates of the mold on each side. Gauge studs were stainless steel studs extended into the specimen and used as the reference for length measurement. The mixture was placed in the mold in two approximately equal layers. Molds were sprayed with commercial form oil before the mixture was placed into the mold to facilitate sample removal.

A standard Proctor hammer was used to compact the predetermined amount of mixture at OMC and MDD in two layers. Samples were covered with plastic sheets and transferred to a moist room with +96% RH for 23.5 ± 0.5 hr. The time was measured after water was added to the cement during mixing. Then samples were moved from the moist room and removed from the molds. The

length of each sample was measured using two reference metal gauge studs buried at each end of the sample. Soil-cement samples made for this study were not sturdy enough to hold the studs in place after removal from the mold; thus, upon removal, the gauge studs were glued into the sample using an epoxy adhesive. Samples were then transferred to a $50 \pm 4\%$ RH room for air storage at a temperature of 73 ± 3 °F. A length comparator was used to take length measurements of the specimens according to requirements specified in ASTM D490. Although ASTM C157 dictates that the first length measurement of concrete specimens should be taken upon removal of the sample from the mold (24 ± 0.5 hour after the addition of water to the cement during mixing), the first length measurement in this study was taken 48 ± 1 hour after adding water to allow enough setting time for the glued studs. The studs were essential for creating fixed reference points for shrinkage measurement, especially since autogenous shrinkage due to chemical agent hydration typically accounts for the most significant volume change during the first day after mixing and tends to be high for low water-to-cement ratios (0.2–0.42) (Aly & Sanjayan, 2009; Wu et al., 2017). The water-to-cement ratios of all mixes in this study were higher than 0.8, meaning the amount of shrinkage on the first day after mixing was expected to be minimal (Aly & Sanjayan, 2009). Comparator readings of each sample were taken over time at certain intervals, as specified in ASTM D157. Time intervals for this study were 48 ± 1 hour; 4, 7, 14, 21, and 28 days; and after 8 and 16 weeks. The length change of specimens at any age was calculated per ASTM C157. Figure 3.7 shows the mold set up, samples in the drying room and the measurement device.

Figure 3.7: Shrinkage Test Setup, Curing, and Length Measurement

3.10.2 CBR Test on Soil-Cement Mixtures

ASTM D1883 (2016), *Standard Test Method for California Bearing Ratio of Laboratory-Compacted Soils*, was followed to measure the CBR of the stabilized mixtures, including the determination of pavement subgrade, subbase, and base course materials from the laboratory-compacted specimens, to evaluate potential strength of the specific pavement layer. All pavement materials, including recycled and self-cementing materials, used in the design of road and airfield pavements can be tested in this procedure. Self-cementing materials, however, should be cured to best represent the long-term service condition of the material. The test method covers the CBR measurement at OMC or over a range of water contents from a specified compaction test and a specified dry unit weight.

In this study, all samples were compacted at OMC. Compaction energy was specified using the specific number of blows per layer. The 100% MDD was achieved following the procedure specified in ASTM D698. The compaction energy for this study was 56 blows per each layer of three layers to reach 100% MDD. ASTM D1883 allows the CBR measurement of soaked or unsoaked samples prior to testing. Due to equipment limitations of this study, CBR measurements of unsoaked samples were taken because study objectives could be satisfied by comparing unsoaked CBR of stabilized mixtures with or without RCA. The loading machine was a manual CBR testing machine with a maximum capacity of 11,000 lb. The procedure required sufficient surcharge weights on the specimen to produce an intensity of the pavement weight, or a minimum of 10 lb if pavement weight was not specified. This study adhered to the minimum requirement (10 lb) of ASTM D1883. Sample preparation for compaction was in accordance with method C of test procedure ASTM C698. The mold containing the sample was put in a plastic bag in a moist room with +96% RH for moist curing for 7 days. After completion of the curing period, the penetration test was performed on the sample. Penetration stress in lb/in^2 was measured by dividing the measured loading force by the cross-sectional area of the piston. The stress versus penetration curve was plotted, and the bearing ratio was defined as the ratio of stress at 0.10 inches penetration to 1,000 psi. Figure 3.8 shows the test set up and a tested sample.

Figure 3.8: CBR Test Setup and a Tested Specimen
Source: ASTM C157 (2017)

3.11 Performance Prediction Using AASHTOWare Pavement ME Design

To predict the long-term performance of stabilized mixtures developed in the laboratory, flexible pavements were designed with AASHTOWare PMED software (version 2.6.2.2). Laboratory-measured properties of the stabilized mixtures were used as inputs for the stabilized subgrade layer.

3.11.1 Mechanistic-Empirical Pavement Design Procedure

The MEPDG analyzes a trial design versus traffic loads and environmental conditions given a specified design period and target agency performance criteria. Each trial uses specific pavement structure layering and material properties, and pavement stress and strain response due to traffic loading and climate conditions is computed through MEPDG mechanistic models. Pavement distresses at the end of the analysis period are then empirically predicted based on mechanically estimated pavement responses (AASHTO, 2015; Gedafa et al., 2006). Estimated damage levels are compared against agency performance indicator criteria for a specific road classification. Indicator criteria include key pavement distresses (i.e., permanent deformation, fatigue cracking, and international roughness index [IRI]) and pavement smoothness, which is measured with respect to the IRI. If the trial design fails to satisfy the required performance criteria, a pavement structure is changed until the design satisfies the performance criteria, materials,

54

material layering, or layer thickness over the specified design period. The procedure is repeated until the revised design meets all performance indicator criteria over the design period.

3.11.2 Study Road Sections

This study designed flexible pavement structures for three levels of traffic, and traffic and climate properties were taken for actual projects in Kansas. Selected sections included parts of a minor arterial road (K-57), a principal arterial road (US-81), and an interstate (I-70). These projects were chosen because they had comparable natural soil properties and climatic conditions. The original pavement structure of all sections were rigid pavements. Table 2.3 summarizes characteristics of the study sections. Because the existing concrete pavements were assumed to be reconstructed as flexible pavements, all sections were designed as new flexible pavements with a design life of 10 years, as specified in the KDOT policy. The year 2019 was selected as the initial construction year of all sections.

Table 3.3: Highway Segment Pavement Cross-Section Details

Road Name	County	Road category	Traffic (AADTT)	Existing pavement
K-57	Marion-KS	Minor Arterial	415	Concrete
US-81	Cloud-KS	Principal Arterial	1,501	Concrete
I-70	Wabaunsee-KS	Interstate	2,671	Concrete

3.11.3 Pavement Performance Criteria and MEPDG Calibration Coefficients

The flexible pavement structure was designed to satisfy specific MEPDG performance criteria, including IRI (in./mile), terminal IRI, asphalt concrete (AC) top-down fatigue cracking (ft/mile), AC bottom-up fatigue cracking (% lane area), AC thermal cracking (ft/mile), permanent deformation - total pavement (in.), and permanent deformation - AC only (in.). Terminal IRI refers to the IRI specified by the agency as the failure/threshold IRI for minimum serviceability. In other words, it is the lowest acceptable ride quality before a significant routine maintenance action is needed to improve the ride quality of the existing pavement. In addition, a design reliability level was considered for each performance parameter. Design reliability is the probability that each key

distress type and smoothness will be less than a critical level over the design period (Gedafa et al., 2006; AASHTO, 2015). The target value for each performance criterion, as well as the level of reliability, depends on the road classification. This study used KDOT-developed performance criteria to analyze the designed pavements, and the calibration factors were KDOT-developed local calibration coefficients for flexible pavements (Islam et al., 2018; Islam et al., 2019).

3.11.4 Traffic

Basic traffic data include annual average daily truck traffic (AADTT) for the base year, number of lanes, percentage of trucks in the design direction, percentage of trucks in the design lane, operational speed, vehicle class distribution and growth, axle load spectra, axle configuration, and monthly and hourly adjustment factors. Except for AADTT, traffic characteristics such as vehicle distribution were the same for the design analysis of all flexible pavement structures. Table 3.4 shows general traffic characteristics of the study sections. The 2% annual growth rate was assumed based on the automatic vehicle classifier (AVC) data from 2012–2014. Results showed no significant difference in traffic growth irrespective of arterial type (major or minor).

Table 3.4: Traffic Characteristics

Road	Traffic (AADTT)	10 years ESALs (millions)	Growth rate (%)	No. of lanes	Trucks in design direction (%)*	Trucks in design lane (%)	Operational speed (mph)
K-57	415	0.26	2	2	50	100	60
US-81	1,501	0.93	2	2	50	100	65
I-70	2,671	1.66	2	24	50	90	70

*AADTT is two-way

Traffic volume adjustment factors were developed from 11 AVC stations in Kansas, and axle load spectra and axle group per vehicle were developed from 10 weigh-in motion stations. The derived traffic parameters were statewide Level 2 traffic inputs (Islam et al., 2018; Islam et al., 2019). Figure 3.9 shows the axle load spectra for single and tandem axle loads developed for class 9 trucks in the state of Kansas. The monthly adjustment factors (MAFs) and vehicle class distribution for Kansas are presented in Figure 3.10.
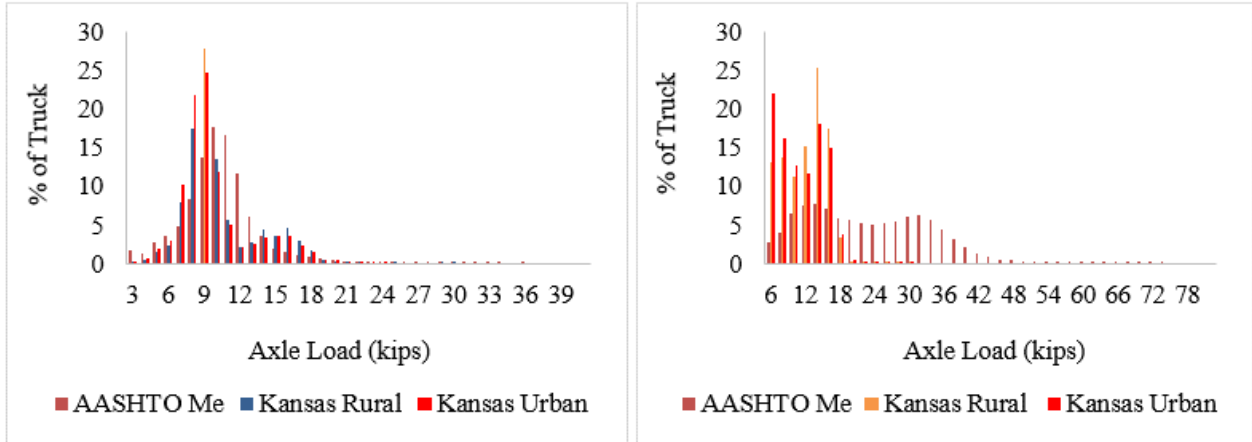
Figure 3.9: Single (left) and Tandem (right) Axle Load for Class 9 Trucks in Kansas
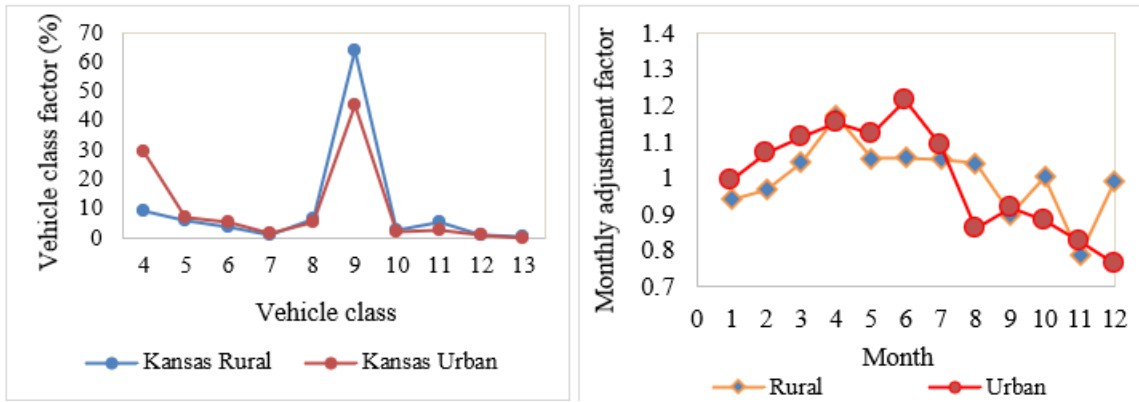
Figure 3.10: Vehicle Class Distribution (left) and Monthly Adjustment Factors (right) for Kansas

3.11.5 Pavement Structure

A full-depth asphalt pavement structure, commonly constructed in Kansas, was designed for all flexible pavements. The asphalt concrete layer surface thickness was 1.5 inches and the intermediate layer thickness was 2.5 inches, resulting in a total thickness of 4 inches for the surface and top base layers. This 4-in. thickness on top was maintained for all projects and adhered to KDOT common practice. Thickness of the asphalt concrete base layer also satisfied all KDOT criteria for flexible pavement design. Based on KDOT (2015) specifications, the top 18 inches of subgrade was compacted, and when subgrade treatment was required, the top 6 inches of the subgrade layer were treated. This study defined a control section based on the KDOT common practice of subgrade preparation for treated subgrades. The control section consisted of a 6-in.

treated top layer and a compacted 12-in. layer directly beneath the treated subgrade. Other sections were based on laboratory results of this study for soil-cement mixtures. The stabilized subgrade thickness was reduced to 4 inches, while compacted subgrade thickness was changed to 14 inches. The stabilized layer thickness reduction was due to increased stiffness of the stabilized soil-cement mixtures compared to lime-treated mixtures commonly used in Kansas. Figure 3.11 shows a schematic of the designed pavement structure.

1.5 in. asphalt (AC Surface)
2.5 in. asphalt (AC Binder)

Var. thickness asphalt (AC Base)

6.0 in. treated subgrade (Control Section)
or
4.0 in. Stabilized subgrade (Alternative Section)

12.0/14.0 in. compacted subgrade

Natural clay subgrade soil
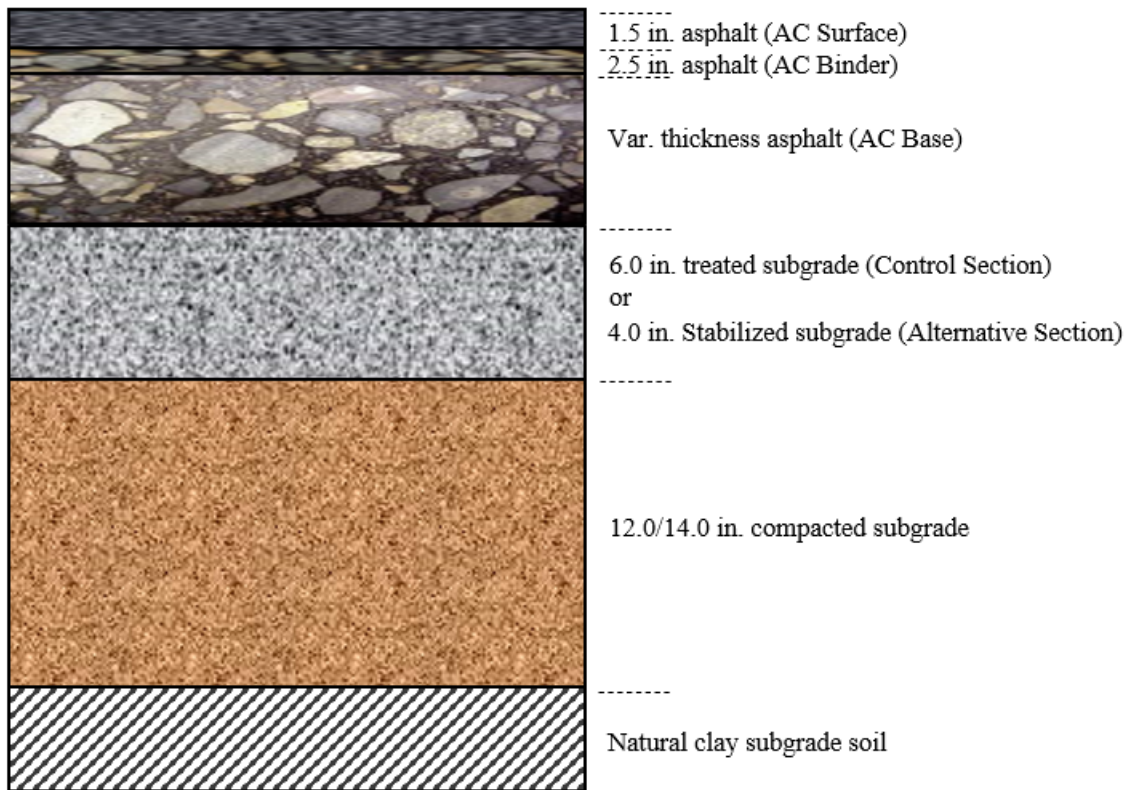
Figure 3.11: Schematic of Designed Pavement Structure

3.11.6 Material Properties

The binder performance grade (PG) for each layer of asphalt concrete was determined based on KDOT requirements, total equivalent single axle loads (ESALs), and percentage of RAP in the mixtures. Table D.4 (Appendix D) shows KDOT requirements. All study sections carried less than 3 million ESALs, and the RAP range was 10%–15%. Asphalt layer properties are shown in Table 3.5.

Table 3.5: MEPDG Inputs for Asphalt Layers

Item	Surface	Intermediate	Base
Thickness (in.)	1.5	2.5	Var.
Binder grade	PG 64-28	PG 64-28	PG 64-22
NMAS (mm)	9.5	19	19
Unit weight (pcf)	145	145	145
Effective binder content (% volume)	11	11	11
Air voids (%)	8	8	7
Poisson's ratio	0.35	0.35	0.35
Reference temperature (°F)	70	70	70
Thermal conductivity (BTU/hr-ft-°F)	0.67	0.67	0.67
Heat capacity (BTU/lb-°F)	0.23	0.23	0.23
Thermal contraction	1.326E-05	1.326E-05	1.25E-05

A 4-in.-thick layer of stabilized subgrade or a 6-in.-thick layer of treated subgrade was taken immediately beneath the asphalt concrete layers. The thickness of the stabilized subgrade was based on results of this research, while common KDOT practice utilizes a 6-in. chemically treated subgrade. Properties of the stabilized subgrade were estimated based on laboratory results for soil-cement mixtures designed in the laboratory, and properties of original pavement in Kansas were used as inputs for the chemically treated layer. The current version of MEPDG does not allow a chemically stabilized/treated subgrade layer under a flexible pavement structure; therefore, a non-stabilized base layer was selected in the software, but properties of the stabilized/treated subgrade were used. MEPDG software requires subgrade resilient modulus as the main design input for subgrade beneath full-depth asphalt pavement, so the modulus of chemically stabilized mixtures in this study was calculated according to the MEPDG (AASHTO, 2015). The elastic modulus of soil-cement mixtures was calculated based on the measured UCS as follows:

$$E = 1200(q_u)$$

Equation 3.2

Where,

E = elastic modulus (psi), and

q_u = unconfined compressive strength of soil-cement measured according to ASTM D1633 (psi).

Other essential inputs for subgrade soil material included gradation, Atterberg limits, specific gravity of solids, MDD, and optimum water content. Corresponding laboratory-measured values were used for stabilized subgrade with soil-cement mixtures, and parameters from original KDOT pavement structures were used for the treated subgrade. For the Poisson's ratio, a KDOT-recommended value of 0.2 was used for all treated or stabilized subgrades; a typical value for Poisson's ratio for soil-cement is 0.15–0.35 (Applied Research Associates, Inc., 2004). A 12-in. compacted subgrade underneath the chemically stabilized/treated subgrade was used in all designs. Properties of the compacted subgrade were taken from the selected projects. All original rigid pavement structures were built over AASHTO A-7-6 soil.

3.11.7 Climate

This study utilized the climate inputs of hourly temperature, precipitation, wind speed, RH, and cloud cover. The closest weather stations were selected for the K-57 and US-81 route projects. The station used for the K-57 project was near Marion, Kansas, while the US-81 project was near Cloud County, Kansas. For the I-70 route project, a virtual weather station was created in Wabaunsee County.

3.12 Economic Analysis Method

Economic analysis for pavements is commonly done at network and project levels. Network-level analysis determines project feasibility, while project-level analysis compares alternatives that meet project needs over the same time period but have variable costs and benefits. Life-cycle cost analysis (LCCA) compares project alternatives rationally by estimating the total cost incurred during the complete life cycle of the pavement, including initial construction, maintenance, rehabilitation, and salvage value. To calculate costs occurring during the analysis period, alternatives must first be established and timing and associated costs must be determined. Two commonly used economic indicators in LCCA estimates are NPV and the equivalent uniform annual cost (EUAC). NPV is the discounted monetary value of expected net benefits (i.e., benefits minus cost), calculated as follows (Mallick & El-Korchi, 2018):

$$NPV = intial\ cost + \sum_{K=1}^{N} Rehabilitation\ Cost_k \left[\frac{1}{(1 + i)^{n_k}}\right]$$

<div align="right">**Equation 3.3**</div>

Where,

i = discount rate (%), and

N = the year of expenditure.

The discount rate is used to calculate the present value of money during the analysis period. NPV can be calculated using a deterministic or a probabilistic approach. In the deterministic approach, a specific value is calculated, while the probabilistic approach considers the discount rate for the variability of factors, such as initial cost. The output of the probabilistic method is a normal distribution rather than a single value. Agency costs and user costs are also considered in the LCCA method. Agency costs include initial construction, routine maintenance, and rehabilitation, while user costs are imposed on users throughout construction and maintenance/rehabilitation activities. Costs that are the same between alternatives are usually excluded from LCCA. Design life for LCCA could be the same as for all evaluated alternatives or different for a specific alternative, but the remaining service life of all alternatives is usually considered.

This study conducted LCCA following the KDOT common practice except it was based only on the initial cost of construction. The deterministic method, according to Equation 3.3, was used to calculate NPV for various pavement alternatives. The analysis period was 40 years according to KDOT requirements for LCCA, and costs were considered only if they differed between alternatives. The initial cost of construction and cost of rehabilitation were estimated at 10-year periods. KDOT does not include user costs, so they were not included in this study. The initial cost of construction included asphalt concrete for traveled way (shoulders were identical for alternatives and not considered), a 6-in. treated or 4-in. stabilized subgrade, existing concrete pavement removal, crushing, and disposal. Rehabilitation actions mentioned were in accordance with KDOT policy for LCCA rehabilitation based on the cumulative ESALs over 10 years but there is no consensus on it. KDOT provided current unit prices of materials and representative rehabilitation actions. Table 3.6 shows initial construction and example rehabilitation actions for each road type.

Table 3.6: Initial Construction and Rehabilitation Actions for Each KDOT Road Category

Year	K-Route	US-Route	Interstate-Route
0	Asphalt concrete construction	Asphalt concrete construction	Asphalt concrete construction
	Treated/stabilized subgrade construction	Treated/stabilized subgrade construction	Treated/stabilized subgrade construction
	Existing concrete Pavement removal, crushing or disposal	Existing concrete Pavement removal, crushing or disposal	Existing concrete Pavement removal, crushing or disposal
10	2-in. surf. recycling + chip seal	1.5-in. cold mill + 1.5-in. overlay	1.5-in. cold mill + 1.5-in. overlay
20	1-in. cold mill + 1-in. overlay	1.5-in. cold mill + 1.5-in. overlay	1.5-in. cold mill + 1.5-in. overlay
30	2-in. surf. recycling + chip seal	1-in. cold mill + 2-in. overlay	1-in. cold mill + 2-in. overlay
40	Salvage value = 0	Salvage value = 0	Salvage value = 0

As shown in Table 3.6, typical rehabilitation actions were identical for each road category (this was due to not having stabilized base in current practice for HMA pavements in Kansas), so the LCC Analysis of this study only considered the initial cost of construction. The control section and stabilized sections were also compared. The control section refers to the common KDOT practice of treating a 6-in. subgrade layer underneath full-depth asphalt concrete; control section properties came from the original KDOT projects. Stabilized sections contained a 4-in. stabilized subbase with the properties of soil-cement or soil-cement-fly ash mixtures as measured in the laboratory in this study. The first scenario assumed the existing concrete pavement was disposed after removal, while the second scenario assumed that the existing concrete pavement was crushed on site and mixed with clay. The objective of the comparison was to identify potential cost savings from stabilization with RCA versus treating clay subgrade.

3.13 Scanning Electron Microscopy

SEM samples were cored from compacted specimens prepared according to the procedure described for the UCS test in Section 3.9.2. Compacted specimens were cured for 28 days and then prepared for coring. A representative sample was obtained from the middle of the compacted specimen and placed in a plastic container and covered with potting epoxy. To facilitate epoxy

curing and remove air from the sample, the epoxied sample was then put into a vacuum chamber with a maintained pressure of 1.2 ± 0.12 in Hg for 45 min. The sample then set overnight to allow the epoxy to cure and harden. SEM samples were cored from the prepared sample using a 0.5-in. core drill. The cored sample was then cut using a saw-cut machine to a thickness of approximately 0.1 inches. Figure 3.12 illustrates sample preparation for SEM.

Figure 3.12: SEM Sample Preparation, Epoxy Curing, and Sample Coring and Cutting

The prepared SEM samples were then mounted onto an aluminum stub using double-sided conductive tape. Soil samples were coated with palladium to prevent a charging effect, or a rapid charge of material under the electron beam that can cause a dielectric breakdown in certain regions of the specimen, leading to complex image artifacts (Sabahfar, 2016). Charging causes astigmatism instabilities, excessive brightness, and spurious X-ray signals. The charging effect occurs in nonconductive materials with high resistivity and can be mitigated by creating a conductive layer of metal on the sample (Sabahfar, 2016).

Although samples of this study were initially scanned without treatment, charging occurred. Therefore, after applying the conductive layer of palladium, samples were analyzed using a Hitachi S-3500N scanning electron microscope. Images with a magnification of 500, 2,000, and 5,000 with 10 KV beam accelerating voltage were taken. All SEM images were produced by a secondary electron (SE) signal. Magnification refers to the ratio of the dimension of the area scanned on the monitor device to the area on the specimen (Hafner, 2007). Magnification increases

in correlation with reduced size of the magnified area. Beam-accelerating voltage occurs when electrons accelerate down the microspore column. The interaction of a beam electron with the electric charge field of a specimen produces signal types such as backscattered electrons, SEs, and X-rays (Hafner, 2007). Energy transfer to the specimen atom results in a potential expulsion of an electron known as an SE. The most common SEM mode is the detection of the emitted SE to produce SEM images (Hafner, 2007). Mixtures selected for SEM were 100% clay, 50% clay-50% RCA, 100% clay-8% lime, 50% clay-50% RCA-8% lime, 100% clay-c/f 1:1, and 50% clay-50% RCA-c/f 1:1. Untreated mixtures, or control mixes, were compared with mixtures with highest and lowest improvement caused by RCA. Figure 3.13 shows the SEM mounted samples and the scanning electron microscope.
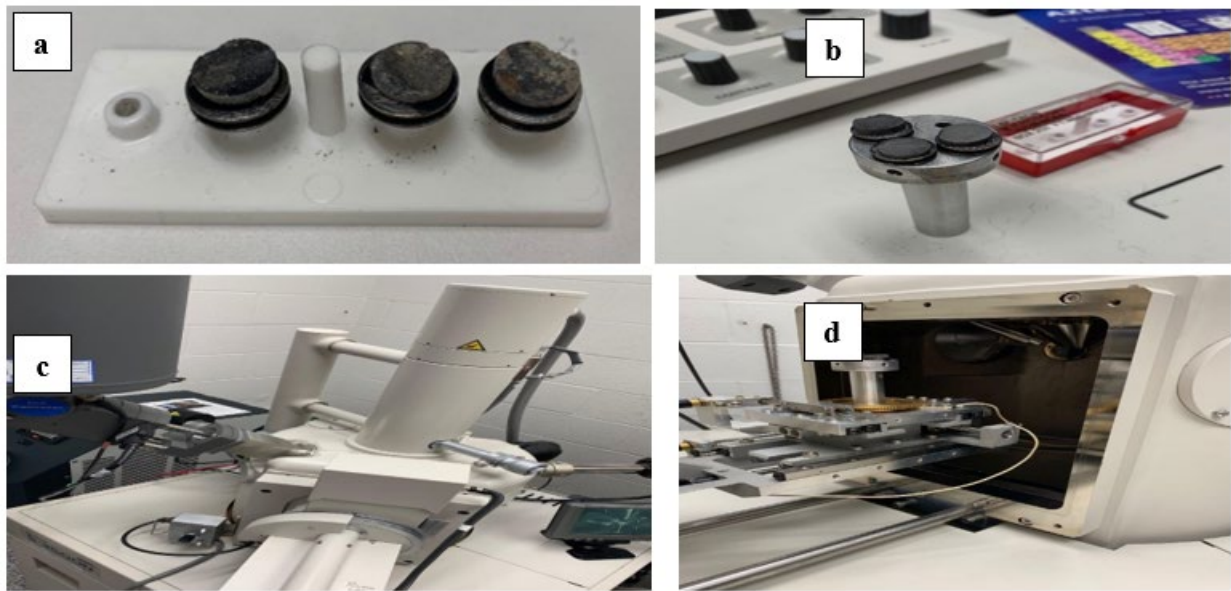
Figure 3.13: a), b) SEM Mounted Samples; c), d) Scanning Electron Microscope

Chapter 4: Results and Discussion

This chapter presents laboratory testing results, performance prediction results using MEPDG, and LCC analysis. Aggregate and A-6 clay test results are presented first, followed by a discussion of designed mixtures and correlating mechanical tests, SEM, MEPDG, and LCCA results. The chapter concludes with laboratory test results of A-4 soil.

4.1 Sieve Analysis, Hydrometer, and Atterberg Limits Test Results

Clay hydrometer analysis parameters were calculated according to ASTM D422 (2007). Results of the sieve analysis of RCA and the combined clay sieve analysis and hydrometer analysis are shown in Figure 4.1, where the curve provides a semi-quantitative sense of aggregate density. The 0.45 power maximum density curve equation is:

$$P = \left(\frac{d}{D}\right)^{0.45}$$

Equation 4.1

Where,

P = % finer than the sieve;

d = aggregate size being considered; and

D = maximum aggregate size to be used.
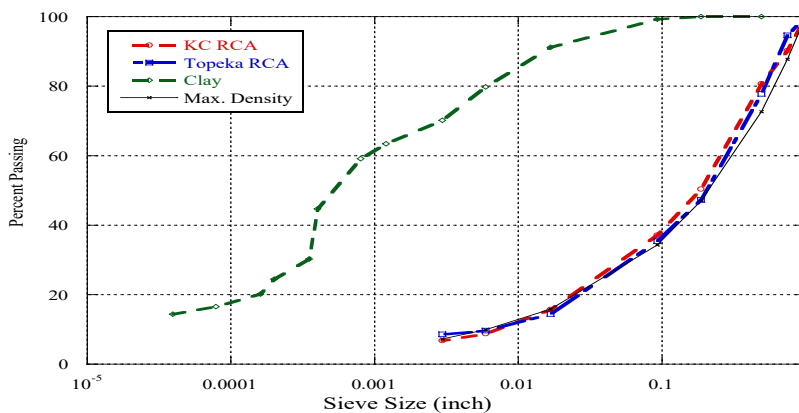
Figure 4.1: Gradation Chart for Topeka RCA, KC RCA, and Clay

As shown in Figure 4.1, the gradations of both RCA sources were close to the maximum density line of a blend with a maximum aggregate size of 1 in., indicating a high density of aggregates. Also, the amount of coarse (retained on the No. 4 sieve) and fine aggregates (passing the No. 4 sieve) were almost equal to 50% for both sources.

Liquid and plastic limits of the clay were determined for the portion of soil passing through the No. 40 sieve. The clay was classified as low plasticity with a plastic limit of 23%, a liquid limit of 38%, and a plasticity index of 15%. The clay in this study was classified according to AASHTO as group A-6 and the USCS as clay with low plasticity.

4.2 Specific Gravity and Absorption of RCA and Clay

The specific gravity and absorption of RCA and clay were measured in the lab according to ASTM D854 and KT-6, a Kansas test procedure. Results are shown in Table 4.1. According to specific gravity test results, RCA bulk specific gravity was lower than the average bulk specific gravity of virgin aggregates used in common concrete or asphalt applications. The amount of absorption, especially for coarse aggregates, was higher than average normal virgin aggregate absorption because the old mortar attached to RCA increased absorption capacity and decreased specific gravity (Verian et al., 2013).

Table 4.1: Specific Gravity and Absorption of RCA and Clay

Item	Topeka RCA	KC RCA	Clay
Bulk specific gravity of coarse aggregates	2.26	2.15	-
Bulk specific gravity of fine aggregates	2.02	1.70	-
Bulk specific gravity of combined aggregates	2.13	1.90	2.50
Absorption of coarse aggregates (%)	5.71	7.51	-
Absorption of fine aggregates (%)	12.64	20.58	-

4.3 Soundness of RCA Aggregates by Freezing and Thawing

The KTMR-21 procedure was used to evaluate the ability of RCA to withstand freezing and thawing, as shown in the results in Table 4.2. Although KDOT does not specify limits for the F-T durability of aggregates for soil stabilization, the KDOT limit for use of RCA in cement-

treated bases is 0.85. No RCA sources in this study demonstrated considerable loss; both RCA sources had an F-T value of 0.85, so no RCA sources were susceptible to F-T mass loss.

Table 4.2: F-T Test Results for RCA Aggregates

Descriptions	Topeka	KC
Loss Ratio	0.96	0.94

4.4 Los Angeles Abrasion Test

Resistance of RCA coarse aggregate to degradation was assessed via the LA abrasion test. A representative sample of approximately 11 lb was prepared according to gradation B of ASTM C131. Table 4.3 shows average LA abrasion test results from two samples. Abrasion loss of the KC aggregate was higher than the Topeka aggregate, which lost approximately 50% of the test fraction. The maximum acceptable wear of aggregates for KDOT concrete and cement-treated base applications ranges from 40% to 60%, specifically 50%–60% for on-grade applications and 40% for not-on-grade applications. Both RCA sources showed high potential to wear, likely due to the old mortar in the RCA (Verian et al., 2013).

Table 4.3: Average LA Test Results for RCA Aggregates

RCA Aggregate	LA Abrasion Loss (%)	Gradation of Test Sample (ASTM C131)
Topeka	36	B
KC	52	B

4.5 Stabilized Soil-Cement-RCA Mixture Design

Study mixtures were designed according to the USACE procedure, beginning with the selection of blends of clay and RCA. Candidate blends of 100% clay (by weight), 50% RCA-50% clay, and 100% RCA were selected for further evaluation. An initial percentage of binder content to achieve minimum 250 psi UCS in 28 days as specified in the USACE procedure and additional mixtures with varying binder contents were developed and tested for UCS. Mixture design results are presented in the following sections.

4.5.1 Selected Blends of RCA and Clay

The first step in designing clay-RCA mixtures was to select clay and RCA blends. Mixtures containing clay only (i.e., 100% clay) were studied as control mixtures to obtain base requirements for clay stabilization. RCA replaced 50% by weight of clay in order to assess RCA effectiveness. The second blend was 50% clay-50% RCA; mixtures of 100% RCA were also studied to obtain information about RCA material characteristics. The procedure to stabilize all three blends was identical, with minor modifications to observe various material characteristics, including modifications to specimen size and the procedure to estimate the initial chemical agent content. Figure 4.2 shows the gradation graph for 50% clay-50% RCA blends. The gradation of 100% clay and 100% RCA are shown for comparison.
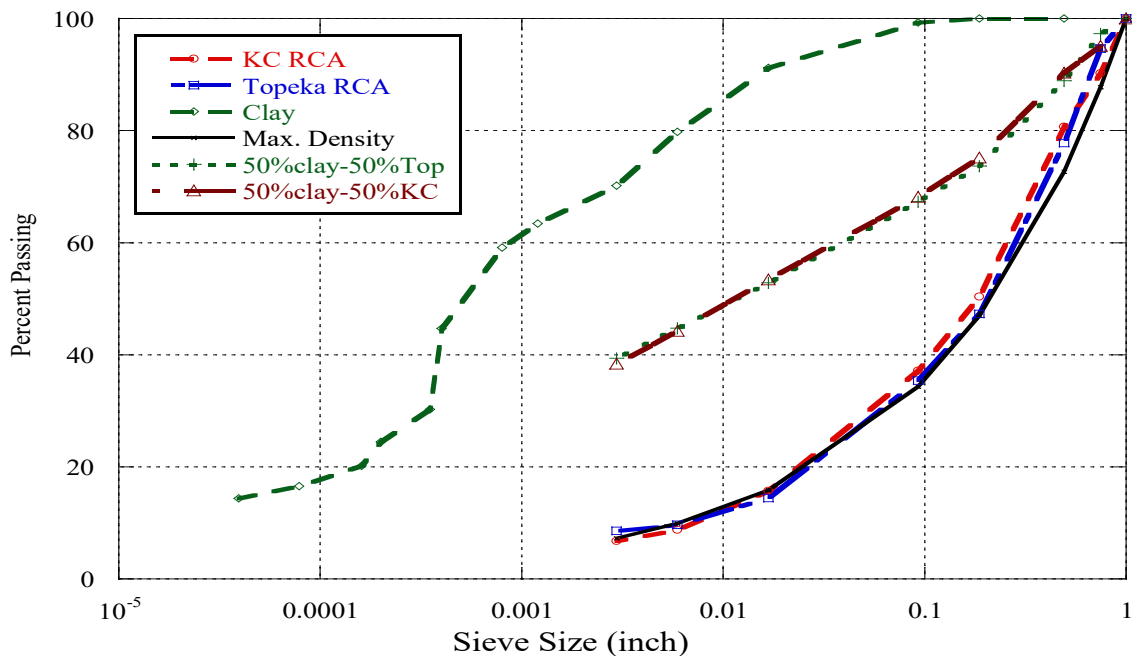
Figure 4.2: Gradation Chart for 50% Clay-50% RCA Blends

4.5.2 Initial Binder Content Estimation

Chemical binders used in this study were lime, Class C fly ash, and a combination of Class C fly ash and portland cement. An initial binder percentage was selected for each type of stabilizer in accordance with methods described in Chapter 3.

4.5.2.1 Initial Binder Content for Lime Mixtures

The initial binder content of lime mixtures was estimated by measuring the pH of various blends of lime-clay-RCA. A varying percentage of lime, based on the total dry weight of the sample, was added to a portion of sample that passed through the No. 40 sieve. The pH of the blended slurry of soil, lime, and water was measured (Table 4.4).

Table 4.4: Measured pH for Various Blends

% Lime	3%	4%	5%	6%	6.5%	7.5%	8%	9%	2 gm lime
100% clay	13.21	13.26	13.29	13.28	13.30	13.30	13.31	13.32	13.34
50% clay-50% Topeka	12.56	12.59	12.61	12.62	12.70	12.73			12.73
50% clay-50% KC	12.65	12.68	12.69	12.71	12.72	12.73			12.73
100% Topeka	12.77	12.77	12.78	12.79	12.79	12.80			12.81
100% KC	12.71	12.72	12.73	12.73	12.74	12.74			12.74

All samples had a measured pH above 12.4. For soils with pH greater than 12.4, the lowest percentage of lime, where the pH value did not rise for at least two successive test samples, was the optimum lime content (i.e., the initial lime estimation). For 100% clay, the pH test results for two consecutive tests after 6% were identical, so 6% was selected as the initial estimation for lime content of 100% clay mixtures. The pH of 50% clay-50% Topeka and 50% clay-50% KC mixtures became stable around 4% and 6%, respectively. The 100% RCA lime mixtures did not show any significant change in pH when lime content increased. Both RCA mixtures were comprised of limestone with a high calcium concentration; therefore, the addition of lime did not increase the pH of the sample. The pH of the lime-water slurry was nearly identical to the pH of lime-water-RCA slurries. All test results indicated a range of 4%–6% as the optimum lime content, so an initial lime content of 6% was selected for all blends. The standard Proctor test (ASTM D698, 2012) was performed on mixtures with 6% lime. Additional mixtures with 8% lime were also developed, and the UCS test was run on both mixture types.

4.5.2.2 Initial Binder Content for Fly Ash Mixtures

A single-point standard Proctor test was conducted on mixtures with fly ash contents varying between 10% and 20% to estimate the initial percentage of fly ash. The single-point Proctor test is a compaction test that keeps water content constant while changing the percentage of fly ash. The amount of fly ash yielding the highest MDD was selected as the initial estimation of fly ash content. For 100% clay, fly ash content of 13%–25% was tested at 3% intervals. Water additions to all mixtures remained constant as a trial estimation for the OMC of fly ash mixtures. Figure 4.3 shows the results of the single-point standard Proctor test when estimating initial fly ash content of 100% clay mixtures. As suggested by the results, the optimum percentage of fly ash was 19% to achieve the highest MDD.
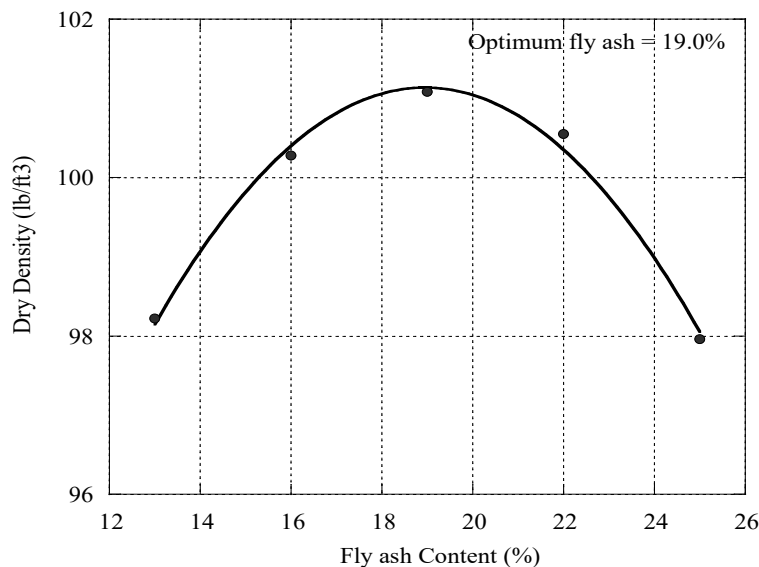
Figure 4.3: Estimation of Initial Fly Ash Content for 100% Clay (Water Content 13%)

The standard Proctor test was performed on mixtures with 13%, 16%, and 19% fly ash (Appendix C, Figures C.1–C.3) to verify results of the single-point compaction curve. The mixture with 19% fly ash resulted in the highest MDD, confirming the results shown in Figure 4.3. Thus, for 100% clay mixtures, 19% fly ash was selected as the initial estimation of the optimum binder content. Mixtures with $19 \pm 3\%$ were made and tested with the UCS test.

A single-point standard Proctor test was first performed on mixture blends of 50% clay-50% RCA with fly ash ranges of 5%–20% at 3% intervals. Figure 4.4 shows the single-point compaction test results on 50% clay-50% KC. Based on the results, 12% fly ash resulted in the highest MDD for the KC RCA.
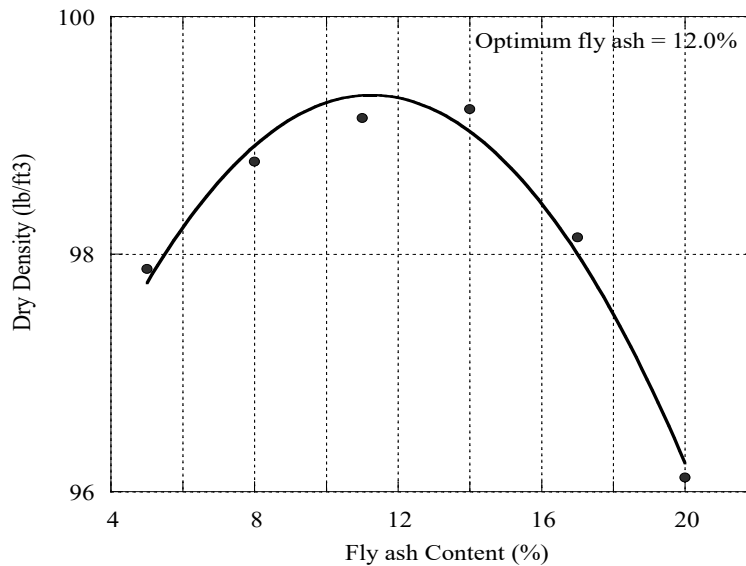
Figure 4.4: Estimation of Initial Fly Ash Content for 50% Clay-50% RCA (Water Content 19%)

A standard Proctor test (i.e., dry density as a function of water content) was then performed on mixtures with 50% clay-50% KC with 12% and 14% fly ash to verify the single-point compaction test results. The compaction curve of the mixture with 14% fly ash suggested a higher MDD than the 12% fly ash, contradicting the single-point findings. These curves are included in Appendix C and shown in Figures C.4 and C.5. Because the highest MDD was obtained with 14% standard Proctor test, 14% was selected as the initial binder content to make UCS specimens. Mixtures of 50% clay-50% RCA with 14% and 17% fly ash were initially developed, but based on UCS test results, none of these mixtures achieved the design target strength of 250 psi. Thus, additional mixtures with 20% fly ash were tested. The overall results for estimating a binder content range for 50% clay-50% RCA mixtures resulted in the development of mixtures with 17 $\pm 3\%$ fly ash. The USACE method was not followed for 100% RCA because the procedure applies to soil stabilization only. Instead, 5% was selected as the initial estimation for fly ash content based

on the results of another study of Topeka and KC RCA for developing cement-treated base mixtures (Daily, 2018).

4.5.2.3 Initial Binder Content for Fly Ash-Portland Cement Mixtures

According to USACE, the initial estimation for fly ash content is used as the total binder content of fly ash-portland cement mixtures. Therefore, total binder contents of 19%, 14%, and 5% were selected for 100% clay, 50% clay-50% RCA, and 100% RCA mixtures, respectively. The ratio of cement to fly ash yielding the highest strength was determined by selecting 1:1 and 1:2 as trial ratios of portland cement to fly ash. Mixtures with total binder content and proportions of portland cement to fly ash were developed and tested for UCS.

In summary, 36 mixtures were studied, including 31 stabilized mixtures containing blends of RCA, clay, and chemical stabilizers, and five control, untreated mixtures with no chemical agent. Table 4.5 summarizes the developed mixtures.

Table 4.5: Mixtures Developed with Various Stabilizers

Mix	Lime (%)	Fly ash (%)	Fly ash-Portland cement
100% clay	6–8	19 ± 3	19 (c/f ratio of 1:1&1:2)
50% clay-50% RCA	6–8	17 ± 3	14 (c/f ratio of 1:1&1:2)
100% RCA	6–8	5	5 (c/f ratio of 1:1&1:2)

*c/f represents the ratio of portland cement to fly ash

4.6 Standard Proctor Test Results

This study measured the compaction curve parameters (OMC, MDD) of clay and RCA materials, as well as the developed mixtures with the initial binder content. Figure 4.5–Figure 4.9 show the results of the standard Proctor test for untreated materials. Other results for mixtures with initial binder estimation are shown in Figures C.6–C.15 in Appendix C.
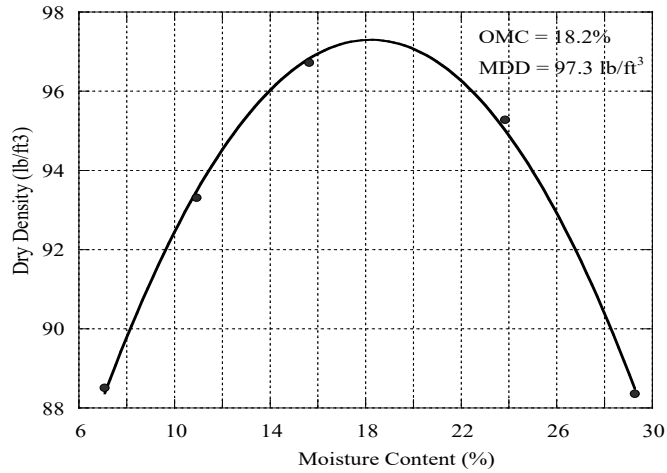
Figure 4.5: Compaction Curve for Untreated Clay
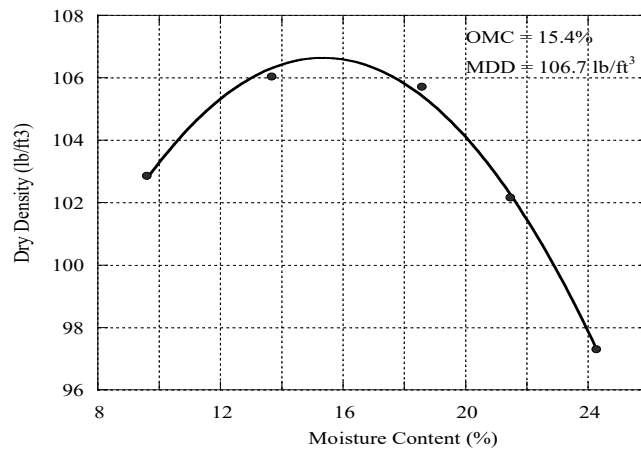
Figure 4.6: Compaction Curve for 50% Clay-50% Topeka
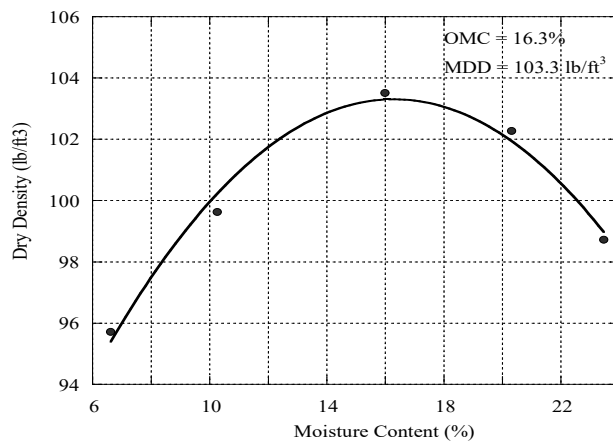
Figure 4.7: Compaction Curve for 50% Clay-50% KC
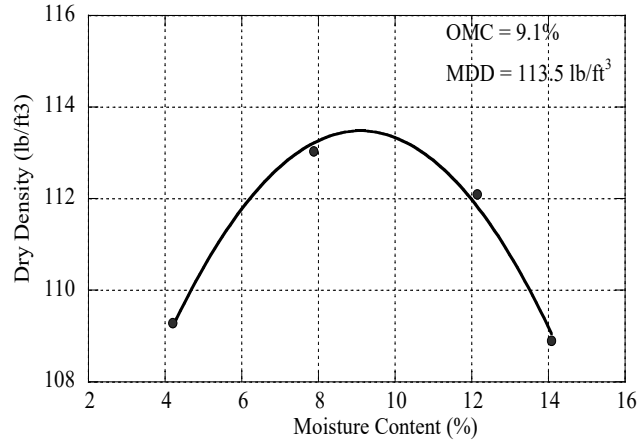
Figure 4.8: Compaction Curve for Untreated 100% Topeka RCA
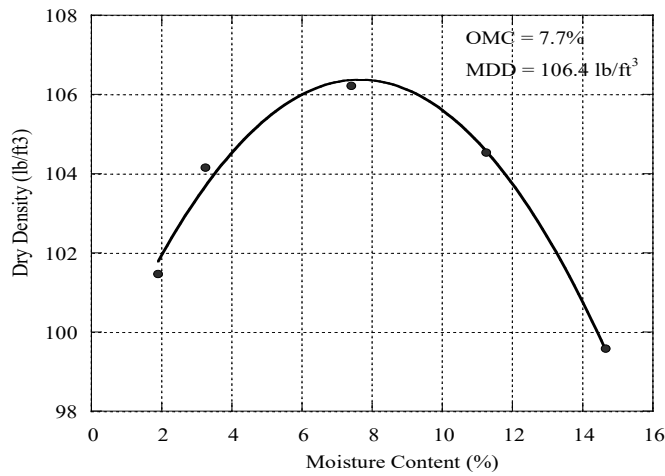
Figure 4.9: Compaction Curve for Untreated 100% KC RCA

As shown in Figure 4.5–Figure 4.7, the addition of 50% RCA into clay resulted in decreased OMC and increased MDD. The 100% RCA (Figure 4.8 and Figure 4.9) had lower OMC and higher MDD compared to 100% clay and 50% clay-50% RCA mixtures. Results of this study confirmed previously known effects of lime and fly ash on compaction curve parameters. Lime resulted in decreased MDD and increased OMC, but fly ash improved compaction curve parameters because fly ash particles, which have a specific gravity higher than clay, may fill the voids in clay, causing a higher MDD of the compacted clay-fly ash mixture. The decreased OMC may be attributed to the low affinity of fly ash to water. For lime mixtures, decreased MDD is possibly due to the lower specific gravity of lime compared to clay. Second, particle aggregation could alter the clay fabric by reorienting the structure to a more flocculated matrix. In fact, the

SEM and EDX investigations sought to identify the cause of observed effects of the RCA and treatments. The increased OMC may be due to the pozzolanic reaction of lime and clay (Al-Swaidani et al., 2016; Osinubi, 1998). MDD and OMC of stabilized mixtures also depend on the delay between mixing and final compaction of the mixture. However, the addition of fly ash or lime to clay results in flocculation and agglomeration of clay particles (Banda, 2003), and flocculated particles have less tendency to be compacted. Thus, compactive effort must overcome cementation, resulting in decreased MDD (Banda, 2003). In this study, the delay between mixing and compaction was approximately 1 hr for both lime and fly ash mixtures. The change in compaction properties caused by lime and fly ash were the same for all mixtures, even in the presence of RCA. Table 4.6 summarizes compaction test results of all mixtures in this study.

Table 4.6: Standard Proctor Test Results for Various Mixtures

Mixture		OMC (%)	MDD (lb/ft3)
100% clay	Untreated	18.2	97.3
	19% fly ash	16.0	104.0
	6% lime	19.8	95.8
50% clay-50% KC	Untreated	16.3	103.3
	14% fly ash	15.7	106.4
	6% lime	17.1	101.7
50% clay-50% Topeka	Untreated	15.4	106.7
	14% fly ash	15.8	109.3
	6% lime	17.4	104.2
100% KC	Untreated	7.7	106.4
	5% fly ash	8.6	109.2
	6% lime	8.4	103.3
100% Topeka	Untreated	9.1	113.5
	5% fly ash	10.2	116.9
	6% lime	10.8	114.2

4.7 UCS Test Results

The UCS test was run on mixtures with an initial binder estimation and a percentage above or below that estimation (percentages shown in Table 4.5). The purpose of testing different mixtures was to identify a binder content resulting in the design target compressive strength of 250 psi at 28 days, as specified in the USACE method. A total of six specimens were made for each mixture, and three replicate specimens were tested at 7 and 28 days after the curing period. In addition, untreated control mixtures containing no chemical agent were developed and tested. All specimens were compacted at OMC and MDD. The UCS was calculated as:

$$UCS = \frac{F_{max}}{A}$$

Equation 4.2

Where,

UCS = unconfined compressive strength (psi),

F_{max} = maximum recorded load of the specimen during test (lb), and

A = specimen cross section (in^2).

Tables B.1–B.18 (Appendix B) include UCS results for each specimen. The average compressive strength of each mixture computed based on the results of three specimens is summarized in Table 4.7–Table 4.9 and Figure 4.10–Figure 4.13.
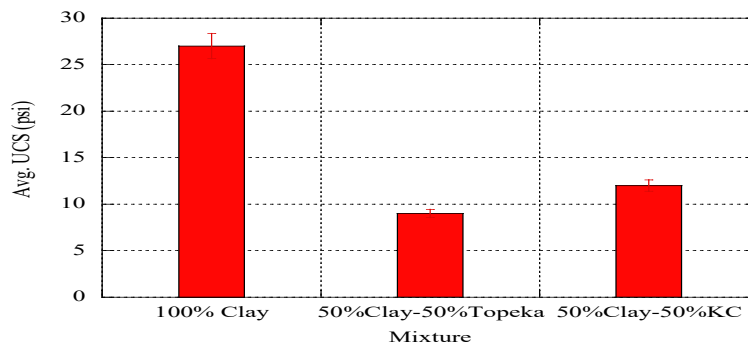
Figure 4.10: Average UCS of Untreated Mixtures

As shown in Figure 4.10, the UCS value of untreated 100% clay was 27 psi. The corresponding value was 12 psi for untreated 50% clay-50% KC RCA and 9 psi for 50% clay-50% Topeka RCA. Thus, mechanically stabilizing clay with 50% RCA was not effective because it

decreased the strength of untreated clay due to the inadequate bond between RCA-clay particles, as validated by SEM results.

However, based on the results of stabilized clay with fly ash, improved UCS of fly ash mixtures was observed as compared to untreated mixtures, although, with the exception of the 50% clay-50% KC mixture with a UCS of 106 psi, the improvement was not notable compared to the target strength. No fly ash mixtures achieved the target design strength of 250 psi. The replacement of clay with 50% RCA helped achieve higher strength levels compared to 100% clay even though lower quantities of fly ash were used. Fly ash results are shown in Table 4.7 and Figure 4.11.

Table 4.7: Average UCS of Fly Ash Mixtures

Mixture	Fly ash content	Avg. 7-day UCS (psi)	Avg. 28-day UCS (psi)
100% clay	16%	13	13
	19%	42	72
	22%	58	65
50% clay-50% Topeka	14%	15	17
	17%	26	44
	20%	70	75
50% clay-50% KC	14%	49	75
	17%	44	106
	20%	43	81
100% Topeka	5%	28	36
100% KC	5%	24	41
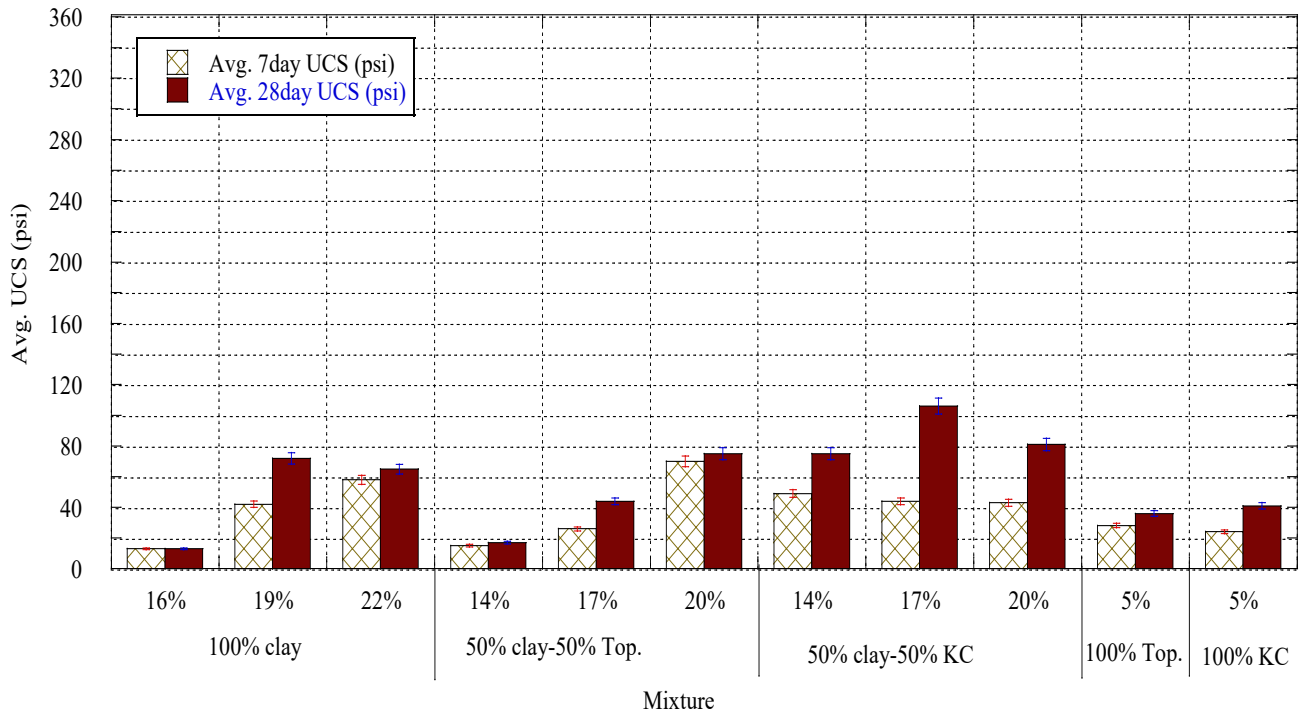
Figure 4.11: Average UCS of Fly Ash Mixtures

The combination of fly ash and portland cement was the only binder type to achieve the design target. However, even this achievement was only possible when RCA was present in the mixture (Table 4.8 and Figure 4.12). As shown in Figure 4.12, 50% clay-50% RCA mixtures with fly ash and portland cement demonstrated considerable improvement in strength. The maximum observed strength for 100% clay was 148 psi, whereas 335 psi was the maximum observed strength for 50% clay-50% RCA. The higher strength was achieved despite the lower total quantity of binder in the mixtures containing RCA. The increased strength of 50% clay-50% RCA mixtures can be attributed to the high strength of RCA aggregates and improved interface of the bond between aggregate-cementitious products. Mixtures with 50% clay and 50% RCA had considerably higher amounts of chemical binders compared to mixtures with 100% RCA; thus, 50% clay-50% RCA mixtures developed higher compressive strength.

Table 4.8: Average UCS of Fly Ash-Portland Cement Mixtures

Mixture	Fly ash-cement content	Avg. 7-day UCS (psi)	Avg. 28-day UCS (psi)
100% clay	c/f 1:2	125	148
	c/f 1:1	91	123
50% clay-50% Topeka	c/f 1:2	132	276
	c/f 1:1	149	335
50% clay-50% KC	c/f 1:2	144	285
	c/f 1:1	258	321
100% Topeka	c/f 1:2	112	159
	c/f 1:1	166	220
100% KC	c/f 1:2	55	150
	c/f 1:1	121	162

*c/f represents the cement to fly ash ratio.
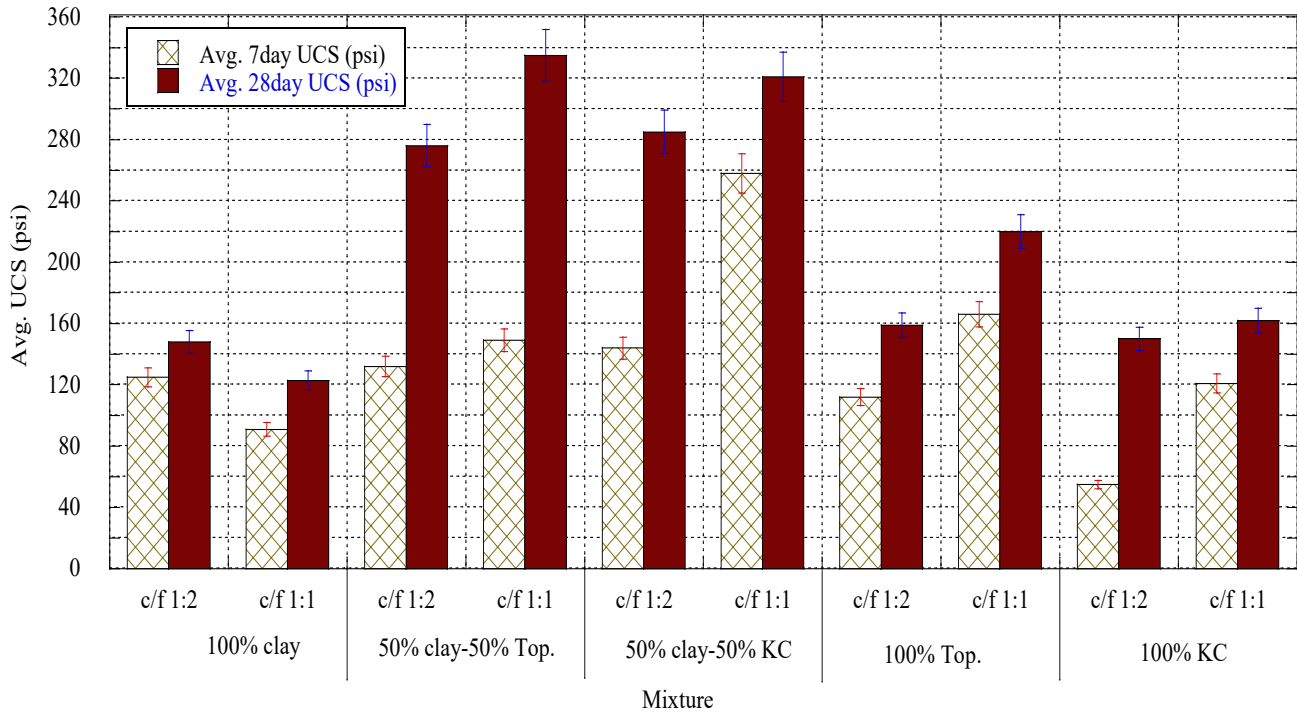
Figure 4.12: Average UCS of Fly Ash-Portland Cement Mixtures

Table 4.9 and Figure 4.13 show the results of the UCS test for lime mixtures. Although lime improved the UCS of all mixtures, the improvement was not sufficient to reach the target strength. The average UCS of lime mixtures was notably lower than the target design strength of

250 psi (maximum UCS was 65 psi). Also, the 50% clay-50% RCA blend did not gain additional strength. The lower strength of lime mixtures compared to other chemical agents was due to the insufficient presence of clay pozzolans that are essential for pozzolanic reaction and strength development. Lime has been shown to effectively stabilize clay with a minimum plasticity index of 12 (USACE, 1994). RCA did not cause additional improvement in strength due to the inadequate bond formed between RCA and clay, as validated by SEM results. Therefore, lime was disqualified from further evaluation in this study.

Table 4.9: Average UCS of Lime Mixtures

Mixture	Lime content	Avg. 7-day UCS (psi)	Avg. 28-day UCS (psi)
100% clay	6%	30	50
	8%	34	61
50% clay-50% Topeka	6%	28	54
	8%	37	61
50% clay-50% KC	6%	29	56
	8%	39	54
100% Topeka	6%	28	41
	8%	24	55
100% KC	6%	55	68
	8%	26	43
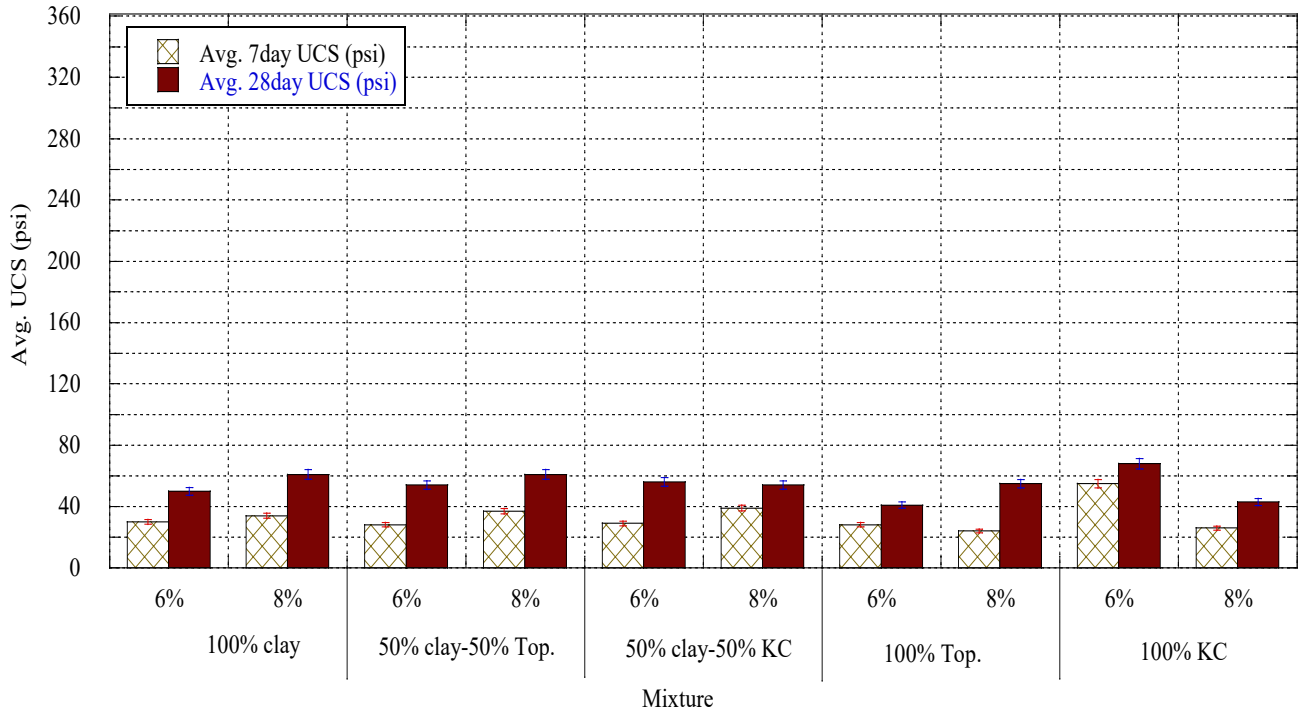
Figure 4.13: Average UCS of Lime Mixtures

4.8 Linear Shrinkage Test Results

This study also measured linear shrinkage of the designed mixtures according to ASTM C157. For each mixture, two replicate specimens were compacted using the standard Proctor effort in two layers at OMC and MDD. Length change of the specimens was tracked over time at certain intervals for up to 112 days. The length change of any specimen at any age after the initial comparator reading (in microstrain) was calculated as:

$$\varepsilon_x = \frac{L_x - L_0}{L_0} \times 10^6$$

Equation 4.3

Where,

ε_x = length change of specimen at any age, microstrain,

Lx = specimen length at any age (in.), and

L_0 = initial specimen length (in.).

Figures 4.14–4.19 summarize the average length change of various mixtures. Results of the untreated mixtures (Figure 4.14) show that most shrinkage occurred during the first two weeks after water was added to the soil or soil aggregate, and then shrinkage progressed due to moisture

loss, finally becoming stable after around three weeks. Although the untreated mixtures showed the highest amount of shrinkage, the untreated 100% clay showed a considerably higher shrinkage level than the 50% clay-50% RCA mixture. The shrinkage strain of untreated 100% clay at 112 days was approximately 33,000 microstrain, while the corresponding value for 50% clay-50% RCA was 5,200–10,700 microstrain. The increased shrinkage of 100% clay was due to the increased amount of water required for compaction and the weaker structure of clay compared to the soil-aggregate matrix. Because moisture loss is the underlying cause of shrinkage, an increased amount of water in the mix has been shown to cause increased shrinkage (Mindess et al., 2002). RCA decreased the required amount of water for compaction. Clay is naturally subject to shrinkage, but coarse RCA aggregates have a restraining influence on volume change because they are dimensionally stable under changing moisture conditions (Mindess et al., 2002).
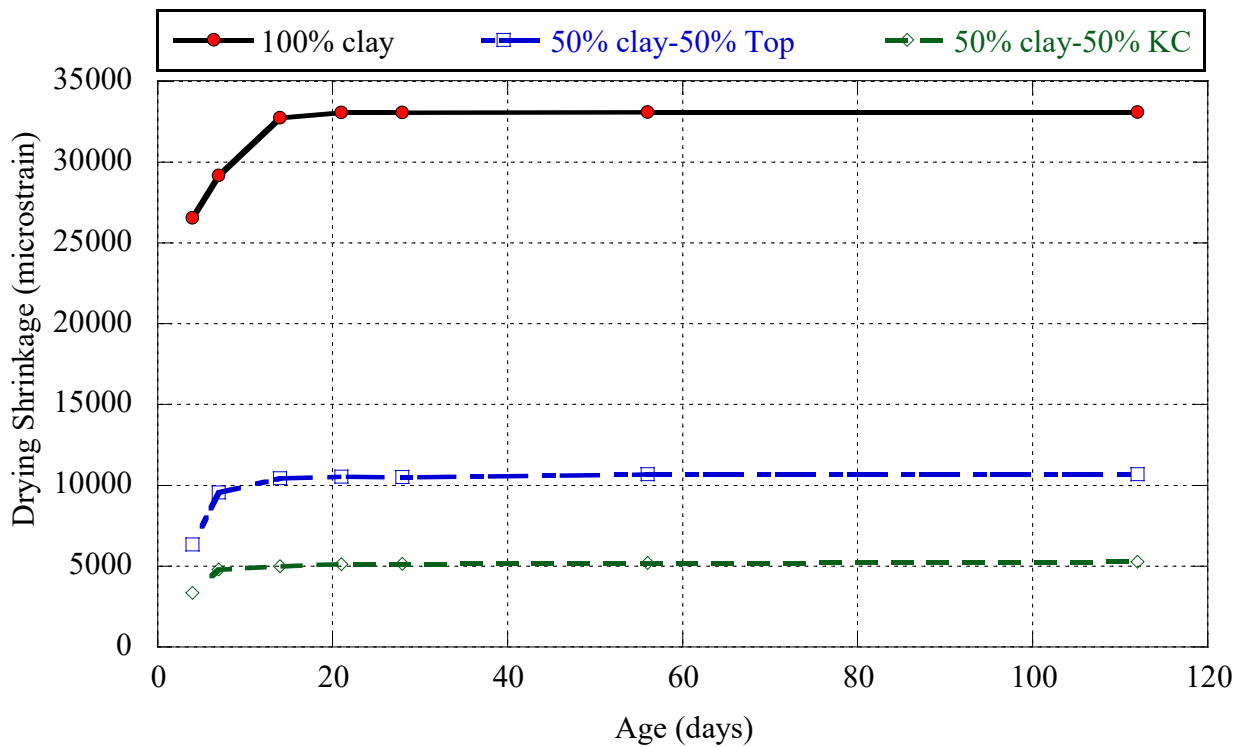
Figure 4.14: Linear Shrinkage Test Results for Untreated Mixtures

Chemically stabilized mixtures (Figure 4.15) showed considerably less shrinkage strain than non-stabilized mixtures. Stabilization causes the rearrangement of soil particles and improves

82

soil texture. The formation of hydration products binds the soil particles, meaning stabilized soil has a strong structure that is less susceptible to deformation due to moisture change (Mindess et al., 2002). Among all stabilized mixtures, fly ash mixtures proved most effective in reducing shrinkage. The improvement due to fly ash increased by an increase in the percentage of fly ash in the mixture because of the dilution effect of fly ash. The slow hydration of fly ash increases the effective water-to-binder ratio, thereby reducing early shrinkage (Kou et al., 2007; Wu et al., 2017).
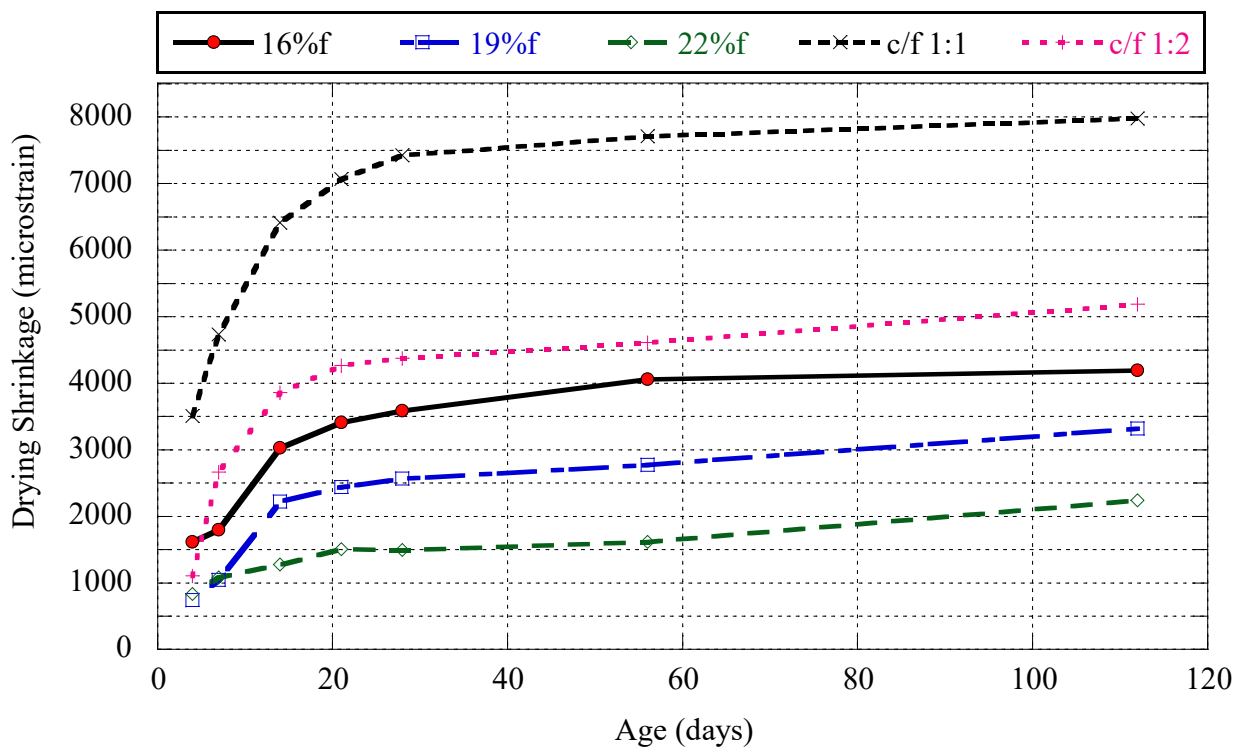
Figure 4.15: Linear Shrinkage Test Results for Stabilized Mixtures of 100% Clay

As shown in Figure 4.16 and Figure 4.17, RCA inhibited shrinkage of the stabilized mixtures. Shrinkage strain of stabilized 100% clay was 2,200–8,000 microstrain at 112 days (Figure 4.15). Comparatively, corresponding shrinkage strain of stabilized soil-RCA mixtures was 650–2,400 microstrain. Previous studies have determined that RCA aggregates act as internal curing agents due to their high porosity, thereby providing water to reduce shrinkage (Gonzalez-Corominas & Etxeberria, 2016; Wu et al., 2017). Over time, free water in the matrix gradually

decreases due to progressive hydration of cement and evaporation, and the reduction in internal RH changes the saturation state of the capillary pore and causes rearrangement and the formation of new pores. Consequently, capillary pore pressure increases. Capillary tension decreases when water from RCA pores transfers to the new cement paste (Wu et al., 2017). Low-quality RCA has been shown to effectively reduce shrinkage because decreased quality of the RCA means increased pore size distribution of the old cement paste, thereby facilitating increased capillary water transportation to the new cement paste (Gonzalez-Corominas & Etxeberria, 2016). Previous findings were further verified by these results, when mixtures of soil and KC RCA showed less shrinkage than Topeka mixtures. KC aggregate had higher absorption and lower specific gravity, indicating a higher porosity of aggregate.
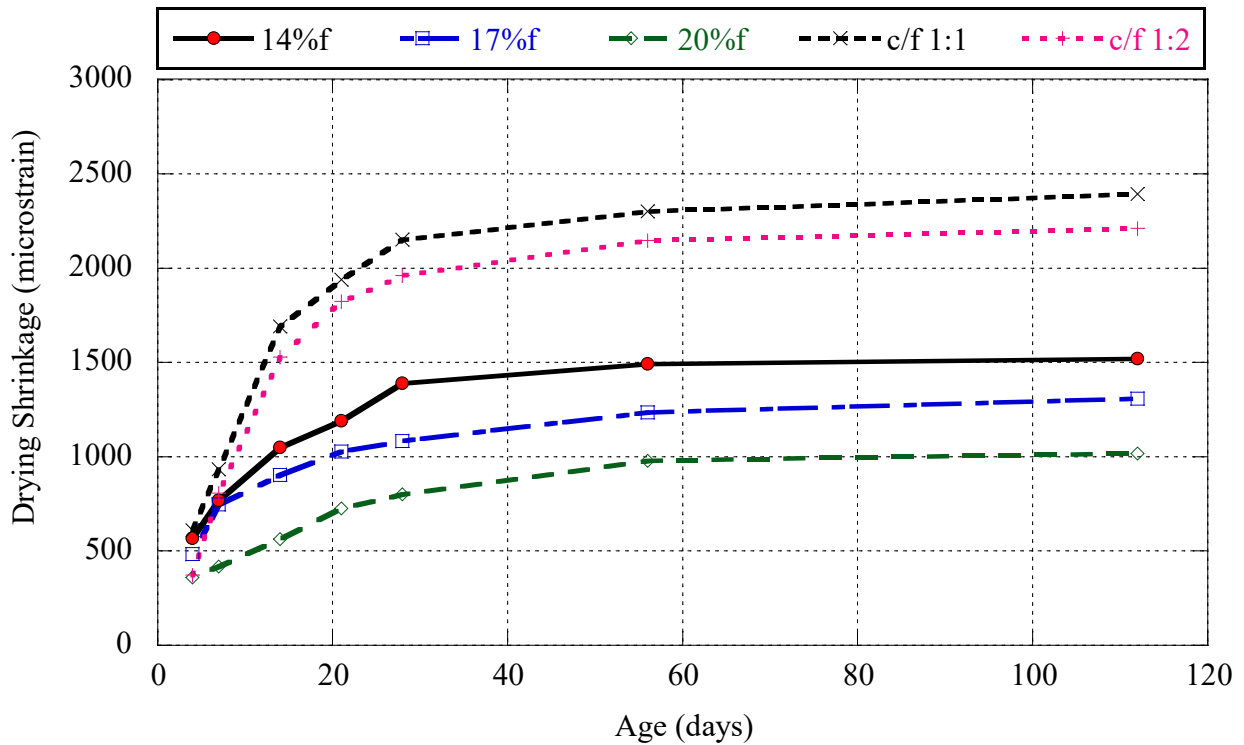
Figure 4.16: Linear Shrinkage Test Results for Stabilized Mixtures of 50% Clay-50% Topeka
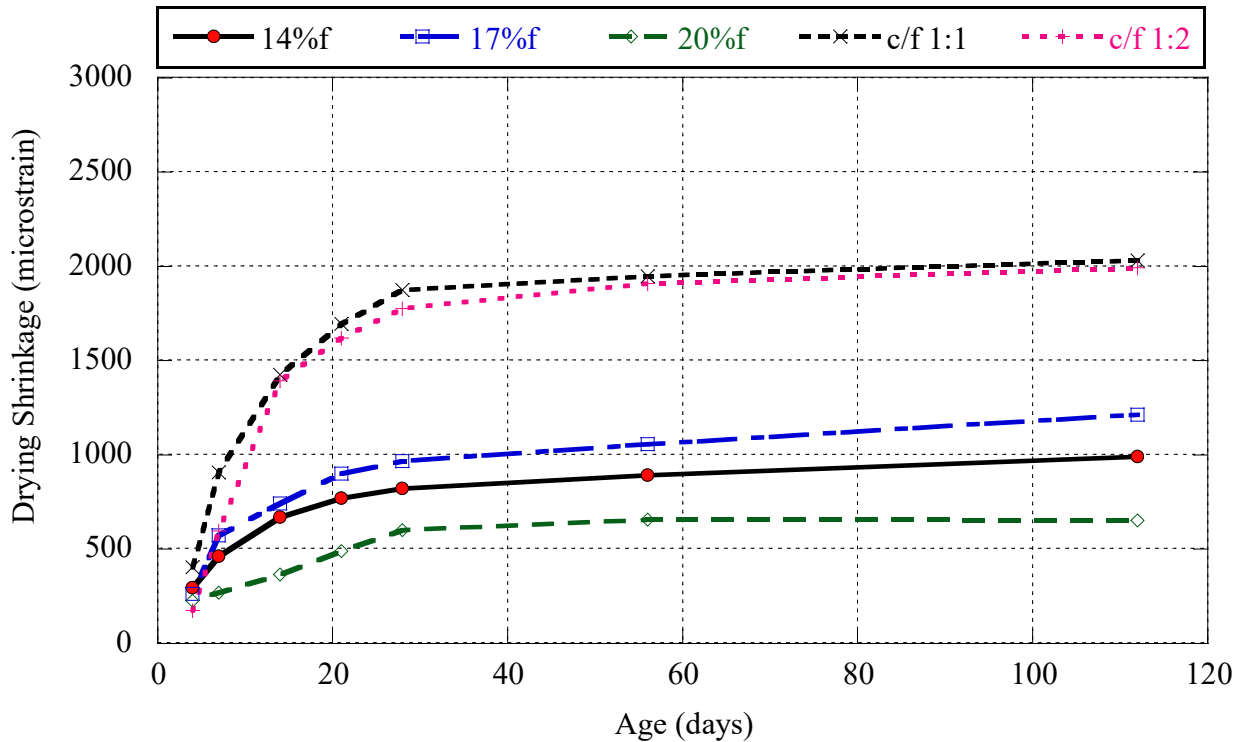
Figure 4.17: Linear Shrinkage Test Results for Stabilized Mixtures of 50% Clay-50% KC

Linear shrinkage test results of 100% RCA are shown in Figure 4.18 and Figure 4.19. The maximum shrinkage strain for 100% RCA at 112 days was approximately 475 microstrain. The linear shrinkage of 100% RCA was considerably lower than other mixtures in this study because, as mentioned, RCA coarse aggregates are dimensionally more stable under moisture change than clay, resulting in less shrinkage. In addition, KC RCA showed less shrinkage than Topeka RCA because, as explained for 50% clay-50% RCA mixes, the high porosity of KC aggregates readily facilitates transportation of capillary water to the new cement paste.
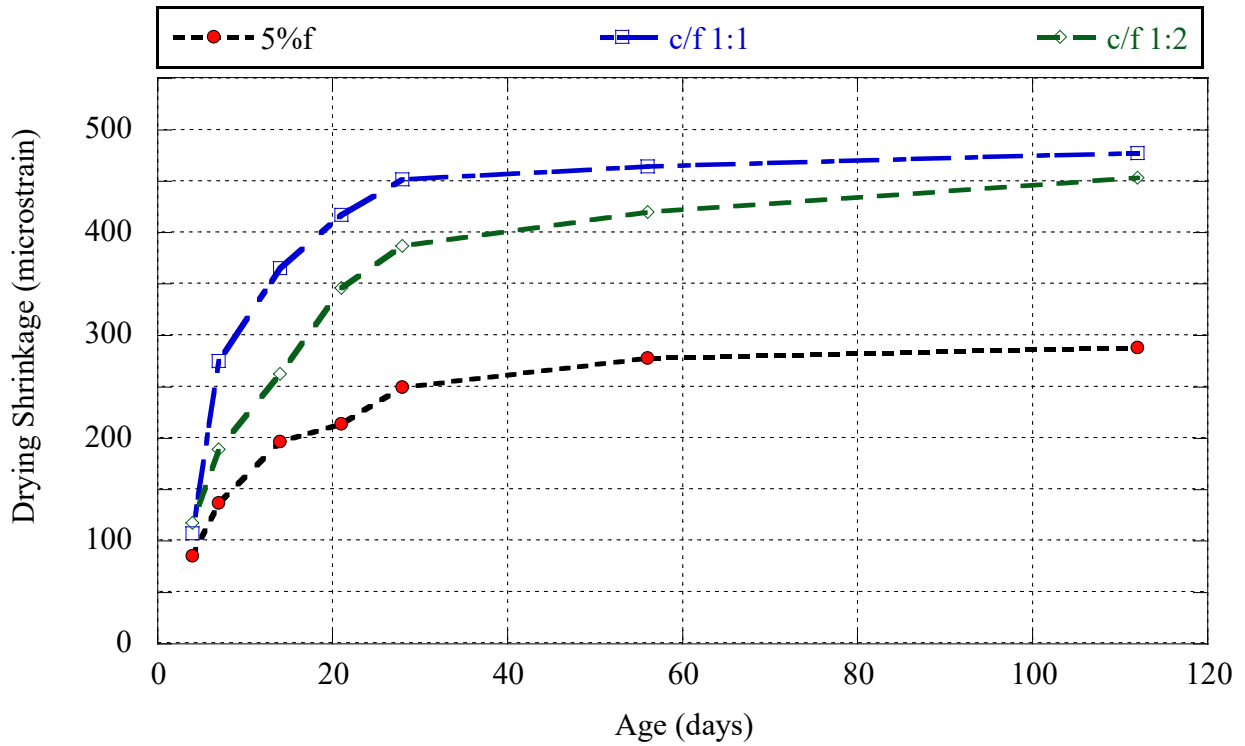
Figure 4.18: Linear Shrinkage Test Results for Stabilized Mixtures of 100% Topeka
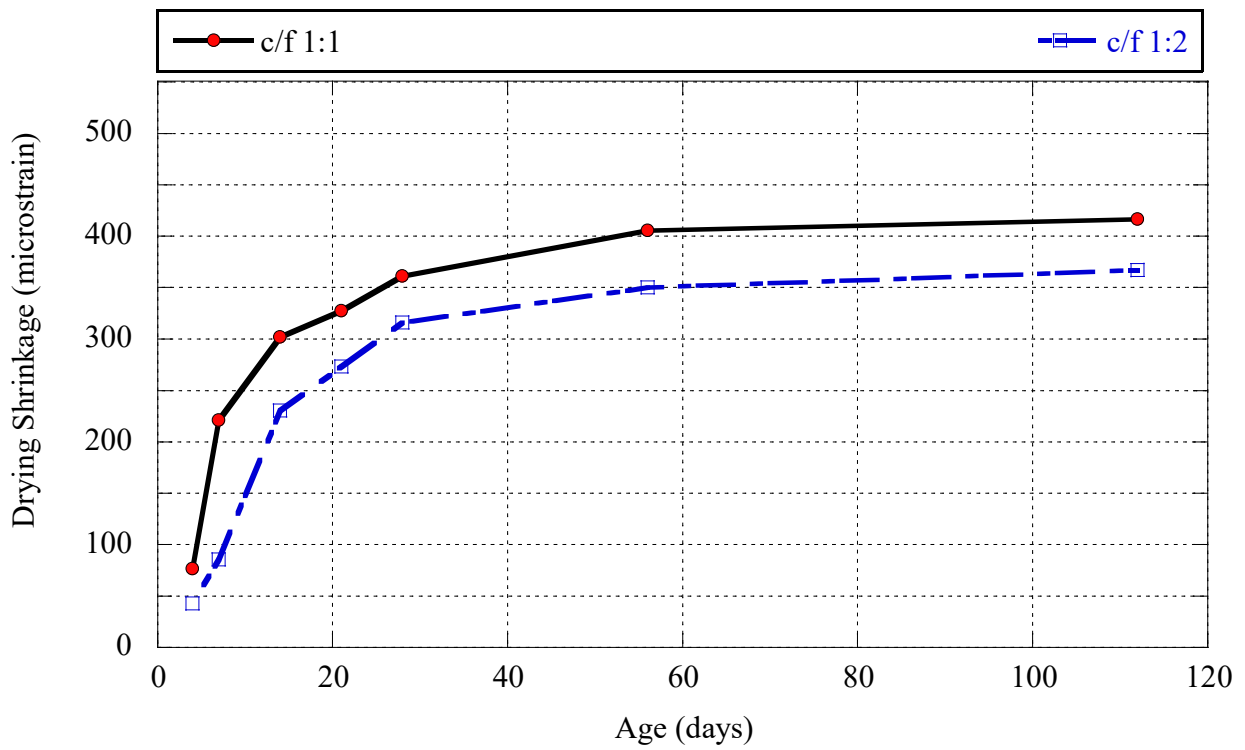
Figure 4.19: Linear Shrinkage Test Results for Stabilized Mixtures of 100% KC

86

4.9 CBR Test Results

This study followed ASTM D1883 to measure mixture stiffness as quantified by unsoaked CBR. The specimens were made at OMC and compacted using 56 blows of the standard Proctor hammer weighing 5.5 lb. The load required for penetration at certain intervals was measured for up to 0.5 in. penetration. Penetration stress in pounds per square inch (psi) was calculated as:

$$\sigma = \frac{F}{A}$$

Equation 4.4

Where,

σ = the penetration stress (psi),

F = measured loading force (lb), and

A = sectional area of the piston (in.).

The stress-penetration curve was plotted and corrected for cases in which the curve was initially concave upward due to surface irregularities, thereby requiring the zero point to be adjusted as required by ASTM D1833. Figure 4.20–Figure 4.24 show stress-penetration curves of the mixtures. According to Figure 4.20, stabilization caused improvement in the stiffness of untreated clay. Mixtures of portland cement and fly ash showed the highest amounts of stiffness. The overall trend of the stress-penetration curve for various c/f ratios was comparable, and different fly ash mixtures showed a similar trend with no notable difference between their stress-penetration curves.
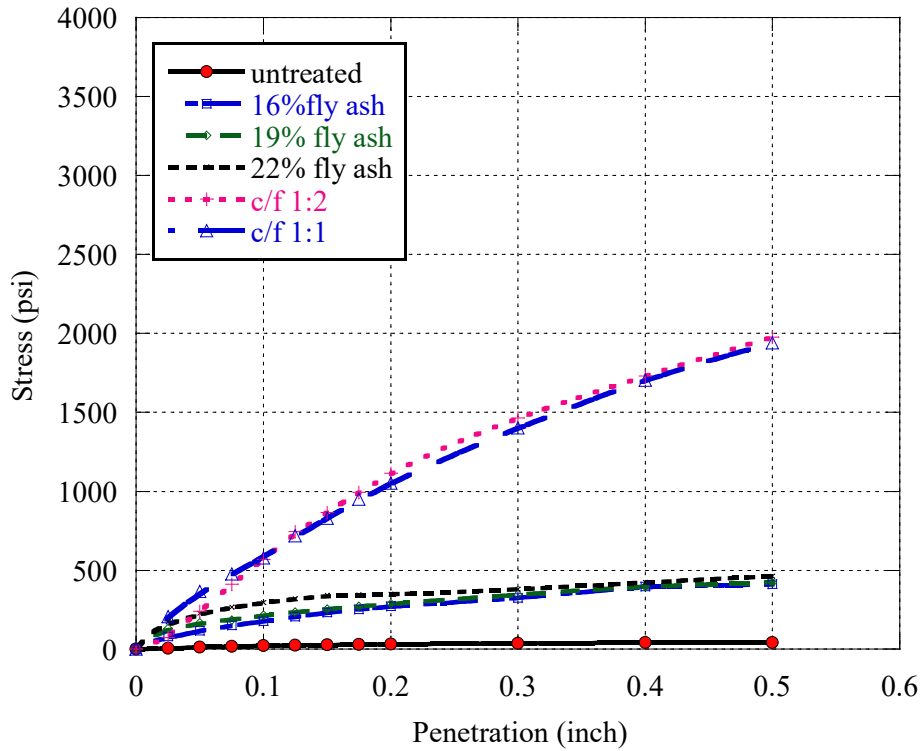
Figure 4.20: Stress-Penetration Curve for 100% Clay Mixtures

Stress-penetration results of 50% clay-50% RCA mixtures are shown in Figure 4.21 and Figure 4.22. As with the 100% clay mixtures, stabilization improved stiffness, with portland cement and fly ash stabilized mixtures showing the highest stiffness. Fly ash mixtures also showed improved stiffness, and the improvement increased with an increasing fly ash content. Both sources of RCA showed comparable results, except that the mixture of 50% clay-50% Topeka with c/f ratio of 1:1 showed considerably improved stiffness compared to the other mixtures (Figure 4.21). The same trend was observed for 100% RCA mixtures (Figure 4.23 and Figure 4.24), although Topeka mixtures with portland cement and fly ash showed considerably higher stiffness than the KC mixtures.
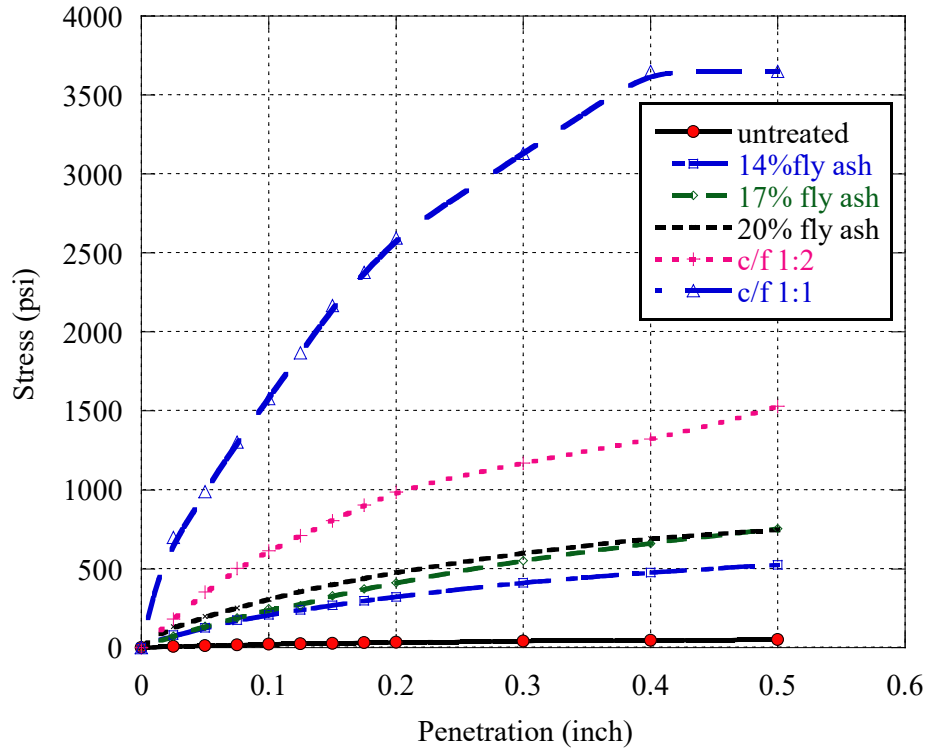
Figure 4.21: Stress-Penetration Curve for 50% Clay-50% Topeka Mixtures
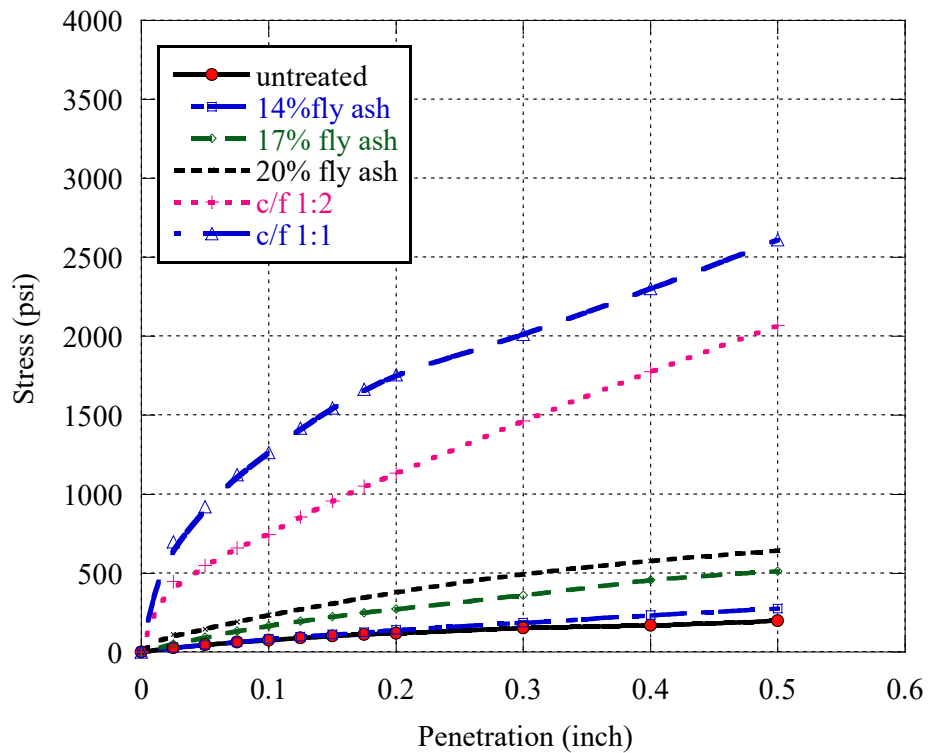
Figure 4.22: Stress-Penetration Curve for 50% Clay-50% KC Mixtures
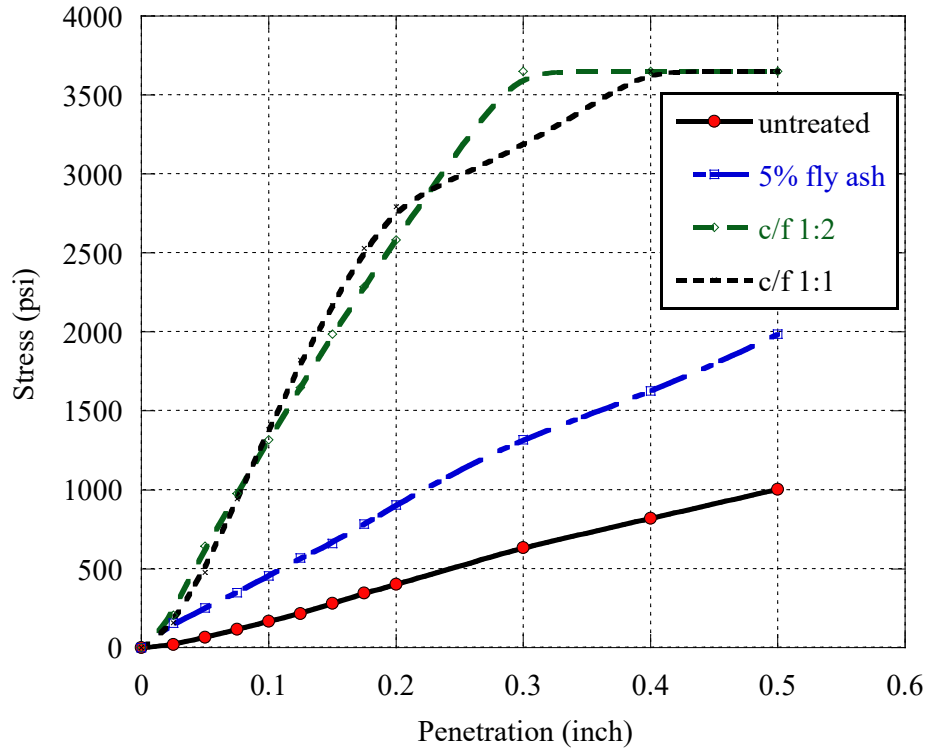
Figure 4.23: Stress-Penetration Curve for 100% Topeka Mixtures
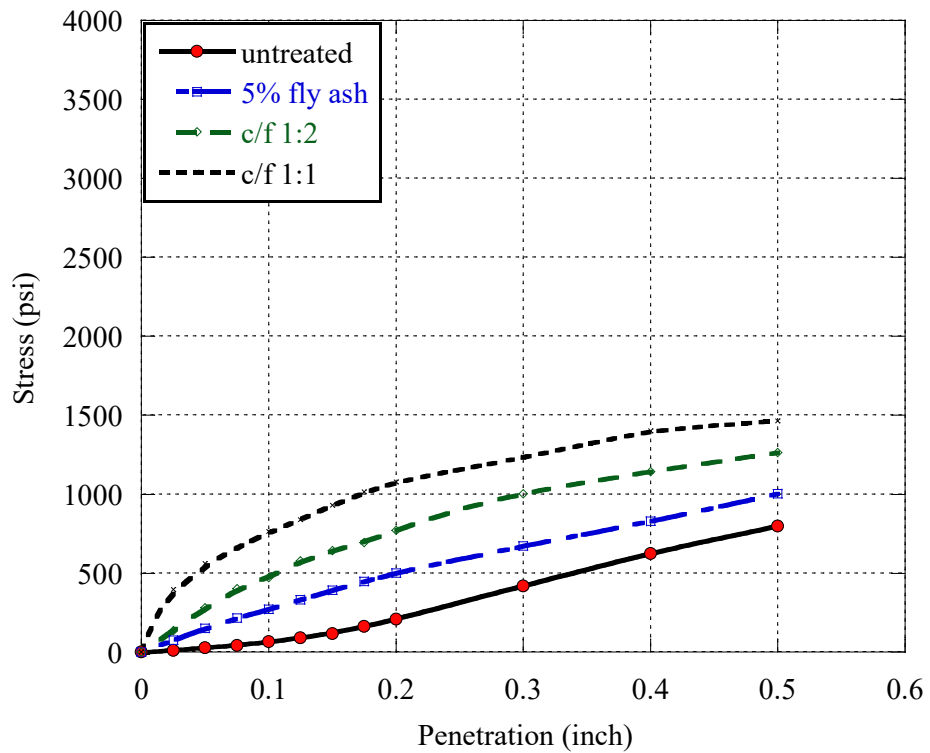
Figure 4.24: Stress-Penetration Curve for 100% KC Mixtures

For mixtures with initially concave upward stress-penetration graphs (100% clay-c/f 1:2, 50% Topeka-50% clay-c/f 1:2, 50% Topeka-50% clay-c/f 1:1, 100% Topeka-untreated, and 100% KC-untreated), corrections were made according to ASTM D1883 guidelines. The CBR of all mixtures was calculated by:

$$CBR\ (\%) = \frac{\sigma_{0.1}}{1000} \times 100$$

<div align="right">**Equation 4.5**</div>

Where,

CBR = the bearing ratio calculated for the standard stress of 1000 psi, and

$\sigma_{0.1}$ = the corrected stress for 0.1 in penetration of piston (psi).

CBR test results, as shown in Figure 4.25, indicated improved stiffness of the stabilized mixtures. The CBR of untreated clay was 2.3%, while all stabilized mixtures (except 50% clay-50% KC with 14% fly ash) attained the 15% minimum CBR value required by many specifications for subgrade (Hossain & Mol, 2011). The improved performance of stabilized soil can be attributed to the cementing and pozzolanic effects of portland cement and fly ash. Although the addition of RCA to clay improved mixture stiffness, only mixtures of RCA-portland cement and fly ash with c/f ratio of 1:1 showed notable improvement. For example, the CBR value of fly ash-100% clay ranged from 17.8% to 29.5%, and the corresponding value for fly ash-50% clay-50% RCA mixtures was 8.39%–30.9%. Mixtures of 100% RCA showed high variability in results for different sources. Topeka aggregates demonstrated considerably higher CBR values compared to KC aggregates. For example, the CBR of 100% Topeka with c/f 1:1 was 182%, while the corresponding value for 100% KC was 76.4%. The observed variability can be attributed to the variability in physical characteristics of RCA, such as gradation, porosity, and the remaining mortar.
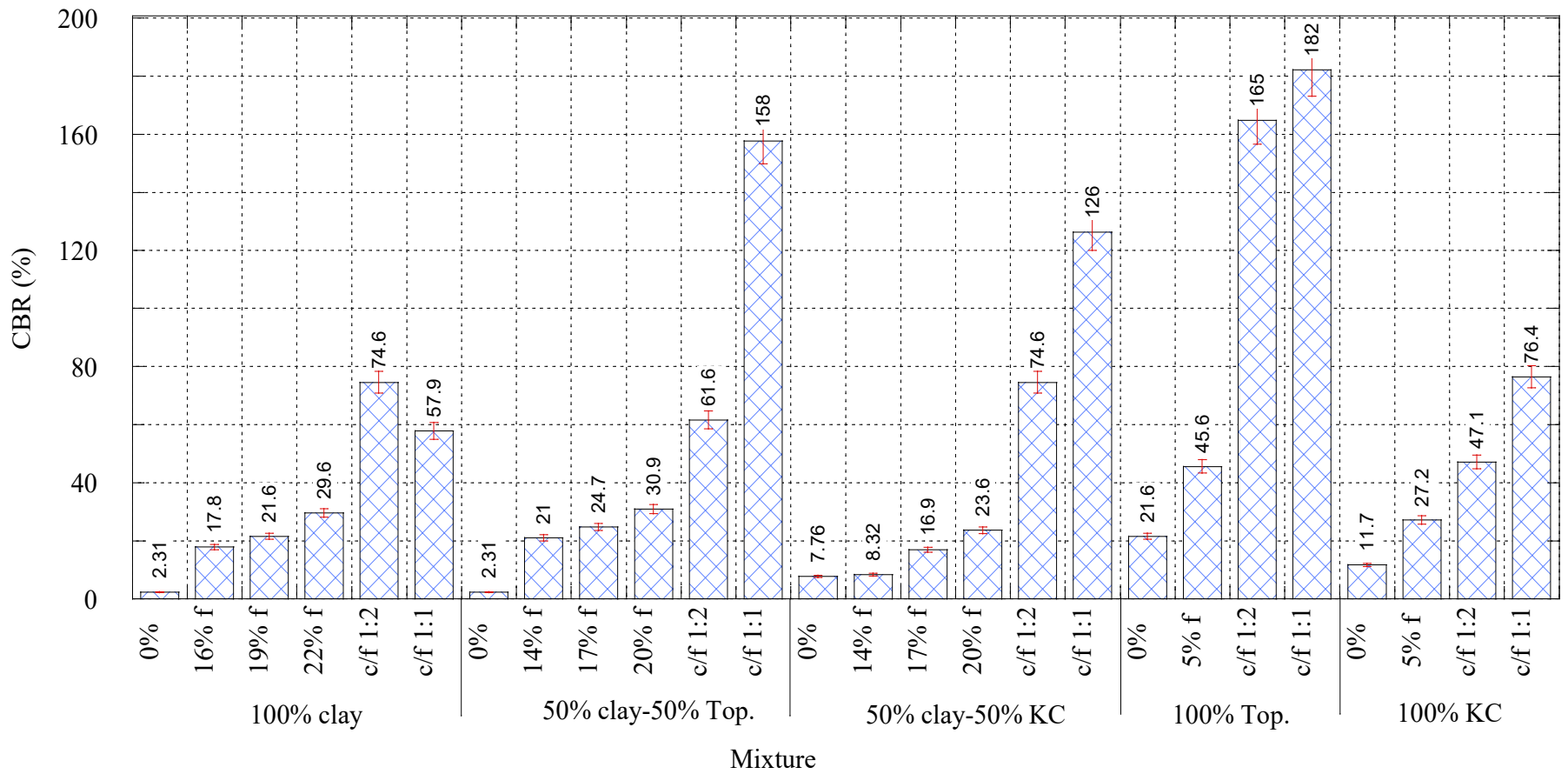
Figure 4.25: CBR Test Results for Various Mixtures

4.10 SEM and EDX Results

SEM and EDX were used to investigate the morphology and elemental composition of the selected mixtures. Figure 4.26–Figure 4.31 show SEM images with 500, 2.0 k, and 5.0 k magnification, as well as EDX results. Figure 4.26 shows that a slightly denser fabric was achieved when RCA was added to 100% clay. The pore structure of the mixture of clay and RCA improved through the interaction of coarse and fine aggregates, but according to the SEM image of 50% clay-50% RCA (Figure 4.27b), no proper bond was formed between the clay and RCA particle, causing a discontinuity in the soil-aggregate matrix. The denser fabric and higher stiffness of the clay-RCA mixture improved shrinkage properties of the mix compared to the 100% clay mixture. The decrease in UCS can be attributed to the observed inadequate bond between clay and RCA. EDX results indicated that the addition of RCA did not considerably change the chemical composition of clay. The main detected elements in clay were Al, Si, K, Mg, Ca, and Fe; therefore, clay mineral is best categorized as illite (Mitchell & Soga, 2005).
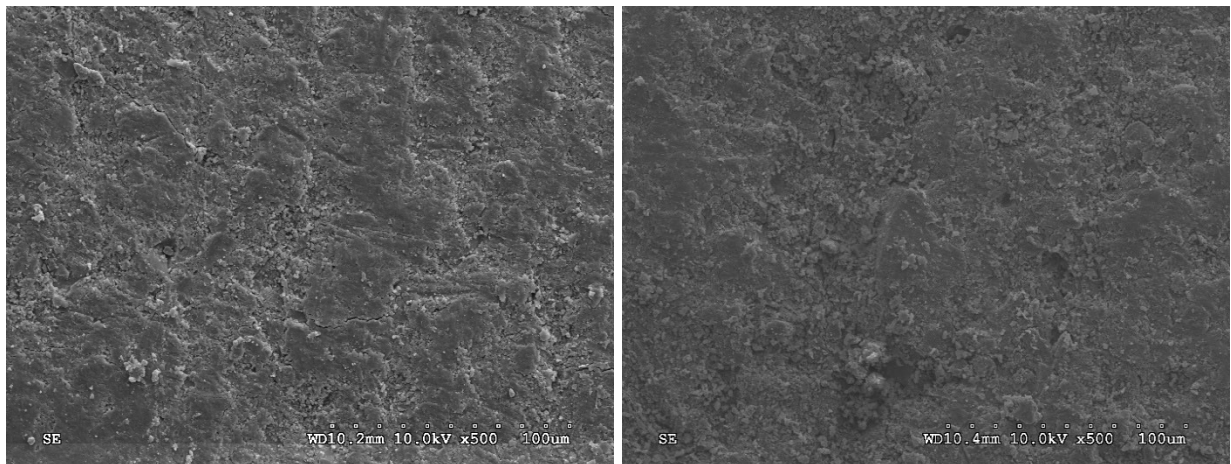
Figure 4.26: SEM Results for Untreated 100% Clay (left) and 50% Clay-50% Topeka (right) (magni. x500)

Element	Atomic%
O	55.37
Mg	0.98
Al	7.61
Si	29.1
K	1.81
Ca	1.19
Fe	3.93

Element	Atomic%
O	58.22
Mg	0.65
Al	4.46
Si	28.85
Ca	0.91
Pd	6.92
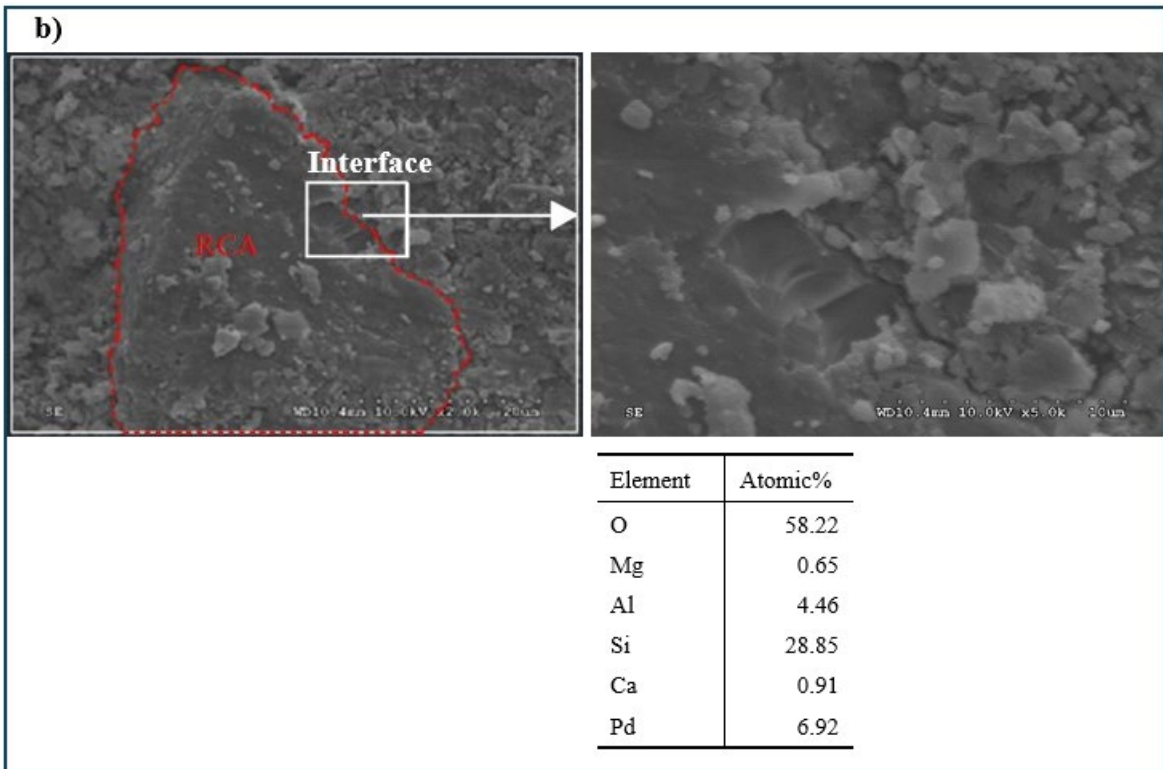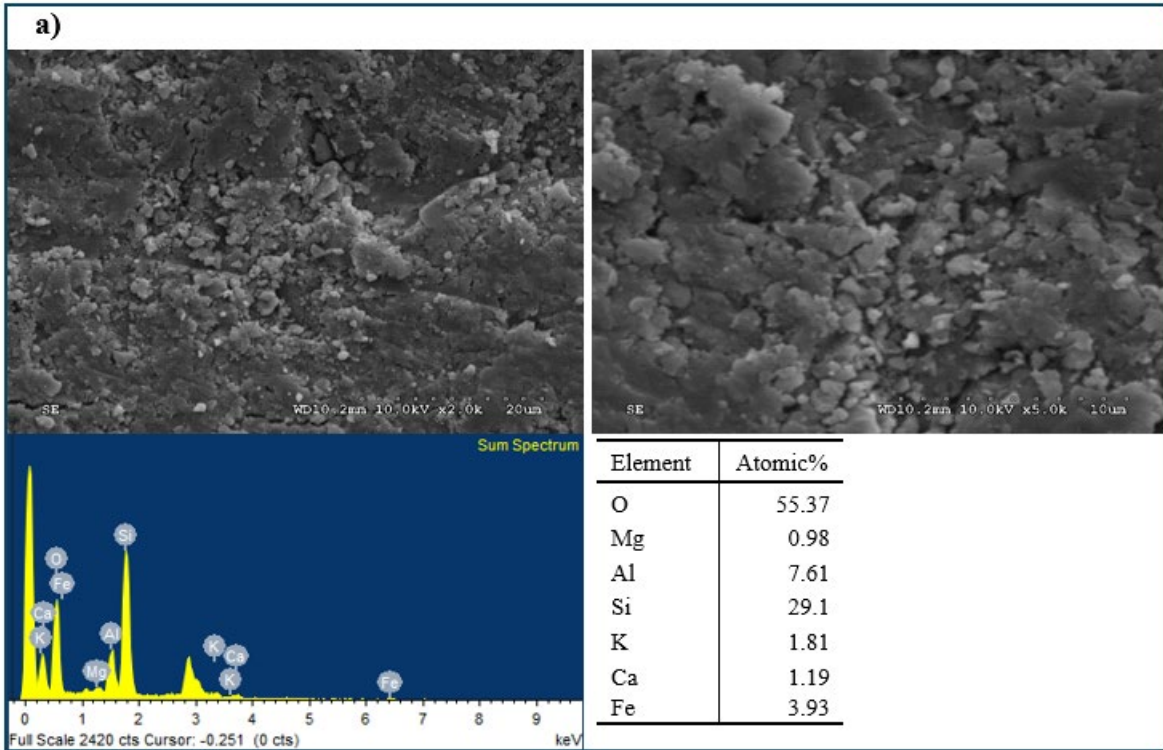
Figure 4.27: SEM and EDX Results for a) Untreated 100% Clay; b) 50% Clay-50% Topeka

Figure 4.28 shows SEM results of lime mixtures with 500 magnifications. A dispersed soil fabric was detected for both 100% clay and 50% clay-50% Topeka mixtures. Although Figure 4.29 shows that lime caused the formation of clay clumps, the formed clumps were dispersed, causing a discontinuous soil fabric with a high void ratio. The observed soil structure was the primary reason the clay was not effectively stabilized with lime due to lime's mechanism of soil stabilization. Calcium ions (Ca^{++}), provided by the addition of lime to clay, replace weak ions such as sodium (Na^+) or potassium (K^+) on the surface of clay particles. Cation exchange results in the flocculation of clay and the formation of clay clumps. However, lime relies on clay pozzolans to form cementitious compounds necessary to bind the clay clumps. The clay in this study did not provide sufficient pozzolans to form the cementitious compounds. SEM results did not show improvement in soil fabric due to the addition of RCA, proving that no improvement in strength was achieved by adding RCA. The main elements found in lime mixtures with or without RCA were Si, Al, and Ca. The concentration of Ca was higher for lime mixtures than untreated mixtures.
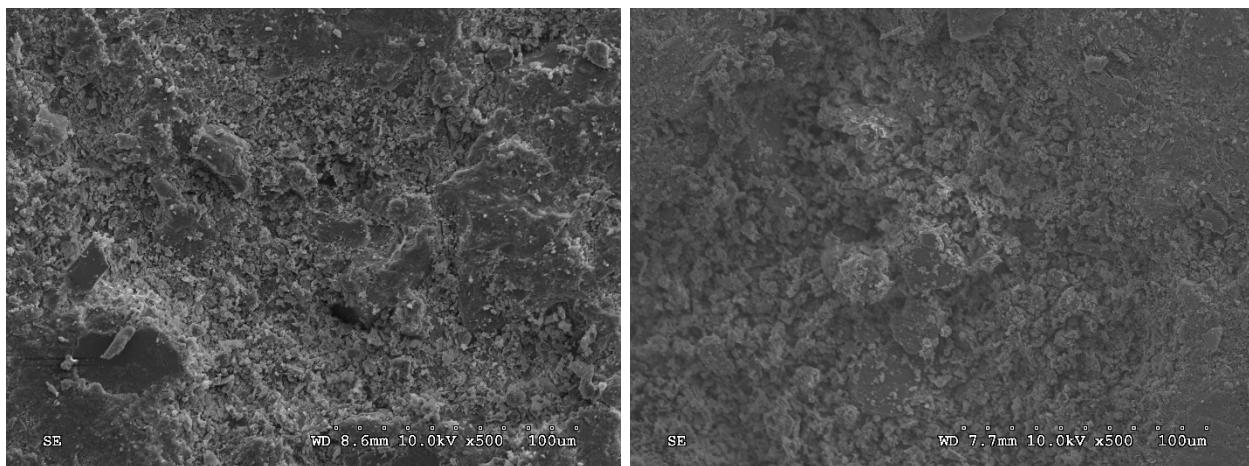
Figure 4.28: SEM Results for 8% Lime, 100% Clay (left), and 8% Lime, 50% Clay-50% Topeka (right) (magni. x500)

a)

Element	Atomic%
O K	63.7
Al K	6.91
Si K	24.13
Ca K	5.26

b)

Element	Atomic%
O K	58.36
Al K	1.39
Si K	5.17
Ca K	23.57
Pd L	11.52
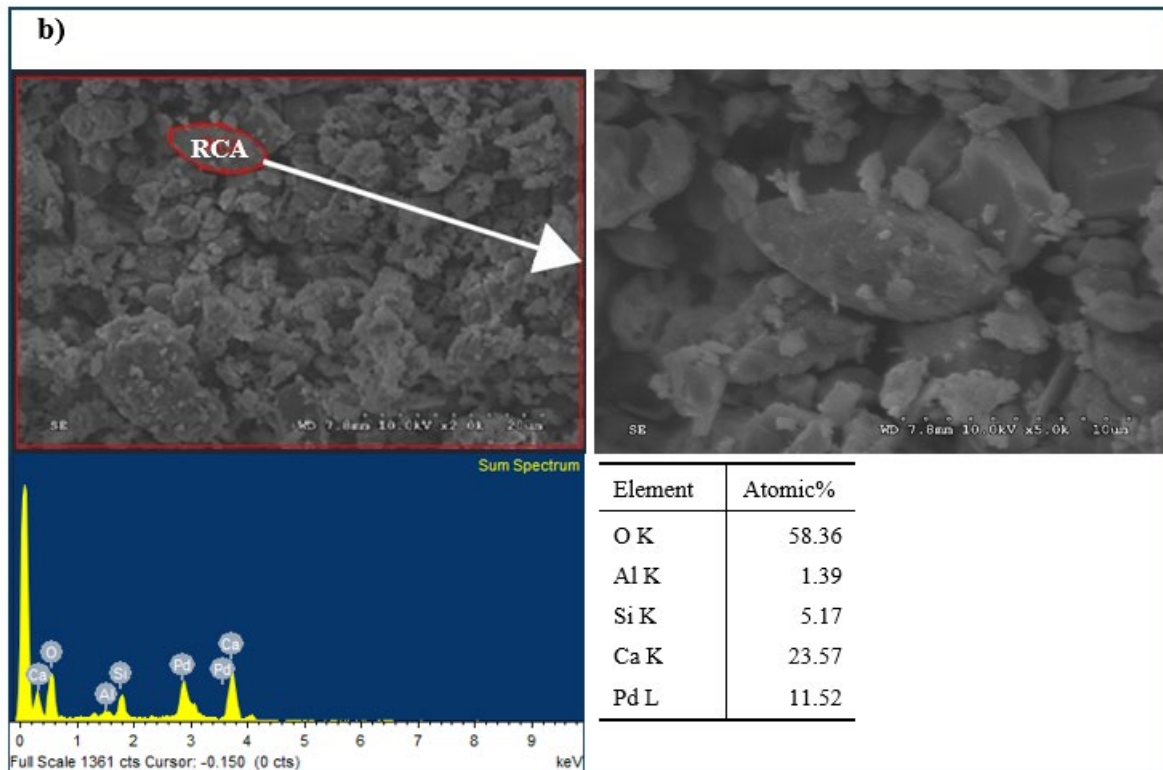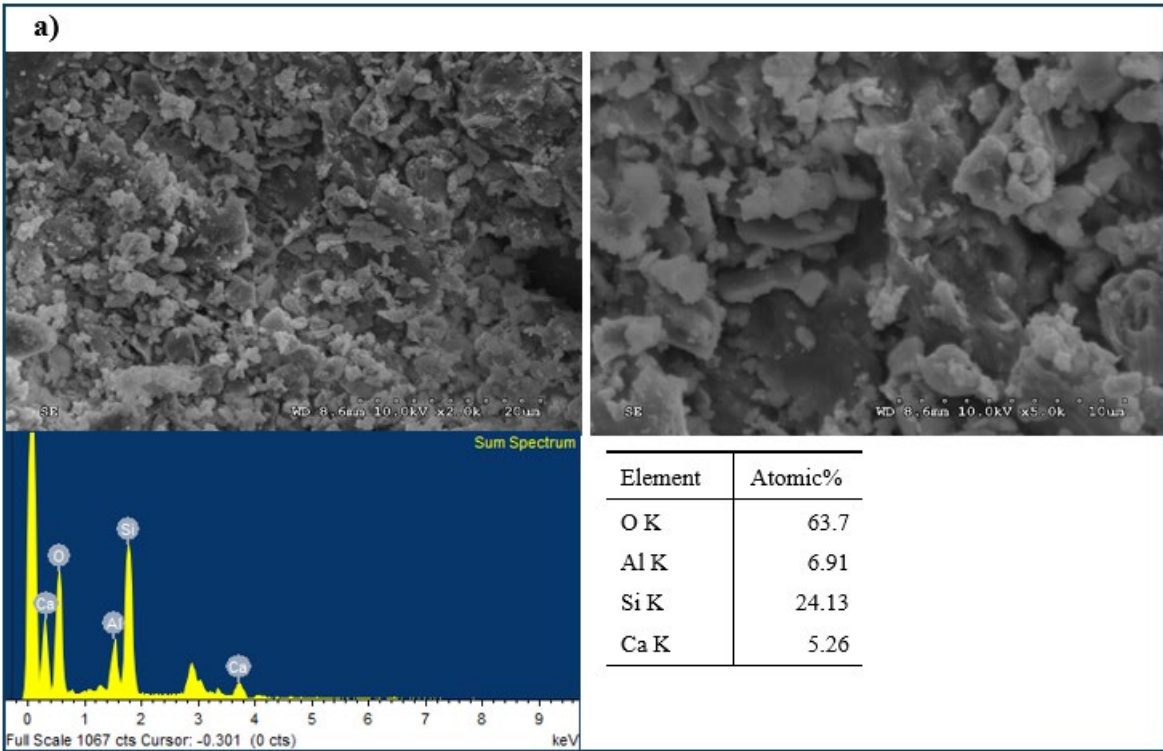
Figure 4.29: SEM and EDX Results for a) 100% Clay-8% Lime; b) 50% Clay-50% Topeka-8% Lime

The mixture of clay-portland cement and fly ash showed some improvement in soil fabric compared to clay (Figure 4.26 and Figure 4.30). However, soil fabric improvement was significant when RCA was added to the mix. A considerably improved soil fabric with low void content was observed in SEM images of RCA-clay-portland cement and fly ash, as shown in Figure 4.30. RCA modified the soil pore structure via the interaction of coarse and fine aggregates, causing an improved soil fabric. Also, cementitious products bonded RCA and clay together, thereby improving the soil-aggregate interface, as shown in Figure 4.31b. Overall enhanced strength, stiffness, and shrinkage were achieved due to the higher strength of RCA aggregates, improved soil fabric, and the adequate bond between clay and RCA, as shown in Figure 4.31b.
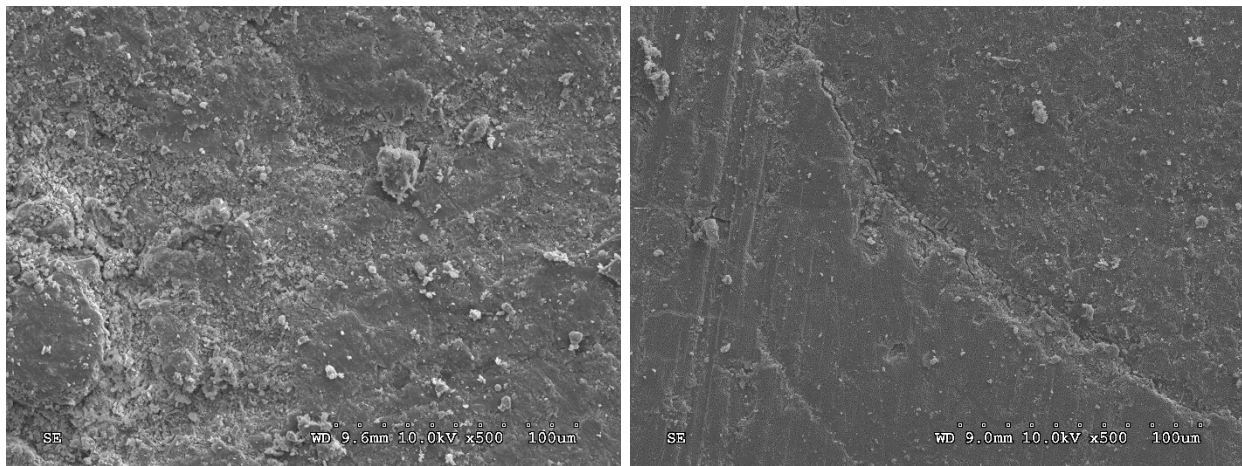
Figure 4.30: SEM Results for Untreated 100% Clay-c/f 1:1 (left) and 50% Clay-50% Topeka-c/f 1:1 (right) (magni. x500)
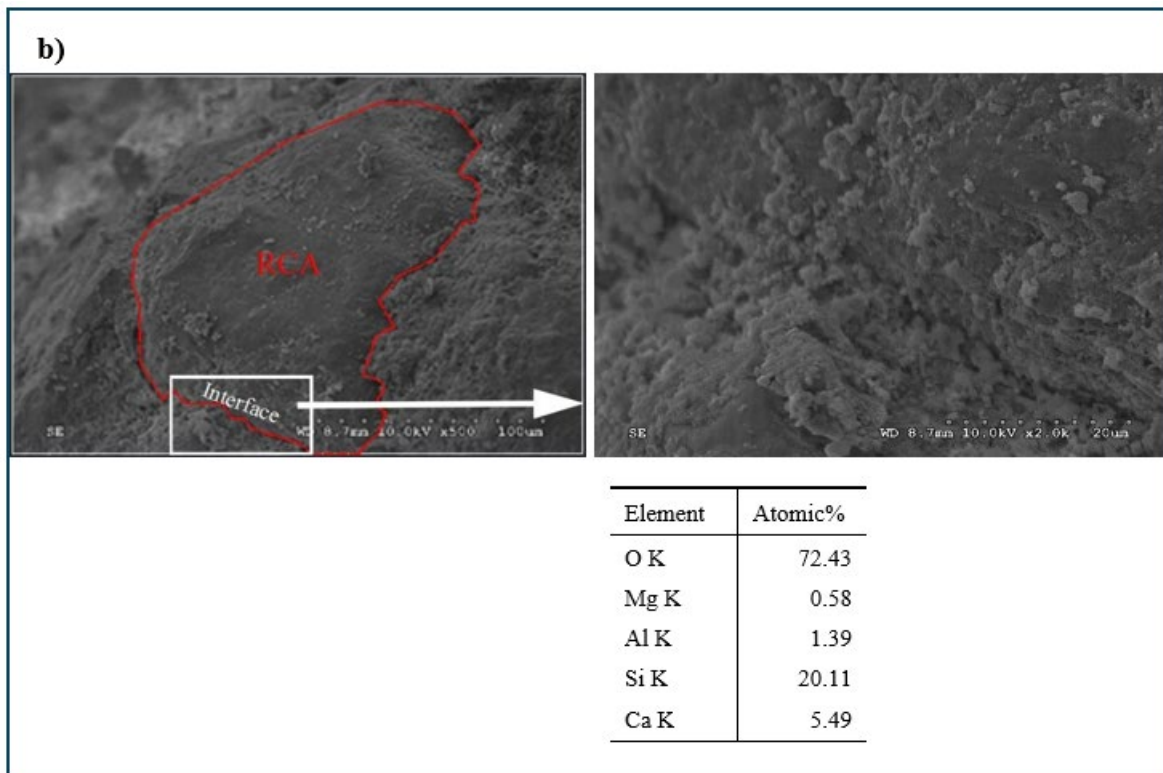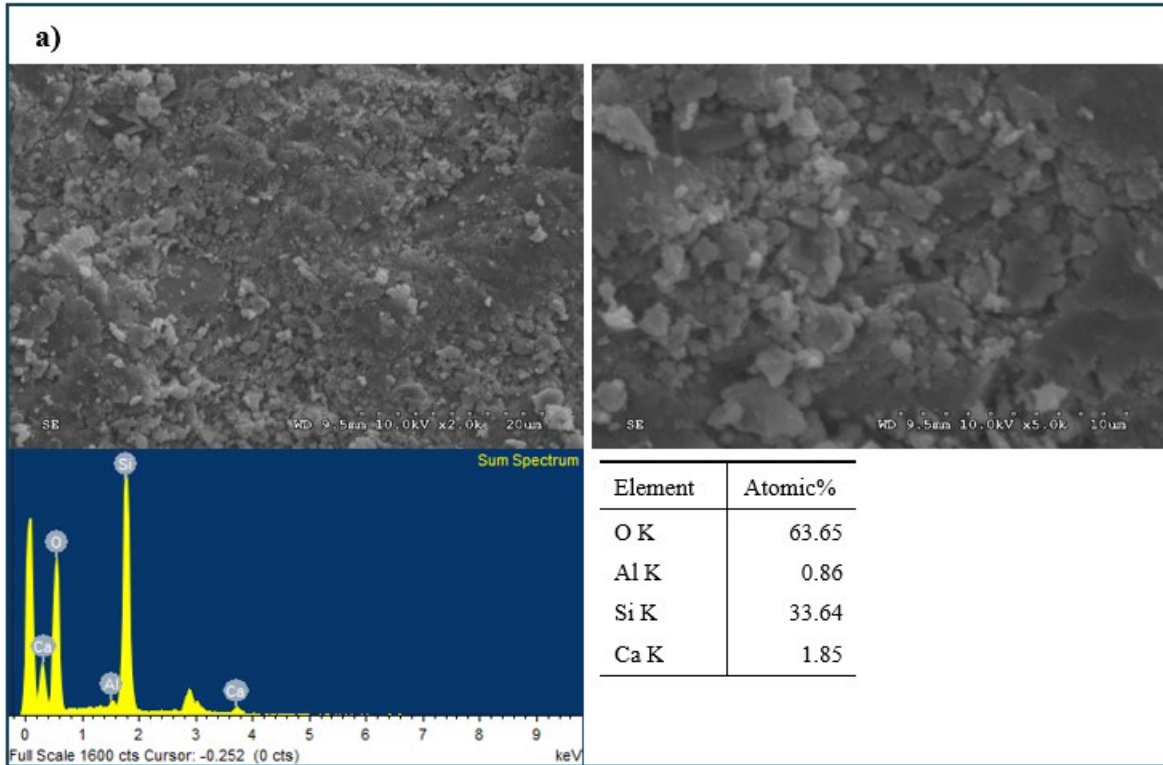
Figure 4.31: SEM and EDX Results for a) 100% Clay-c/f 1:1; b) 50% Clay-50% Topeka c/f 1:1

SEM and EDX results helped non-quantitatively explain the effect of RCA for clay stabilization. As shown in Figure 4.27b an inadequate bond between RCA and clay reduced the UCS of clay-RCA mixtures, and a dispersed soil fabric and high void content (Figure 4.28 and Figure 4.29) showed that lime mixtures did not develop sufficient strength. Because the addition of RCA did not improve soil fabric, RCA did not contribute additional strength to the mixture. However, overall enhanced strength, stiffness, and shrinkage were achieved for fly ash-portland cement mixtures due to improved soil fabric (Figure 4.30) and the adequate bond formed at the interface of clay and RCA (Figure 4.31b).

4.11 Performance Prediction Using AASHTOWare Pavement ME Design

Pavement section performance was predicted using AASHTOWare PMED software. As mentioned, full-depth HMA pavements were designed using properties of the designed stabilized mixtures for the subgrade layer. Performance of the designed mixtures was compared to the control section, which was full-depth asphalt over a chemically stabilized subgrade. Subgrade material properties of the control sections were from real-world projects in Kansas. Table 4.10 shows the natural soil properties for each project.

Table 4.10: Natural Subgrade Soil Properties from Various Projects

Property	K	US	Interstate
% passing No. 200	90	98	90
AASHTO group	A-7-6	A-7-6	A-7-6
MDD (pcf)	91.6	99	94.5
Liquid limit	60	46	55
Plasticity index	40	24	33
Poisson's ratio	0.35	0.35	0.35
Mr of treated subgrade	5,503	6,315	5,503
Mr of natural subgrade	2,600	3,000	2,600

Table 4.11 shows the calculated M_r based on the UCS of the stabilized mixtures. The M_r was input into the PMED as the main design factor. Other engineering properties of the stabilized

mixtures, such as gradation, Atterberg limits, and compaction curve parameters, were also inserted into the PMED software based on measured properties of the soil-cement mixtures.

Table 4.11: Laboratory UCS and Calculated M_r of Stabilized Soil-Cements

Mixture		Avg. UCS (psi)	M_r (psi)
Control	KDOT treated subgrade	-	5,500 (K & Interstate) 6,315 (US)
100% clay	fly ash	72	86,400
	50c+50f	123	147,600
	35c+65f	148	177,600
50% clay-50% KC	fly ash	106	127,200
	50c+50f	321	385,200
	35c+65f	285	342,000
50% clay-50% Topeka	fly ash	80	96,000
	50c+50f	335	402,000
	35c+65f	276	331,200

Total asphalt thickness needed to achieve target KDOT performance criteria for each road category is shown in Figure 4.32. Results are based on a 10-year design life for a 4-in. stabilized or 6-in. treated subgrade (control section). Results showed that a combination of portland cement and fly ash at a mass ratio of 1:1 is the most effective stabilizer for reducing HMA layer thickness. The incorporation of RCA into mixtures was also shown to reduce total HMA thickness. The total reduction for cement and fly ash mixtures ranged from 1.5 in. for the K-57 project to 6.0 in. for the I-70 project. For example, the required HMA thickness for 100% clay stabilized with portland cement and fly ash (c/f 1:1) can be reduced from 22.5 in. to 19 in. with the incorporation of RCA. Increased stiffness and improved plasticity properties of clay stabilized with RCA are the primary reasons for thickness reduction.
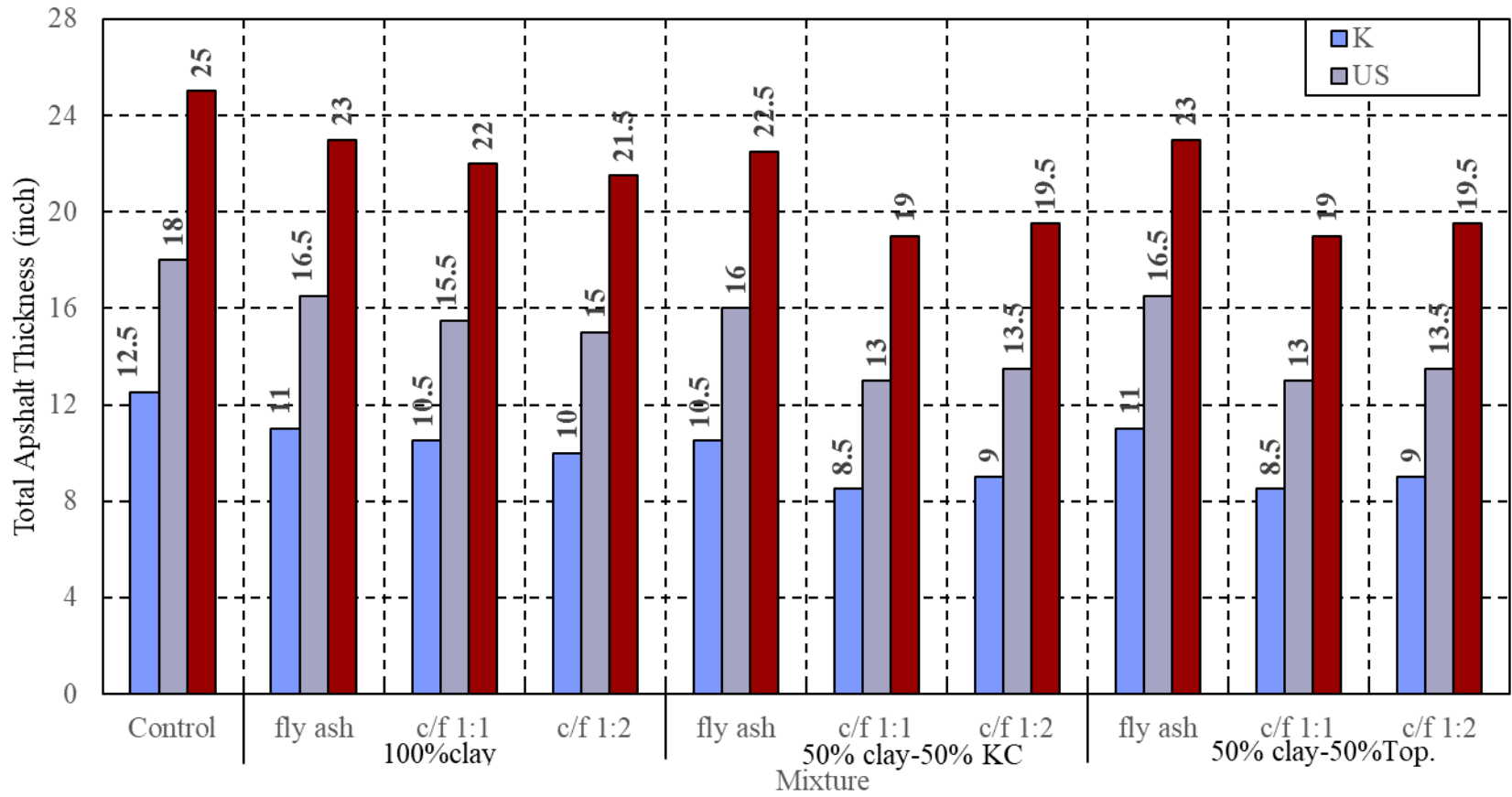
Figure 4.32: MEPDG Outputs for All Road Categories

4.12 Economic Analysis

Economic analysis evaluated potential cost savings from stabilization of the clay subgrade soil. KDOT provided average unit construction costs, and costs associated with RCA were obtained from a local crushing company. Table 4.12 tabulates the unit costs used in this study.

Table 4.12: Unit Costs of Construction Materials and Activities

Description	Unit of Measure	Unit Cost
SR-9.5A (PG64-28)	Ton	$ 80.0
SR-19A (PG64-28)	Ton	$ 69.5
SR-19A (PG64-22)	Ton	$ 60.5
Manipulation (fly ash-treated subgrade)	Sq. yd	$ 3.5
Manipulation (cement-treated subgrade)	Sq. yd	$ 4.7
Fly ash (used alone)	Ton	$ 76.0
Fly ash (in combination with cement, c/f 1:2)	Ton	$ 86.0
Fly ash (in combination with cement, c/f 1:1)	Ton	$ 87.0
Cement (in combination with cement, c/f 1:2)	Ton	$ 130.0
Cement (in combination with cement, c/f 1:1)	Ton	$ 120.0
Water (treated subgrade)	Ton	$ 35.0
Concrete pavement milling & disposal	Ton	$ 3.0
Concrete pavement milling & crushing (on site)	Ton	$ 9.5

Calculations were made for a road section measuring 12 ft wide and 1 mile long with the proposed pavement structure, as shown in Figure 3.11. Construction costs varied according to the scale of the project. Costs considered in this LCCA study were for the construction of a 1-mile section in a 10-mile road. Asphalt layer thickness was based on results of PMED analysis, as shown in Figure 4.32. For RCA mixes, the minimum asphalt layer thickness of Topeka or KC RCA was used in LCCA because the results did not differ significantly. For RCA-stabilized subgrade, the RCA was assumed to be crushed in the plant and mixed with subgrade soil. Concrete slabs were assumed to be removed, transported, and stored/disposed. According to the LCCA results (Table 4.13), all stabilized mixtures resulted in cost reductions compared to the control section in which the subgrade was only chemically treated.

Table 4.13: Cost Estimates for LCCA Scenarios

Section	Subgrade Mixture		Construction ($)	Control Section (%)
K	100% clay	control (KDOT treated subgrade)	$ 379,662	0.0%
		fly ash	$ 371,595	-11.4%
		c/f 1:2	$ 382,641	-13.3%
		c/f 1:1	$ 390,735	-10.7%
	50% clay-50% RCA	fly ash	$ 360,694	-8.8%
		c/f 1:2	$ 347,382	-15.8%
		c/f 1:1	$ 579,858	-18.9%
US	100% clay	control (KDOT treated subgrade)	$ 525,252	0.0%
		fly ash	$ 501,984	-9.4%
		c/f 1:2	$ 513,030	-13.4%
		c/f 1:1	$ 526,932	-11.5%
	50% clay-50% RCA	fly ash	$ 453,027	-9.1%
		c/f 1:2	$ 428,962	-21.9%
		c/f 1:1	$ 800,175	-26.0%
Interstate	100% clay	control (KDOT treated subgrade)	$ 731,586	0.0%
		fly ash	$ 700,888	-8.6%
		c/f 1:2	$ 717,044	-12.4%
		c/f 1:1	$ 738,410	-10.4%
	50% clay-50% RCA	fly ash	$ 642,828	-7.7%
		c/f 1:2	$ 657,547	-19.7%
		c/f 1:1	$ 657,547	-17.8%

The cost reduction as a percentage of the cost of the control section is shown in the last column of Table 4.13. However, the comparison of stabilized mixtures with the control sections (treated subgrade) suggests varying degrees of cost reduction mostly due to the savings in the HMA thickness. For example, the cost reduction for the stabilized base with only fly ash is 8.6% for the interstate project, while the cost reduction with the inclusion of RCA is 7.7%. However, fly ash-portland cement-RCA mixtures can result in up to a 19.7% cost reduction. Thus, portland cement must be used in combination with fly ash to make RCA an economically viable option for stabilization. However, unit prices will fluctuate, and the cost figures used were based on the 2018 prices.

4.13 Mechanical Stabilization of a Source of Lean Clay

Another source of soil with lower plasticity was obtained to further investigate RCA effectiveness for stabilizing different types of soil. Sieve analysis, Atterberg limits, and the standard Proctor test were run to obtain basic engineering properties of the soil. Then various blends of lean clay and RCA were mixed and tested for the UCS test to assess RCA suitability for

mechanically stabilizing the soil. The gradation chart and compaction curve for the clay are shown in Figure 4.33 and Figure 4.34, respectively.
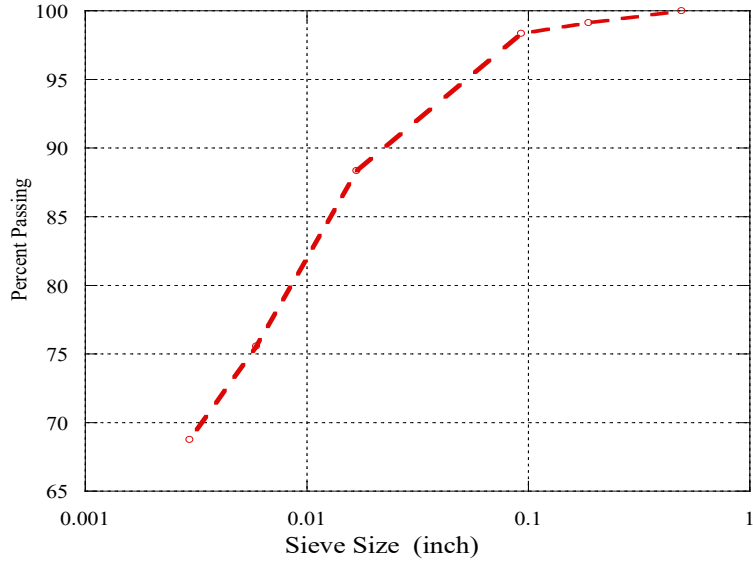
Figure 4.33: Gradation Chart for A-4 Soil
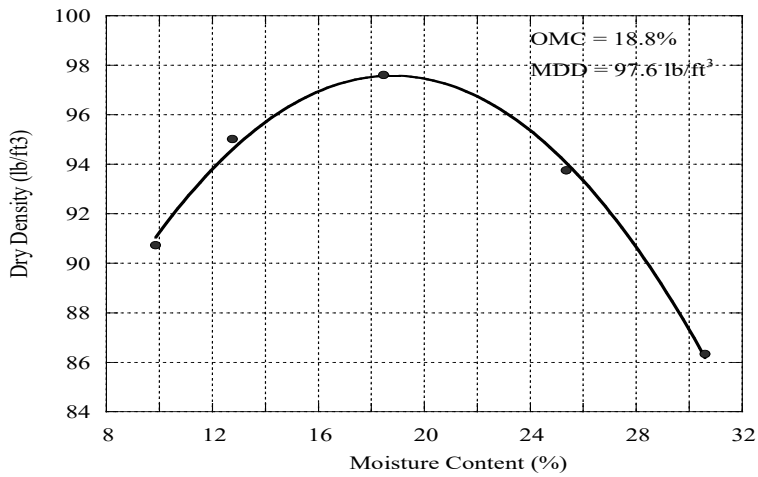
Figure 4.34: Compaction Curve for 100% A-4 Soil

Liquid and plastic limits of the A-4 soil were measured per ASTM D4318. The soil was classified as A-4 soil (CL) according to AASHTO and USCS. Test results and soil classifications are shown in Table 4.14.

Table 4.14: AASHTO and Unified Soil Classifications for Clay

Item	Value
% passing No. 10	98
% passing No. 40	88
% passing No. 200	69
Liquid limit	32
Plasticity index	10
AASHTO Soil Class	**A-4**
Unified Soil Class	**CL**

Various blends of RCA and A-4 soil were also considered for UCS testing. Blends were designed so that at least one blend mimicked AB-3 aggregate gradation, one of three aggregate gradations used in Kansas for base construction that allows the highest plasticity index and liquid limit. Table 4.15 shows KDOT requirements for AB-3 gradation.

Table 4.15: KDOT Gradation and Aggregate Plasticity for Aggregate Base Construction

Type	% Retained-Square Mesh Sieves									P.I.	max. LL (%)
	2 in	1.5 in	1 in	3/4 in	3/8 in	No. 4	No. 8	No. 40	No. 200		
AB-3	0	0–5		5–30		35–60	45–70	60–84	80–92	1–8	30

Blends of 75%–100% RCA, by total weight of the blend, and 0–25% A-4 soil were in the range of KDOT AB-3 gradation. A blend of 75% RCA-25% A-4 was selected for further investigation. The highest possible limit for A-4 to achieve AB-3 gradation was selected to incorporate enough cohesive soil into the mix to enable the creation of UCS specimens. Other mixtures of RCA and A-4 were also developed for comparison, as shown in Table 4.16 and Figure 4.35.

The standard Proctor test was performed on the blend of 75% RCA-25% A-4, and the replacement of A-4 with 75% RCA improved compaction properties of the mix. OMC decreased to 12%, and MDD increased to 104.4 lb/ft^3. UCS test specimens were made at the measured OMC and MDD. The procedure for making and testing samples was conducted as described in Chapter

3 for A-6 soil. Three replicate specimens were made and tested for UCS. Table 4.16 shows the results of mechanical stabilization of A-4 soil with RCA.

Table 4.16: UCS Test Results for Blends of RCA and A-4 Soil

Mixture	Specimen#	Binder (%)	Dia. (in.)	Ht. (in.)	Max. Load (lb)	UCS (psi)	Avg. UCS (psi)
0% RCA-100% A-4	1	0	2.8	6.3	91	15	**14**
	2	0	2.8	6.3	79	13	
	3	0	2.8	6.3	89	15	
25% RCA-75% A-4	1	0	2.8	6.3	62	10	**10**
	2	0	2.8	6.3	56	9	
	3	0	2.8	6.3	59	10	
50% RCA-50% A-4	1	0	2.8	6.3	42	7	**6**
	2	0	2.8	6.3	36	6	
	3	0	2.8	6.3	33	5	
75% RCA-25% A-4	1	0	2.8	6.3	28	5	**5**
	2	0	2.8	6.3	30	5	
	3	0	2.8	6.3	26	4	
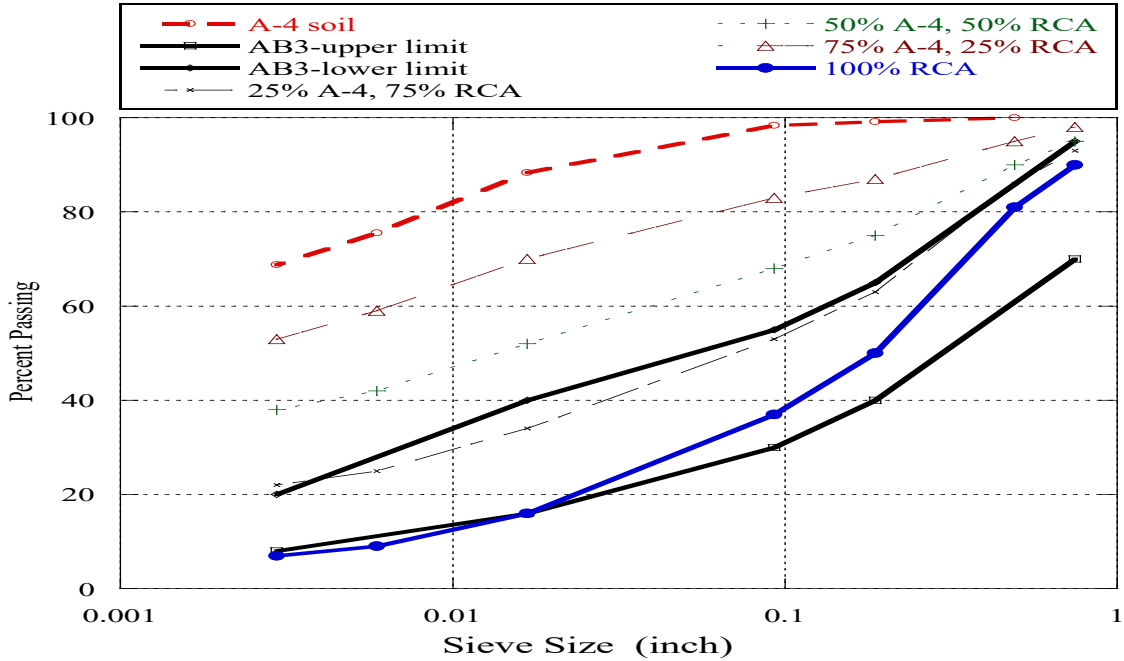
Figure 4.35: Gradation Chart for AB-3 and Blends of A-4 and RCA

UCS test results indicated that replacing A-4 soil with RCA decreased the compressive strength of the blends. The higher the replacement level, the lower the UCS due to the weak bond formed between RCA and A-4 soil and alteration of the effective soil particle arrangement. Based on the results, RCA was disqualified for mechanical stabilization of A-4 soil since the purpose of stabilization is to improve compressive strength of the soil. However, the addition of RCA improved compaction properties of the soil.

Chapter 5: Conclusions and Recommendations

State highway agencies are confronted with environmental and economic concerns regarding the massive production of a waste stream from discarded concrete pavements. Recycling concrete waste into new paving applications is one way to resolve this critical issue. However, RCA usage is questionable when RCA is derived from low-quality pavements, such as pavements with D-cracking, which often end up in landfills. Although D-cracked RCA could be utilized for soil stabilization, to date, no known work has evaluated the effect of RCA from D-cracked pavements on subgrade soil stabilization.

This study evaluated the potential improvement in mechanical properties of a clay soil stabilized with D-cracked RCA for HMA subgrade stabilization. RCA blends, a clay source, and chemical stabilizers such as lime, Class C fly ash, and a combination of Class C fly ash and portland cement were developed according to the USACE method. Blends were tested in the laboratory for compaction properties, UCS, linear shrinkage, and CBR. The microstructures of the selected mixtures were studied using SEM and EDX, and laboratory test results were input into the MEPDG software to predict the long-term performance of stabilized mixtures. LCCA economic analysis was conducted to evaluate potential cost savings of RCA usage. The following conclusions were drawn from study results:

1. Mechanically stabilizing clay with RCA lowered the UCS of the untreated clay, proving that RCA alone is not effective for soil strength gain. However, the addition of RCA improved compaction, stiffness, and shrinkage properties of clay.

2. Except for lime-stabilized mixtures, the incorporation of 50% RCA into 100% clay mixtures improved the UCS of chemically stabilized mixtures. Lime likely failed to develop an adequate aggregate-soil interface bond.

3. The addition of RCA improved shrinkage performance of stabilized clay mixtures likely due to internal curing caused by RCA's high porosity.

4. CBR test results indicated higher stiffness of 50% RCA-50% clay blends than clay-only mixtures.

5. A combination of Class C fly ash and portland cement was the most effective stabilizer to increase UCS and stiffness.

6. Performance prediction using MEPDG confirmed a potential for reducing HMA thickness up to 3.5 inches by including RCA in chemically stabilized 100% clay subgrade soil in roads with medium- to high-volume traffic compared to stabilized clay without RCA. No significant thickness reduction was predicted for a low-volume traffic road.

7. Based on the LCCA results, the addition of RCA to chemically stabilized clay mixtures would be economical only if a combination of RCA, fly ash, and portland cement was used. RCA-fly ash mixtures did not demonstrate any significant cost savings.

8. SEM and EDX results showed an improved arrangement of soil particles and a lower void content with the addition of RCA to clay. Increased strength and improved shrinkage properties can be achieved if an adequate soil-aggregate bond is reached using chemical agents.

The two sources of RCA used in this study, Topeka and KC, performed satisfactorily, although Topeka mixtures outperformed KC mixtures in strength and stiffness. Topeka had higher qualities of absorption capacity, specific gravity, toughness, soundness, and aggregate stiffness. However, KC showed superior shrinkage performance, which correlated with the higher porosity of KC aggregate. Overall results of this research showed that, although RCA properties vary widely, they can be mechanically and economically effective for stabilizing clay soils when used with fly ash and portland cement.

5.1 Research and Practice Contributions

The literature contains minimal information on the effects of RCA on the mechanical performance of clay, and no known work explores the use of D-cracked RCA for soil stabilization. Therefore, the main contribution of this study was to provide knowledge related to potential improvements in mechanical properties of clay using D-cracked RCA. A comprehensive laboratory study was performed to evaluate the properties of RCA aggregates and their effects on

the essential mechanical properties of stabilized mixtures. Laboratory results of this study are the first guidelines for researchers and decision makers regarding the mechanical properties of stabilized mixtures using D-cracked RCA. Although shrinkage cracking is a major concern of chemically stabilized subgrade, insufficient information is available about shrinkage properties of stabilized soil, especially in Kansas. Results of this study add knowledge about shrinkage characteristics of stabilized mixtures.

The second major contribution of this study was to predict the performance of designed mixtures using MEPDG software and evaluate the potential reduction in pavement thickness. Findings of this investigation showed that stabilization for low-volume traffic roads is not an economically viable option. A primary motivation behind this research was to evaluate potential cost savings when using RCA for soil stabilization. LCCA results provide unprecedented information about the economic efficiency of RCA usage for soil stabilization. The main scientific contribution of this research was to study the interaction of soil-RCA in stabilized mixtures using SEM and XDS analysis. Analysis results are first steps toward understanding the effect of RCA on the microstructure of stabilized mixtures.

The implementation of this research will take careful planning, test plan, and follow up. The planning should include letting the project with the stipulation that existing concrete pavement must be recycled on-site. The test plan should create an economical combination of cementitious materials for use in recycling. Finally, the project must be monitored for long-term performance.

5.2 Recommendations for Future Work

Results of this study highlighted recommendations for future work. First, further investigation of shrinkage properties of developed mixtures using autogenous shrinkage and pore size distribution testing is recommended. This study showed that stabilization, especially with fly ash and RCA, improves shrinkage properties of soil. Thus, understanding the mechanism and factors affecting shrinkage of stabilized soil is essential. Second, development of additional mixtures with different RCA percentages is recommended since RCA replacement levels in this study were only 0%, 50%, and 100%. A combination of lime and portland cement could also be investigated as an alternative stabilizer, and the optimum replacement level of RCA and all

effective stabilizers to improve different mixture properties must be identified. Third, this study calculated the M_r of chemically stabilized mixtures as input for MEPDG based on a linear correlation with UCS, but further calibration of the equation is needed to consider the effect of RCA. CBR test results indicated that the stiffness of RCA-stabilized mixtures can be highly variable, thereby requiring the identification of factors affecting strength and stiffness and comprehensive correlation. Finally, long-term performance of the developed mixtures must be assessed via field investigation. Although this research used MEPDG software to predict satisfactory long-term performance of the stabilized mixtures, field performance can have various results, such as high stiffness of the stabilized layer underneath a flexible surface may cause top-down longitudinal and bottom-up reflective cracking.

References

AASHTO M 85. (2017). *Standard specification for portland cement*. American Association of
     State Highway and Transportation Officials.

Al-Swaidani, A., Hammoud, I., & Meziab, A. (2016). Effect of adding natural pozzolana on
     geotechnical properties of lime-stabilized clayey soil. *Journal of Rock Mechanics and
     Geotechnical Engineering, 8*(5), 714–725.

Aly, T., & Sanjayan, J. G. (2009). Mechanism of early age shrinkage of concretes. *Materials and
     Structures, 42*(4), 461–468.

American Association of State Highway and Transportation Officials (AASHTO). (1993).
     AASHTO guide for design of pavement structures.

American Association of State Highway and Transportation Officials (AASHTO). (2015).
     Mechanistic-empirical pavement design guide: A manual of practice (2nd ed.).

American Coal Ash Association. (2003). *Fly ash facts for highway engineers* (Report No.
     FHWA-IF-03-019). Federal Highway Administration.

American Concrete Pavement Association (ACPA). (2009). *Recycling concrete pavements*
     (Engineering Bulletin EB043P).

Applied Research Associates, Inc. (2004). *Guide for mechanistic-empirical design of new and
     rehabilitated pavement structures* (NCHRP Project 1-37A). Transportation Research
     Board.

Arulrajah, A., Piratheepan, J., Disfani, M. M., & Bo, M. W. (2012). Geotechnical and
     geoenvironmental properties of recycled construction and demolition materials in
     pavement subbase applications. *Journal of Materials in Civil Engineering, 25*(8), 1077–
     1088.

ASTM C131-06. (2006). *Standard test method for resistance to degradation of small-size coarse
     aggregate by abrasion and impact in the Los Angeles machine*. ASTM International. doi:
     10.1520/C0131-06, www.astm.org

ASTM C136/C136M-14. (2014). *Standard test method for sieve analysis of fine and coarse
     aggregates*. ASTM International. doi: 10.1520/C0136_C0136M-14, www.astm.org

ASTM C157/C157M-17. (2017). *Standard test method for length change of hardened hydraulic-cement mortar and concrete*. ASTM International. doi: 10.1520/C0157_C0157M-17, www.astm.org

ASTM C192/C192M-16. (2016). *Standard practice for making and curing concrete test specimens in the laboratory*. ASTM International. doi: 10.1520/C0192_C0192M-16, www.astm.org

ASTM C490/C490M-17. (2017). *Standard practice for use of apparatus for the determination of length change of hardened cement paste, mortar, and concrete*. ASTM International. doi: 10.1520/C0490_C0490M-17, www.astm.org

ASTM C618-17. (2017). *Standard specification for coal fly ash and raw or calcined natural pozzolan for use in concrete*. ASTM International. doi: 10.1520/C0618-17, www.astm.org

ASTM D422-63. (2007). *Standard test method for particle-size analysis of soils*. ASTM International. doi: 10.1520/D0422-63R07, www.astm.org

ASTM D698-12. (2012). *Standard test methods for laboratory compaction characteristics of soil using standard effort*. ASTM International. doi: 10.1520/D0698-12, www.astm.org

ASTM D854-14. (2014). *Standard test methods for specific gravity of soil solids by water pycnometer*. ASTM International. doi: 10.1520/D0854-14, www.astm.org

ASTM D1632-17. (2017). *Standard practice for making and curing soil-cement compression and flexure test specimens in the laboratory*. ASTM International. doi: 10.1520/D1632-17, www.astm.org

ASTM D1633-17. (2017). *Standard test methods for compressive strength of molded soil-cement cylinders*. ASTM International. doi: 10.1520/D1633-17, www.astm.org

ASTM D1883-16. (2016). *Standard test method for California bearing ratio (CBR) of laboratory-compacted soils*. ASTM International. doi: 10.1520/D1883-16, www.astm.org

ASTM D2216-10. (2010). *Standard test methods for laboratory determination of water (moisture) content of soil and rock by mass*. ASTM International. doi: 10.1520/D2216-10, www.astm.org

ASTM D3551-17. (2017). *Standard practice for laboratory preparation of soil-lime mixtures using mechanical mixer*. ASTM International. doi: 10.1520/D3551-17, www.astm.org

ASTM D4318-17. (2017). *Standard test methods for liquid limit, plastic limit, and plasticity index of soils*. ASTM International. doi: 10.1520/D4318-17, www.astm.org

ASTM D5239-12. (2012). *Standard practice for characterizing fly ash for use in soil stabilization*. ASTM International. doi: 10.1520/D5239-12, www.astm.org

ASTM D6276. (2006). *Standard test method for using pH to estimate the soil-lime proportion requirement for soil stabilization*. ASTM International. doi: 10.1520/D6276-99AR06, www.astm.org

Banda, S. K. (2003). *Laboratory evaluation of chemical stabilization of Kansas embankment soils* (Master's thesis). Kansas State University.

Bandara, N., Binoy, T. H., Aboujrad, H. S., & Sato, J. (2015). Pavement subgrade stabilization using recycled materials. In *Airfield and Highway Pavements 2015* (pp. 605-616). American Society of Civil Engineers.

Bell, F. G. (1993). *Engineering treatment of soils*. CRC Press.

Bennert, T., & Maher, A. (2008). *The use of recycled concrete aggregate in a dense graded aggregate base course* (Report No. FHWA-NJ-2008-002). New Jersey Department of Transportation.

Bhandari, R. (1973). Shrinkage of cement treated mixtures. *Australian Road Research, 5*(3), 3–21.

Cabalar, A. F., Zardikawi, O., & Abdulnafaa, M. D. (2017). Utilisation of construction and demolition materials with clay for road pavement subgrade. *Road Materials and Pavement Design, 20*(3), 702–714.

Cavalline, T. (2022). *Recycled concrete aggregates: Current practice, implementation challenges and new guidance*. Presented at NIST Workshop: Fostering a circular economy and carbon sequestration for construction materials, Gaithersburg, Maryland, June 8, 2022. https://www.nist.gov/document/circular-economy-cement-workshop-tara-cavalline-recycled-concrete-aggregates-concrete

Chakrabarti, S., & Kodikara, J. (2003). Basaltic crushed rock stabilized with cementitious additives: Compressive strength and stiffness, drying shrinkage, and capillary flow characteristics. *Transportation Research Record, 1819*, 18–26.

Choobbasti, A. J., & Kutanaei, S. S. (2017). Microstructure characteristics of cement-stabilized sandy soil using nanosilica. *Journal of Rock Mechanics and Geotechnical Engineering, 9*(5), 981–988.

Daily, K. (2018). *Evaluation of lower quality recycled PCCP for portland cement treated base (PCTB)* (Master's thesis). Kansas State University.

Danyluk, L. S. (1986). *Stabilization of fine-grained soil for road and airfield construction*. US Army Corps of Engineers, Cold Regions Research & Engineering Laboratory.

Dastgerdi, A. S., Peterman, R. J., Riding, K., & Beck, B. T. (2019). Effect of concrete mixture components, proportioning, and compressive strength on fracture parameters. *Construction and Building Materials, 206*, 179–192.

Epps, J. A., Little, D. N., Holmgreen, R. J., & Terrel, R. L. (1980). *Guidelines for recycling pavement materials* (NCHRP Report 224). Transportation Research Board.

Etxeberria, M., Vázquez, E., Mari, A., & Barra, M. (2007). Influence of amount of recycled coarse aggregates and production process on properties of recycled aggregate concrete. *Cement and Concrete Research, 37*(5), 735-742.

Federal Highway Administration (FHWA). (2002). *Life-cycle cost analysis primer* (Report No. FHWA-IF-02-047).

Federal Highway Administration (FHWA). (2004). *Recycled concrete aggregate Federal Highway Administration national review*. https://www.fhwa.dot.gov/pavement/recycling/rca.cfm

Garber, N. J., & Hoel, L. A. (2014). *Traffic and highway engineering* (5th ed.)*. Cengage Learning.

Gedafa, D. S., Hossain, M., & Gisi, A. J. (2006). *Mechanistic-empirical design guide analysis of asphalt pavements with granular base course*. 10th International Conference on Asphalt Pavements – August 12 to 17, 2006, Quebec City, Canada.

George, K. P. (1968). Shrinkage characteristics of soil-cement mixtures. *Highway Research Record, 255*, 42–58.

Gomez, J. N., & Anderson, D. M. (2012). *Soil cement stabilization – Mix design, control and results during construction*. International Symposium on Ground Improvement, May 31 to June 1, 2012, Brussels, Belgium.

Gonzalez, G. P., & Moo-Young, H. K. (2004). *Transportation applications of recycled concrete aggregate* (FHWA State of the Practice National Review). Federal Highway Administration. https://www.fhwa.dot.gov/pavement/recycling/applications.pdf

Gonzalez-Corominas, A., & Etxeberria, M. (2016). Effects of using recycled concrete aggregates on the shrinkage of high performance concrete. *Construction and Building Materials, 115*, 32–41.

Guthrie, W. S., Sebesta, S., & Scullion, T. (2002). *Selecting optimum cement contents for stabilizing aggregate base materials* (Report No. FHWA/TX-05/7-4920-2). Texas Transportation Institute.

Hafner, B. (2007). *Scanning electron microscopy primer*. Characterization Facility, University of Minnesota – Twin Cities.

Hossain, K., & Mol, L. (2011). Some engineering properties of stabilized clayey soils incorporating natural pozzolans and industrial wastes. *Construction and Building Materials, 25*(8), 3495–3501.

Islam, S., Hossain, M., Jones, C., Bose, A., Barrett, R., & Velasquez, N. (2019). Implementation of AASHTOWare Pavement ME Design Software for asphalt pavements in Kansas. *Transportation Research Record, 2673*(4), 490–499.

Islam, S., Sufian, A., Hossain, M., Velasquez, N., Barrett, R. (2018). *Practical issues in local calibration and implementation of AASHTOWare Pavement ME design procedure for concrete pavements* (Paper No. 18-05022). Transportation Research Board 97th Annual Meeting, Washington, D.C.

Jones, D., Rahim, A., Saadeh, S., & Harvey, J. T. (2010). *Guidelines for the stabilization of subgrade soils in California*. California Department of Transportation.

Kansas Department of Transportation (KDOT). (2007). *Kansas Department of Transportation geotechnical manual*.

Kansas Department of Transportation (KDOT). (2015). *Standard specifications for state road & bridge construction*.

Kestler, M. A. (2009). *Stabilization selection guide for aggregate- and native-surfaced low volume roads*. U.S. Department of Agriculture, National Technology & Development Program.

Kodikara, J., & Chakrabarti, S. (2001). *Shrinkage behaviour of cemented materials as applicable to in situ pavement stabilisation*. ARRB Transport Research LTD Conference, 20th, 2001, Melbourne, Victoria, Australia

Kou, S. C., Poon, C. S., & Chan, D. (2007). Influence of fly ash as cement replacement on the properties of recycled aggregate concrete. *Journal of Materials in Civil Engineering, 19*(9), 709–717. https://doi.org/10.1061/(ASCE)0899-1561(2007)19:9(709)

KT-6 Kansas Test Method. (2004). Specific gravity and absorption of aggregates. *Kansas Department of Transportation construction manual, Part V*. Kansas Department of Transportation.

KTMR-21 Kansas Test Method. (1999). *Soundness & modified soundness of aggregates by freezing and thawing*. Kansas Department of Transportation.

Latifi, N., Meehan, C. L., Majid, M. Z. A., & Horpibulsuk, S. (2016). Strengthening montmorillonitic and kaolinitic clays using a calcium-based non-traditional additive: A micro-level study. *Applied Clay Science, 132*, 182–193.

Latifi, N., Vahedifard, F., Ghazanfari, E., Horpibulsuk, S., Marto, A., & Williams, J. (2017). Sustainable improvement of clays using low-carbon nontraditional additive. *International Journal of Geomechanics, 18*(3).

Little, D. N. (1998). *Evaluation of structural properties of lime stabilized soils and aggregates*. National Lime Association.

Little, D. N., & Nair, S. (2009). *Recommended practice for stabilization of subgrade soils and base materials* (NCHRP Web-Only Document 144). Transportation Research Board.

Maher, M., Marshall, C., Harrison, F., & Baumgaertner, K. (2005). *Context sensitive roadway surfacing selection guide* (FHWA-CFL/TD-05-004). Federal Highway Administration.

Mallick, R. B., & El-Korchi, T. (2018). *Pavement engineering: Principles and practice* (3rd ed.). CRC Press.

McNeil, K., & Kang, T.-H. (2013). Recycled concrete aggregates: A review. *International Journal of Concrete Structures and Materials, 7*, 61–69.

Mindess, S., Young, J. F., & Darwin, D. (2002). *Concrete* (2nd ed.). Prentice Hall.

Mitchell, J. K., & Soga, K. (2005). *Fundamentals of soil behavior* (3rd ed.). John Wiley & Sons.

Oikonomou, N. D. (2005). Recycled concrete aggregates. *Cement and Concrete Composites, 27*(2), 315–318.

Osinubi, K. J. (1998). Influence of compactive efforts and compaction delays on lime-treated soil. *Journal of Transportation Engineering, 124*(2), 149–155.

Ozdemir, M. A. (2016). Improvement in bearing capacity of a soft soil by addition of fly ash. *Procedia Engineering, 143*, 498–505.

Parsons, R. L., Johnson, C. P., & Cross, S. A. (2001). *Evaluation of soil modification mixing procedures* (Report No. K-TRAN: KU-00-6). Kansas Department of Transportation.

Petry, T. M., & Little, D. N. (2002). Review of stabilization of clays and expansive soils in pavements and lightly loaded structures—History, practice, and future. *Journal of Materials in Civil Engineering, 14*(6), 447–460.

Poon, C. S., & Chan, D. (2006). Feasible use of recycled concrete aggregates and crushed clay brick as unbound road sub-base. *Construction and Building Materials, 20*(8), 578–585.

Portland Cement Association (PCA). (1956). *Soil-cement laboratory handbook.*

Portland Cement Association (PCA). (1992). *Soil-cement laboratory handbook.*

Rao, A., Jha, K. N., & Misra, S. (2007). Use of aggregates from recycled construction and demolition waste in concrete. *Resources, Conservation and Recycling, 50*(1), 71–81.

Rawlings, R. E., Williams, D. J., & Gordon, R. G. (1988). Laboratory and field comparisons of cement treated paving materials. In *Australian Road Research Board (ARRB) Conference, 14th, 1988, Canberra* (Vol. 14, No. 7).

Romero, E., & Simms, P. H. (2008). Microstructure investigation in unsaturated soils: A review with special attention to contribution of mercury intrusion porosimetry and environmental scanning electron microscopy. *Geotechnical & Geological Engineering, 26*(6), 705–727.

Sabahfar, N. (2016). *Effect of asphalt rejuvenating agent on aged reclaimed asphalt pavement and binder properties* (Doctoral dissertation). Kansas State University.

Schwartz, D. R. (1987). *D-cracking of concrete pavements* (NCHRP Synthesis of Highway Practice 134). Transportation Research Board.

Silva, R. V., de Brito, J., & Dhir, R. K. (2016). Establishing a relationship between modulus of elasticity and compressive strength of recycled aggregate concrete. *Journal of Cleaner Production, 112*(4), 2171–2186.

Snyder, M. B. (2016). Concrete pavement recycling and the use of recycled concrete aggregate in concrete paving mixtures. https://intrans.iastate.edu/app/uploads/2019/11/MAPbriefMarch2016.pdf

Snyder, M. B., Vandenbossche, J. M., Smith, K. D., & Wade, M. (1994). *Synthesis on recycled concrete aggregate* (Interim Report–Task A, DTFH61-93-C-00133). Federal Highway Administration.

Tastan, E. O., Edil, T. B., Benson, C. H., & Aydilek, A. H. (2011). Stabilization of organic soils with fly ash. *Journal of Geotechnical and Geoenvironmental Engineering, 137*(9), 819–833.

U.S. Army Corps of Engineers (USACE). (1994). *Soil stabilization for pavements* (TM 5-822-14).

U.S. Environmental Protection Agency (EPA). (2014). *Construction and demolition debris generation in the United States*. Office of Resource Conservation and Recovery.

Verian, K. P., Whiting, N. M., Olek, J., Jain, J., & Snyder, M. B. (2013). *Using recycled concrete as aggregate in concrete pavements to reduce materials cost* (Report No. FHWA/IN/JTRP-2013/18). Indiana Department of Transportation.

Walker, P. J. (1995). Strength, durability and shrinkage characteristics of cement stabilised soil blocks. *Cement and Concrete Composites, 17*(4), 301–310.

Walls, J., III., & Smith, M. R. (1998). *Life-cycle cost analysis in pavement design* (Report No. FHWA-SA-98-079). Federal Highway Administration.

Westover, T. M., Labuz, J. F., & Guzina, B. B. (2007). *Resilient modulus development of aggregate base and subbase containing recycled bituminous and concrete for 2002 Design Guide and Mn/Pave pavement design* (Report No. MN/RC-2007-25). Minnesota Department of Transportation.

Wu, L., Farzadnia, N., Shi, C., Zhang, Z., & Wang, H. (2017). Autogenous shrinkage of high performance concrete: A review. *Construction and Building Materials, 149*(2), 62–75.

Yoder, E. J., & Witczak, M. W. (1975). *Principles of pavement design* (2nd ed.). John Wiley & Sons.

Zha, F., Liu, S., Du, Y., & Cui, K. (2008). Behavior of expansive soils stabilized with fly ash. *Natural Hazards, 47*(3), 509–523.

Appendix A: Mill Reports of Fly Ash and Portland Cement

KCPC
MATERIALS LAB
Kansas City Performance Center
15100 E. Courtney Atherton Rd. Sugar Creek, MO 64056
Phone: (816)257-4093 Fax: (816)257-5930

REPORT DATE 04/20/2017
FLY ASH SOURCE latan
COMPOSITE START DATE 3/1/2017 1:03:00 PM
COMPOSITE END DATE 3/15/2017 1:03:00 PM
SAMPLE IDENTIFICATION 1A1170301-0315

CHEMICAL ANALYSES

Analysis	Value	ASTM C 618 CLASS C	AASHTO M295 CLASS C
SiO2 (silicon dioxide), %	42.28		
Al2O3 (aluminum oxide), %	18.34		
Fe2O3 (iron oxide), %	5.74		
SiO2+Al2O3+Fe2O3, %	66.36	50 min	50 min
CaO (calcium oxide), %	23.01		
MgO (magnesium oxide), %	4.51		
SO3 (sulfur trioxide), %	1.10	5.0 max	5.0 max
Moisture content, %	0.11	3.0 max	3.0 max
Loss On Ignition, %	0.19	6.0 max	5.0 max
Na2O (sodium oxide), %	1.45		
K2O (potassium oxide), %	0.49		

PHYSICAL ANALYSES

Fineness, amount retained on #325 sieve, %	26.6	34 max	34 max
variation, points from average	2.9	5 max	5 max
Density, g/cm3	2.55		
variation from average, %	-4.1	5 max	5 max
Strength Activity Index with Portland Cement at 7 days, % of cement control	79		
Water Requirement, % of cement control	95	105 max	105 max
Soundness, autoclave expansion or contraction, %	0.06	0.8 max	0.8 max

We hereby certify that the fly ash represented by the above chemical and physical analysis meets the requirements of ASTM C 618 and AASHTO M 295.

04/20/2017

Tina M. Tucholski
KCPC Laboratory Manager

ASTM C 618 Note 1 - Finely divided materials may tend to reduce the entrained air content of concrete. Hence, if a mineral admixture is added to any concrete for which entrainment of air is specified, provision should be made to assure that the specified air content is maintained by air content tests and by use of additional air-entraining admixture or use of an air-entraining admixture in combination with air-entraining hydraulic cement.

Figure A.1: Class C Fly Ash Mill Report

Central Plains Cement Company

Cement Mill Test Report
Month of Issue: April-17

Plant:	Sugar Creek Plant
Product:	Portland Cement Type I-II (MH)
Shipped:	Mar-17
Manufactured:	Mar-17

The current version of ASTM C 150 and AASHTO M 85 Standard Requirements
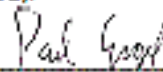
CHEMICAL ANALYSIS

Item	Spec limit	Test Result
Rapid Method, X-Ray (C 114)		
SiO2 (%)	—	21.2
Al2O3 (%)	6.0 max	4.7
Fe2O3 (%)	6.0 max	3.1
CaO (%)	—	64.0
MgO (%)	6.0 max	1.2
SO3 (%)	3.0 max *	3.0
Loss on Ignition (%)	3.5 max	2.6
Insoluble residue (%)	1.5 max	0.27
CO2 (%)	—	1.8
Limestone (%)	5.0 max	4.5
CaCO3 in Limestone (%)	70 min	93
Adjusted Potential Phase Composition (C 150)		
C3S (%)	—	55
C2S (%)	—	17
C3A (%)	8 max	7
C4AF (%)	—	9
C3S+4.75*C3A (%)	100 max	90

PHYSICAL ANALYSIS

Item	Spec limit	Test Result
Air content of mortar (%) (C 185)	12 max	8
Blaine fineness (m2/kg) (C 204)	260 - 430	361
-325 (%) (C 430)	—	95.8
Autoclave expansion (%) (C 151)	0.80 max	-0.01
Compressive strength (PSI) (C 109)		
1 day	—	2143
3 days	1740 min	3803
7 days	2760 min	5063
28 days (Reflects previous month's data)	—	7053
Time of setting (minutes)		
Vicat Initial (C 191)	45 - 375	97
Mortar Bar Expansion (%) (C 1038) *	0.020 max	0.005
Specific Gravity (C 188)	—	3.15

ASTM C 150-18 and AASHTO M 85-18 Optional Chemical Requirements:

Na2e (%)	0.60 max	0.55

* May exceed 3.0% SO3 maximum, based on our C 1038 results of <0.020 expansion at 14 days.

We certify that the above described cement meets the chemical and physical requirements of Type I and Type II (MH) for the current version of ASTM C 150 & AASHTO M 85 STANDARD.

Certified By:

_____
Paul Engel - Quality Coordinator

4/7/2017

Sugar Creek Plant
2200 N Courtney Rd.
Sugar Creek, MO 64050
816-257-3600

Figure A.2: Portland Cement Mill Report

Appendix B: UCS Test Results

Table B.1: UCS Test Results for 100% Untreated Clay (No Chemical Agent)

Sample#	Binder (%)	Age (days)	Dia. (in.)	Ht. (in.)	Max. Load (lb)	UCS (psi)	Avg. UCS (psi)
1	0	0	2.8	6.3	165	27	
2	0	0	2.8	6.3	167	28	27
3	0	0	2.8	6.3	162	27	

Table B.2: UCS Test Results (7 and 28 Days) for 100% Clay-Fly Ash Mixtures

Sample#	Binder (%)	Age (days)	Dia. (in.)	Ht. (in.)	Max. Load (lb)	UCS (psi)	Avg. UCS (psi)
7 days							
1	22	7	2.8	6.3	295	49	58
2	22	7	2.8	6.3	411	68	
1	19	7	2.8	6.3	345	59	
2	19	7	2.8	6.3	183	31	42
3	19	7	2.8	6.3	209	36	
1	16	7	2.8	6.3	85	14	
2	16	7	2.8	6.3	103	17	13
3	16	7	2.8	6.3	54	9	
28 days							
1	22	28	2.8	6.3	361	60	
2	22	28	2.8	6.3	449	74	65
3	22	28	2.8	6.3	376	62	
1	19	28	2.8	6.3	446	73	
2	19	28	2.8	6.3	399	66	72
3	19	28	2.8	6.3	462	76	
1	16	28	2.8	6.3	70	11	13
2	16	28	2.8	6.3	92	15	

Table B.3: UCS Test Results (7 and 28 Days) for 100% Clay-Fly Ash-Portland Cement Mixtures

Sample#	Binder	Age (days)	Dia. (in.)	Ht. (in.)	Max. Load (lb)	UCS (psi)	Avg. UCS (psi)
			7 days				
1	19% -(c/f 1:2)	7	2.8	6.3	714	118	125
2	19% -(c/f 1:2)	7	2.8	6.3	801	132	
1	19% -(c/f 1:1)	7	2.8	6.3	525	87	
2	19% -(c/f 1:1)	7	2.8	6.3	687	113	91
3	19% -(c/f 1:1)	7	2.8	6.3	445	73	
			28 days				
1	19% -(c/f 1:2)	28	2.8	6.3	913	150	
2	19% -(c/f 1:2)	28	2.8	6.3	1011	167	148
3	19% -(c/f 1:2)	28	2.8	6.3	772	127	
1	19% -(c/f 1:1)	28	2.8	6.3	912	150	
2	19% -(c/f 1:1)	28	2.8	6.3	667	110	123
3	19% -(c/f 1:1)	28	2.8	6.3	659	109	

Table B.4: UCS Test Results (7 and 28 Days) for 100% Clay-Lime Mixtures

Sample#	Binder (%)	Age (days)	Dia. (in.)	Ht. (in.)	Max. Load (lb)	UCS (psi)	Avg. UCS (psi)
			7 days				
1	8	7	2.8	6.3	301	50	
2	8	7	2.8	6.3	212	35	34
3	8	7	2.8	6.3	102	17	
1	6	7	2.8	6.3	171	28	
2	6	7	2.8	6.3	194	32	30
			28 days				
1	8	28	2.8	6.3	377	62	
2	8	28	2.8	6.3	437	72	61
3	8	28	2.8	6.3	298	49	
1	6	28	2.8	6.3	239	39	
2	6	28	2.8	6.3	359	59	50
3	6	28	2.8	6.3	305	50	

Table B.5: UCS Test Results for Untreated 50%Clay-50%Topeka (No Chemical Agent)

Sample#	Binder (%)	Age (days)	Dia. (in.)	Ht. (in.)	Max. Load (lb)	UCS (psi)	Avg. UCS (psi)
1	0	0	2.78	6.3	60	10	
2	0	0	2.78	6.3	61	10	9
3	0	0	2.78	6.3	50	8	

Table B.6: UCS Test Results (7 and 28 Days) for 50%Clay-50%Topeka-Fly Ash Mixtures

Sample#	Binder (%)	Age (days)	Dia. (in.)	Ht. (in.)	Max. Load (lb)	UCS (psi)	Avg. UCS (psi)
7 days							
1	20	7	2.8	6.3	402	66	
2	20	7	2.8	6.3	387	64	70
3	20	7	2.8	6.3	489	81	
1	17	7	2.8	6.3	210	35	26
2	17	7	2.8	6.3	100	16	
1	14	0	2.8	6.3	86	14	15
2	14	0	2.8	6.3	92	15	
28 days							
1	20	28	2.8	6.3	559	92	
2	20	28	2.8	6.3	417	69	75
3	20	28	2.8	6.3	394	65	
1	17	28	2.8	6.3	417	69	
2	17	28	2.8	6.3	198	33	44
3	17	28	2.8	6.3	190	31	
1	14	28	2.8	6.3	199	33	
2	14	28	2.8	6.3	34	6	17
3	14	28	2.8	6.3	73	12	

Table B.7: UCS Test Results (7 and 28 Days) for 50%Clay-50%Topeka-Fly Ash-Portland Cement Mixtures

Sample#	Binder (%)	Age (days)	Dia. (in.)	Ht. (in.)	Max. Load (lb)	UCS (psi)	Avg. UCS (psi)
7 days							
1	14% -(c/f 1:2)	7	2.8	6.3	956	158	
2	14% -(c/f 1:2)	7	2.8	6.3	652	107	132
3	14% -(c/f 1:2)	7	2.8	6.3			
1	14% -(c/f 1:1)	7	2.8	6.3	549	90	
2	14% -(c/f 1:1)	7	2.8	6.3	1261	208	149
28 days							
1	14% -(c/f 1:2)	28	2.8	6.3	1752	289	
2	14% -(c/f 1:2)	28	2.8	6.3	1918	316	276
3	14% -(c/f 1:2)	28	2.8	6.3	1354	223	
1	14% -(c/f 1:1)	28	2.8	6.3	1697	280	
2	14% -(c/f 1:1)	28	2.8	6.3	2364	389	335

Table B.8: UCS Test Results (7 and 28 Days) for 50%Clay-50%Topeka-Lime Mixtures

Sample#	Binder (%)	Age (days)	Dia. (in.)	Ht. (in.)	Max. Load (lb)	UCS (psi)	Avg. UCS (psi)
7 days							
1	8	7	2.8	6.3	224	37	
2	8	7	2.8	6.3	220	36	37
1	6	7	2.8	6.3	211	35	
2	6	7	2.8	6.3	129	21	28
28 days							
1	8	28	2.8	6.3	355	58	
2	8	28	2.8	6.3	332	55	61
3	8	28	2.8	6.3	427	70	
1	6	28	2.8	6.3	211	35	
2	6	28	2.8	6.3	373	62	54
3	6	28	2.8	6.3	404	67	

Table B.9: UCS Test Results for Untreated 50%Clay-50%KC (No Chemical Agent)

Sample#	Binder (%)	Age (days)	Dia. (in.)	Ht. (in.)	Max. Load (lb)	UCS (psi)	Avg. UCS (psi)
1	0	0	2.8	6.3	83	14	
2	0	0	2.8	6.3	67	11	12
3	0	0	2.8	6.3	73	12	

Table B.10: UCS Test Results (7 and 28 Days) for 50%Clay-50%KC-Fly Ash Mixtures

Sample#	Binder (%)	Age (days)	Dia. (in.)	Ht. (in.)	Max. Load (lb)	UCS (psi)	Avg. UCS (psi)
7 days							
1	20	7	2.8	6.3	137	23	
2	20	7	2.8	6.3	386	64	43
3	20	7	2.8	6.3			
1	17	7	2.8	6.3	319	53	
2	17	7	2.8	6.3	212	35	44
3	17	7	2.8	6.3		0	
1	14	7	2.8	6.3	332	55	49
2	14	7	2.8	6.3	259	43	
28 days							
1	20	28	2.8	6.3	480	79	
2	20	28	2.8	6.3	471	78	81
3	20	28	2.8	6.3	520	86	
1	17	28	2.8	6.3	703	116	
2	17	28	2.8	6.3	632	104	106
3	17	28	2.8	6.3	597	98	
1	14	28	2.8	6.3	719	118	
2	14	28	2.8	6.3	378	62	75
3	14	28	2.8	6.3	274	45	

Table B.11: UCS Test Results (7 and 28 Days) for 50%Clay-50%KC-Fly Ash-Portland Cement Mixtures

Sample#	Binder (%)	Age (days)	Dia. (in.)	Ht. (in.)	Max. Load (ib)	UCS (psi)	Avg. UCS (psi)
7 days							
1	14% -(c/f 1:2)	7	2.8	6.3	1246	205	
2	14% -(c/f 1:2)	7	2.8	6.3	864	142	144
3	14% -(c/f 1:2)	7	2.8	6.3	521	86	
1	14% -(c/f 1:1)	7	2.8	6.3	1700	280	
2	14% -(c/f 1:1)	7	2.8	6.3	1431	236	258
3	14% -(c/f 1:1)	7	2.8	6.3		0	
28 days							
1	14% -(c/f 1:2)	28	2.8	6.3	2066	340	
2	14% -(c/f 1:2)	28	2.8	6.3	1305	215	285
3	14% -(c/f 1:2)	28	2.8	6.3	1827	301	
1	14% -(c/f 1:1)	28	2.8	6.3	1126	186	
2	14% -(c/f 1:1)	28	2.8	6.3	2267	373	321
3	14% -(c/f 1:1)	28	2.8	6.3	2457	405	

Table B.12: UCS Test Results (7 and 28 Days) for 50%Clay-50%KC-Lime Mixtures

Sample#	Binder (%)	Age (days)	Dia. (in.)	Ht. (in.)	Max. Load (ib)	UCS (psi)	Avg. UCS (psi)
7 days							
1	8	7	2.8	6.3	202	33	39
2	8	7	2.8	6.3	269	44	
1	6	0	2.8	6.3	185	30	
2	6	0	2.8	6.3	102	17	29
3	6	0	2.8	6.3	245	40	
28 days							
1	8	28	2.8	6.3	350	58	
2	8	28	2.8	6.3	301	50	54
3	8	28	2.8	6.3	331	55	
1	6	28	2.8	6.3	359	59	
2	6	28	2.8	6.3	331	55	56
3	6	28	2.8	6.3	325	54	

Table B.13: UCS Test Results (7 and 28 Days) for 100%Topeka-Fly Ash Mixtures

| Sample#	Binder (%)	Age (days)	Dia. (in.)	Ht. (in.)	Max. Load (lb)	UCS (psi)	Avg. UCS (psi)
7 days							
1	5	7	3.9	8.0	355	30	28
2	5	7	3.9	8.0	310	26	
28 days							
1	5	7	3.9	8.0	441	38	
2	5	7	3.9	8.0	407	35	36
3	5	7	3.9	8.0			

Table B.14: UCS Test Results (7 and 28 Days) for 100%Topeka-Fly Ash-Portland Cement Mixtures

Sample#	Binder (%)	Age (days)	Dia. (in.)	Ht. (in.)	Max. Load (lb)	UCS (psi)	Avg. UCS (psi)
7 days							
1	5% -(c/f 1:2)	7	3.9	8.0	1607	137	
2	5% -(c/f 1:2)	7	3.9	8.0	1163	99	112
3	5% -(c/f 1:2)	7	3.9	8.0	1193	101	
1	5% -(c/f 1:1)	7	3.9	8.0	1871	159	166
2	5% -(c/f 1:1)	7	3.9	8.0	2041	174	
28 days							
1	5% -(c/f 1:2)	28	3.9	8.0	1889	161	
2	5% -(c/f 1:2)	28	3.9	8.0	1950	166	159
3	5% -(c/f 1:2)	28	3.9	8.0	1758	149	
1	5% -(c/f 1:1)	28	3.9	8.0	2592	220	220
2	5% -(c/f 1:1)	28	3.9	8.0	2576	219	

Table B.15: UCS Test Results (7 and 28 Days) for 100%Topeka-Lime Mixtures

| Sample#	Binder (%)	Age (days)	Dia. (in.)	Ht. (in.)	Max. Load (lb)	UCS (psi)	Avg. UCS (psi)
7 days							
1	8	7	3.9	8.0	271	23	24
2	8	7	3.9	8.0	294	25	
1	6	7	3.9	8.0	290	25	28
2	6	7	3.9	8.0	359	31	
28 days							
1	8	28	3.9	8.0	738	63	55
2	8	28	3.9	8.0	566	48	
1	6	28	3.9	8.0	398	34	
2	6	28	3.9	8.0	559	48	41
3	6	28	3.9	8.0	477	41	

Table B.16: UCS Test Results (7 and 28 Days) for 100% KC-Fly Ash Mixtures

Sample#	Binder (%)	Age (days)	Dia. (in.)	Ht. (in.)	Max. Load (lb)	UCS (psi)	Avg. UCS (psi)
7 days							
1	5	7	3.9	8.0	283	24	24
28 days							
1	5	28	3.9	8.0	483	41	41

Table B.17: UCS Test Results (7 and 28 Days) for 100% KC-Fly Ash-Portland Cement Mixtures

Sample#	Binder (%)	Age (days)	Dia. (in.)	Ht. (in.)	Max. Load (lb)	UCS (psi)	Avg. UCS (psi)
7 days							
1	5% -(c/f 1:2)	7	3.9	8.0	640	54	55
2	5% -(c/f 1:2)	7	3.9	8.0	645	55	
1	5% -(c/f 1:1)	7	3.9	8.0	1408	120	121
2	5% -(c/f 1:1)	7	3.9	8.0	1437	122	
28 days							
1	5% -(c/f 1:2)	28	3.9	8.0	1736	148	150
2	5% -(c/f 1:2)	28	3.9	8.0	1800	153	
1	5% -(c/f 1:1)	28	3.9	8.0	2016	171	162
2	5% -(c/f 1:1)	28	3.9	8.0	1789	152	

Table B.18: UCS Test Results (7 and 28 Days) for 100% KC-Lime Mixtures

Sample#	Binder (%)	Age (days)	Dia. (in.)	Ht. (in.)	Max. Load (lb)	UCS (psi)	Avg. UCS (psi)
7 days							
1	8	7	3.9	8.0	293	25	26
2	8	7	3.9	8.0	322	27	
1	6	7	3.9	8.0	616	52	55
2	6	7	3.9	8.0	687	58	
28 days							
1	8	28	3.9	8.0	484	41	43
2	8	28	3.9	8.0	522	44	
1	6	28	3.9	8.0	677	58	68
2	6	28	3.9	8.0	932	79	

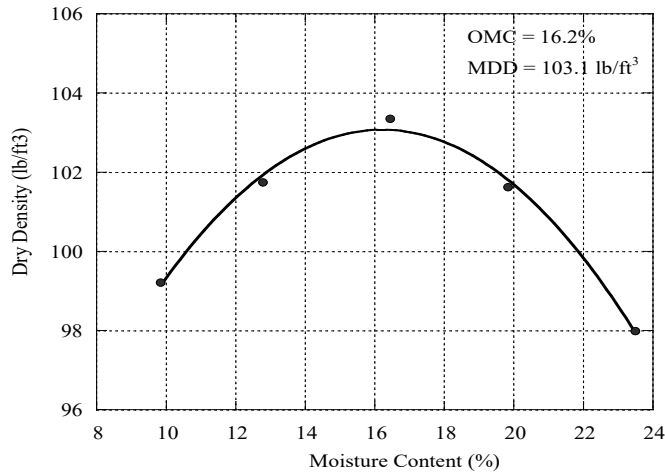# Appendix C: Standard Proctor Test Results
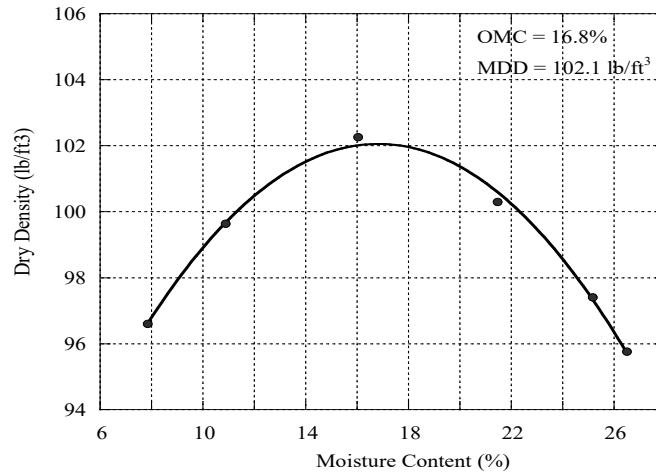
Figure C.1: Estimation of Initial Fly Ash Content for 100% Clay Mixtures (Fly Ash Content 13%)
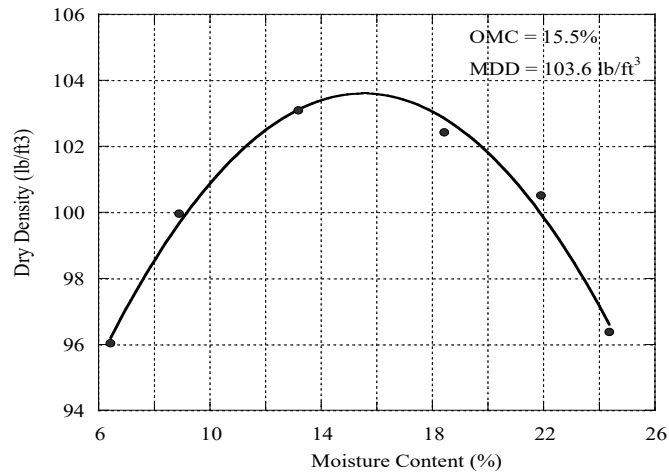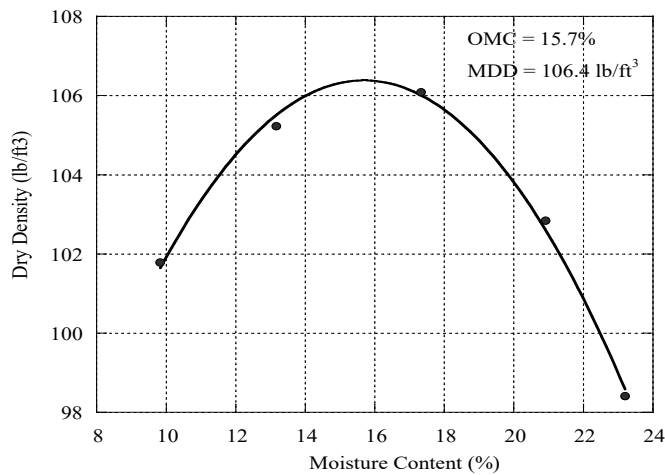

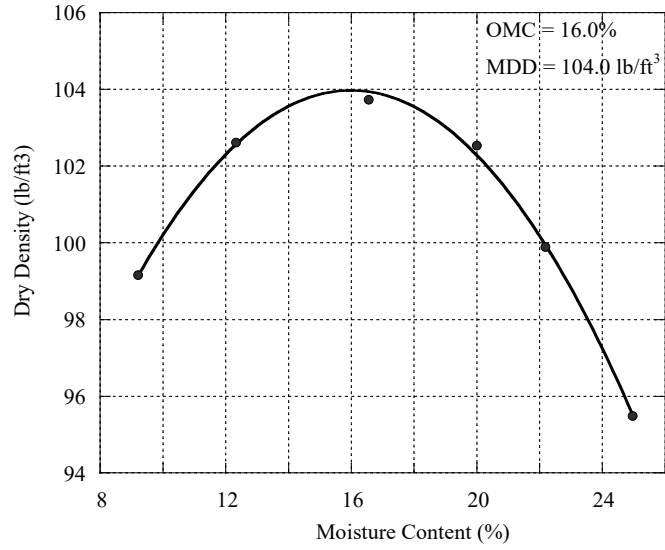**Figure C.2: Estimation of Initial Fly Ash Content for 100% Clay Mixtures (Fly Ash Content 16%)**
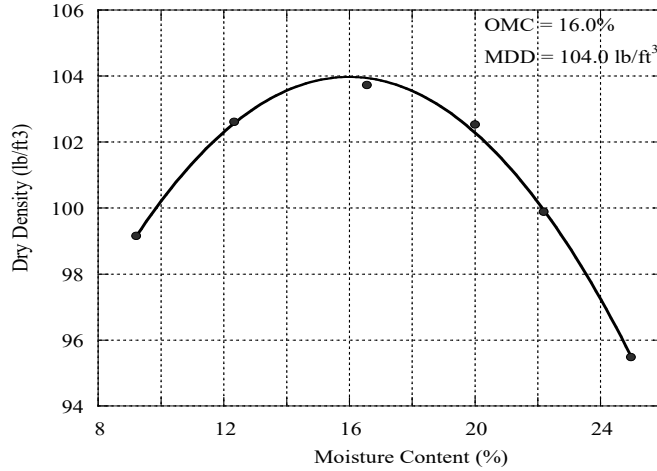
Figure C.3: Estimation of Initial Fly Ash Content for 100% Clay Mixtures (Fly Ash Content 19%)
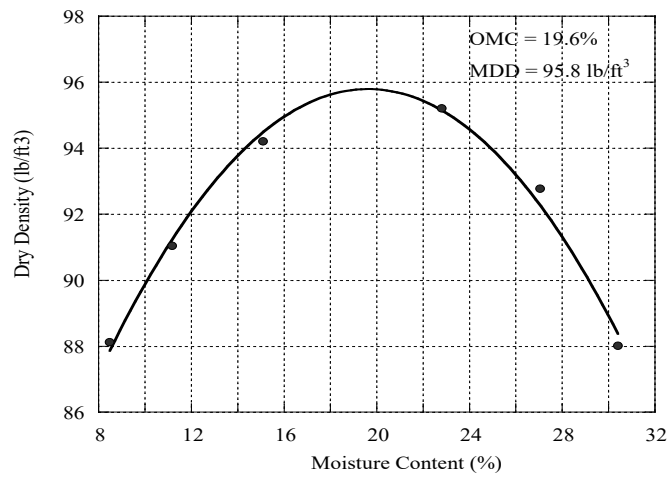

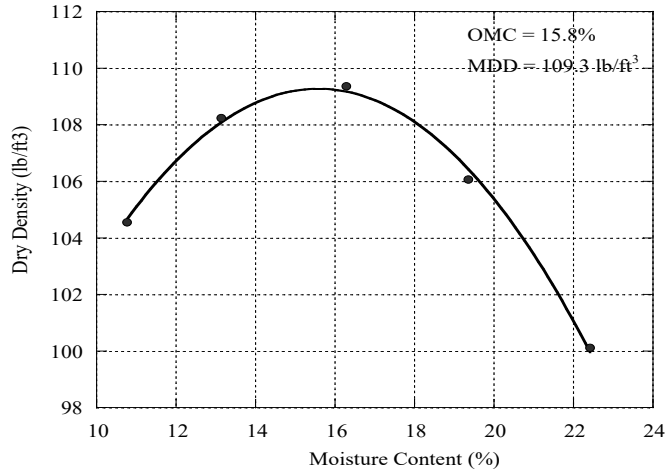**Figure C.4: Estimation of Initial Fly Ash Content for 50% Clay-50% RCA (12% Fly Ash)**

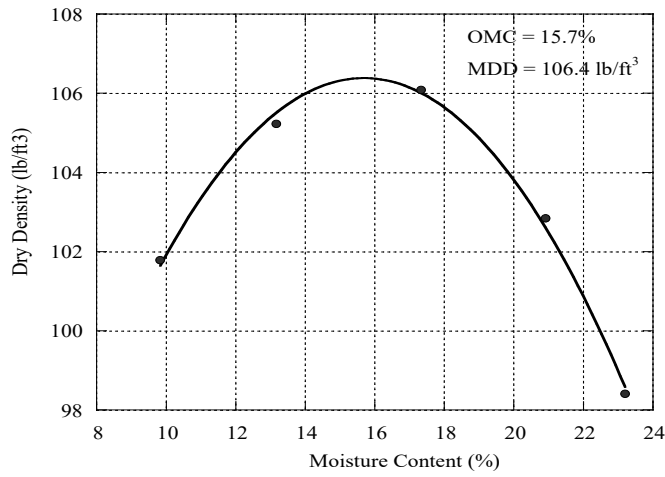**Figure C.5: Estimation of Initial Fly Ash Content for 50% Clay-50% RCA (14% Fly Ash)**

Figure C.6: Compaction Curve for 100% Clay and 19% Fly Ash
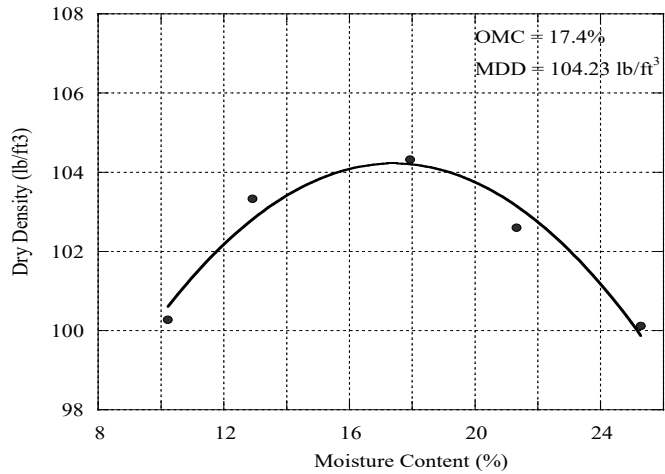

Figure C.7: Compaction Curve for 100% Clay and 6% Lime
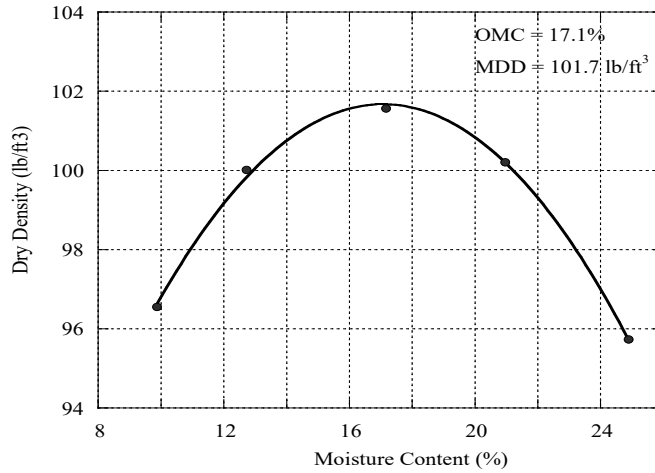
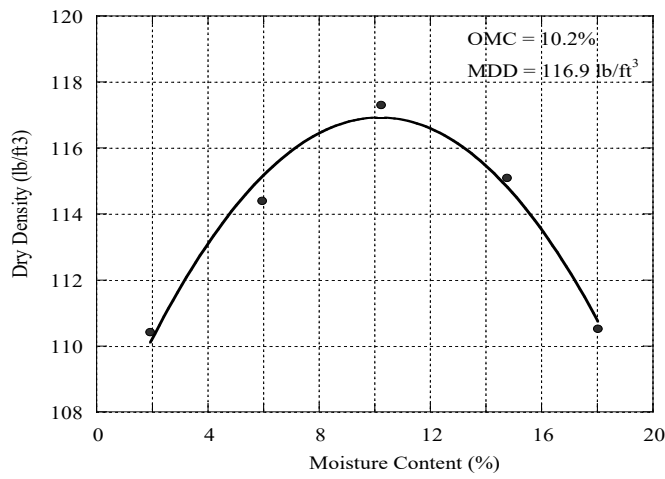**Figure C.8: Compaction Curve for 50% Clay-50% Topeka and 14% Fly Ash**

Figure C.9: Compaction Curve for 50% Clay-50% KC and 14% Fly Ash
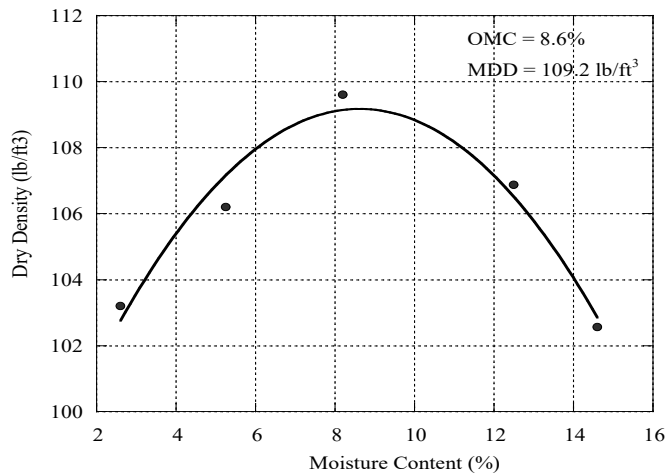

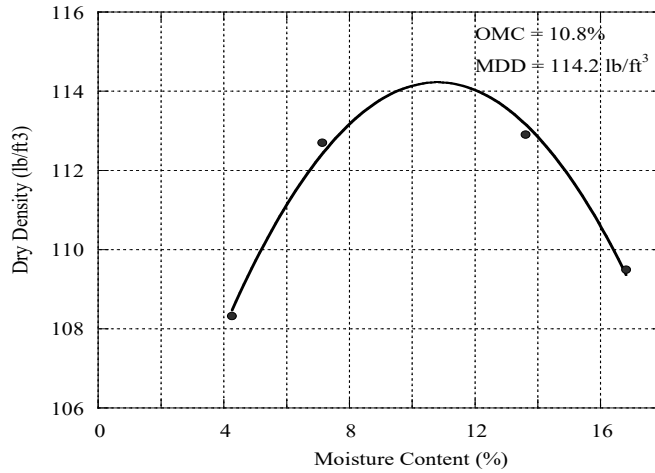**Figure C.10: Compaction Curve for 50% Clay-50% Topeka and 6% Lime**

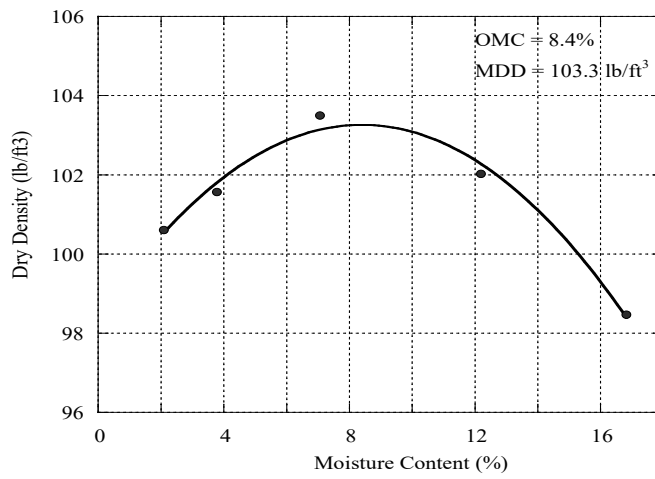**Figure C.11: Compaction Curve for 50% Clay-50% KC and 6% Lime**

Figure C.12: Compaction Curve for 100% Topeka and 5% Fly Ash

Figure C.13: Compaction Curve for 100% KC and 5% Fly Ash

135

Figure C.14: Compaction Curve for 100% Topeka and 6% Lime

Figure C.15: Compaction Curve for 100% KC and 6% Lime

136

Appendix D: MEPDG Inputs

Table D.1: KDOT Calibration Coefficients for New Flexible Pavements

Subgrade Rutting	Bs_1 (fine)= 0.4	Bs_1 (granular)= 1.0		
AC Rutting	$Br_1 = 0.75$	$Br_2 = 1.0$	$Br_3 = 0.85$	
AC Fatigue	$Bf_1 = 1.0$	$Bf_2 = 1.0$	$Bf_3 = 1.60$	
Thermal Fracture	Level 1 = 1.5	Level 2 = 0.5	Level 3 = 1.5	
AC Bottom Up Fatigue Cracking	$C_1 = 1.0$	$C_2 = 1.0$	$C_3 = 6000$	
AC Top Down Fatigue Cracking	C1 = 0.90	C2 = 0.45	C3 = 0	C4 = 1000
IRI	$C_1 = 33$	$C_2 = 0.40$	$C_3 = 0.008$	$C_4 = 0.01$

Table D.2: KDOT Performance Criteria for Each Category of Road

Performance Criteria	Minor Arterial		Principal Arterial		Interstate	
	Target Value	Reliability	Target Value	Reliability	Target Value	Reliability
Initial IRI (in./mile)	30	-	30	-	30	-
Terminal IRI (in./mile)	200	65	180	75	160	85
AC top-down fatigue cracking (ft/mile)	2,500	75	2,000	85	1,500	95
AC bottom-up fatigue cracking (% lane area)	30	75	20	85	10	95
AC thermal cracking (ft/mile)	750	65	750	75	750	85
Permanent deformation - total pavement (in.)	0.65	75	0.55	85	0.35	95
Permanent deformation - AC only (in.)	0.55	75	0.45	85	0.45	95

Table D.3: Distribution of AADTT by Vehicle Class and Number of Axles per Truck

Vehicle class	AADTT Distribution (%) (Level 3)	Single Axle	Tandem Axle	Tridem Axle	Quad Axle
Class 4	29.5%	1.90	0.28	0	0
Class 5	6.9%	2.16	0.68	0.08	0
Class 6	5.2%	1.32	1.70	0	0
Class 7	1.6%	2.20	0.80	0.10	0.13
Class 8	5.3%	2.19	1.52	0	0
Class 9	45.6%	1.54	3.45	0.01	0
Class 10	2.1%	2.64	2.00	1.23	0.01
Class 11	2.9%	4.00	0	0	0
Class 12	0.8%	3.84	1.75	0	0
Class 13	0.2%	2.53	0.82	0.55	0

Table D.4: KDOT Criteria for Superpave Mixtures

Asphalt Layer	Percent RAP	< 3 million ESALs	≥ 3 million ESALs
Top 1.5" (Surface)	0	SM-9.5A (PG64-28)	SM-9.5A (PG70-28)
	1-15	SR-9.5A (PG64-28)	SR-9.5A (PG70-28)
Top 2.5" of Base (Intermediate)	0	SM-19A (PG64-28)	SM-19A (PG70-28)
	1-15	SR-19A (PG64-28)	SR-19A (PG70-28)
	16-25	SR-19A (PG64-34)	SR-19A (PG70-34)
Rest of Base (Base)	0	SM-19A (PG64-22)	SM-19A (PG64-22)
	1-15	SR-19A (PG64-22)	SR-19A (PG64-22)
	16-25	SR-19A (PG58-28)	SR-19A (PG58-28)

K-TRAN

KANSAS TRANSPORTATION RESEARCH
AND
NEW-DEVELOPMENT PROGRAM

AD ASTRA PER ASPERA

Kansas
Department of Transportation